DEVELOPMENT OF ROBOTIC BLACK PEPPER HARVESTING SYSTEM

By

AMSUJA V AJAYAN

(2019-18-011)

DEPARTMENT OF FARM MACHINERY AND POWER ENGINEERING

KELAPPAJI COLLEGE OF AGRICULTURAL ENGINEERING AND TECHNOLOGY, TAVANUR - 679 573, MALAPPURAM

KERALA, INDIA

2022

DEVELOPMENT OF ROBOTIC BLACK PEPPER HARVESTING SYSTEM

By

AMSUJA V AJAYAN

(2019-18-011)

THESIS

Submitted in partial fulfilment of the requirement for the degree of

MASTER OF TECHNOLOGY

IN

AGRICULTURAL ENGINEERING

(Farm Machinery and Power Engineering)

Faculty of Agricultural Engineering and Technology

Kerala Agricultural University

DEPARTMENT OF FARM MACHINERY AND POWER ENGINEERING

KELAPPAJI COLLEGE OF AGRICULTURAL ENGINEERING AND TECHNOLOGY, TAVANUR - 679 573

KERALA, INDIA

2022

DECLARATION

I, hereby declare that this thesis entitled "**DEVELOPMENT OF ROBOTIC BLACK PEPPER HARVESTING SYSTEM**" is a bona-fide record of research work done by me during the course of academic programme in the Kerala Agricultural University and that the thesis has not previously formed the basis for the award of any degree, diploma, associateship, fellowship or other similar title of any other university or society.

Place: Tavanur

Date: 25.07.2022

AMSUJA V AJAYAN

(2019- 18- 011)

CERTIFICATE

Certified that this thesis entitled "**DEVELOPMENT OF ROBOTIC BLACK PEPPER HARVESTING SYSTEM**" is a bona-fide record of research work done independently by **Ms. AMSUJA V AJAYAN (2019-18-011)** under my guidance and supervision and that it has not previously formed the basis for the award of any degree, diploma, fellowship, associateship to her.

Place: Tavanur

Date: 25.07.2022

Er. Sindhu Bhaskar
(Major Advisor)
Assistant Professor
Department of Farm Machinery
and Power Engineering
KCAET, KAU,
Tavanur, Kerala

CERTIFICATE

We, the undersigned members of the Advisory Committee of **Ms. AMSUJA V AJAYAN (2019-18-011)** a candidate for the degree of Master of Technology in Agricultural Engineering with majoring in Farm Machinery and Power Engineering, agree that the thesis entitled "**DEVELOPMENT OF ROBOTIC BLACK PEPPER HARVESTING SYSTEM**" may be submitted by **Ms. AMSUJA V AJAYAN (2019-18-011)** in partial fulfilment of the requirement for the degree.

Er. Sindhu Bhaskar
(Chairman, Advisory Committee)
Asst. Professor
Department of FMPE
KCAET, Tavanur

Dr. Jayan, P. R
(Member, Advisory Committee)
Professor & Head
Department of FMPE
KCAET, Tavanur

Er. Shivaji K. P.
(Member, Advisory Committee)
Asst. Professor (FPME)
RARS, Ambalavayal

Er. Anwar Sadique
(Member, Advisory Committee)
Asst. Professor
Department of Mechanical Engineering
Govt. Engineering College, Thrissur

Mrs. Josephina Paul
(Member, Advisory Committee)
Asst. Professor & Head
Department of BE and AS
KCAET, Tavanur

EXTERNAL EXAMINER

ACKNOWLEDGEMENT

First of all let me thank the Almighty for blessing me and helping me to complete this task as those blessings were invaluable.

My profound gratitude is placed on record to my chairman **Er. Sindhu Bhaskar**, Assistant Professor, Department of Farm Machinery and Power Engineering, KCAET, Tavanur for her deemed support, idea and efficacious advice throughout my project work.

This would be the right moment to thank **Dr. Sathian K. K**., Dean (Ag. Engg), KCAET, Tavanur for his support during the course of the project work.

I am grateful to all the members of advisory committee **Dr. Jayan, P.R**, Professor & Head, FMPE, KCAET, Tavanur, **Er. Shivaji K.P.**, Asst. Professor Dept. of FPME, RARS, Ambalavayal, **Er. Anwar Sadique,** Asst. Professor, Dept. of Mechanical Engineering, Govt. Engineering College, Thrissur and **Mrs. Josephina Paul,** Asst. Professor & Head**,** Dept. of BE and AS**,** KCAET, Tavanur for their help and constructive criticism throughout the work.

It is my pleasure to thank **Dr. Lalu P. P.**, Asst. professor and Coordinator of NCRAI, Govt. Engineering College, Thrissur for his advice and guidance rendered during this study. And I am grateful to **Mr. Vishnu Prasad S.R., Mr. Harrison Seby, Mr. Alfro Robin, Mr. Albin Saju George, and Mr. Adithyan S.**, students of Govt. Engineering College, Thrissur for their immense help and support throughout the work.

Let me take this opportunity to thank **Mr**. **Rajesh A., Mr. Sarath Kumar S., Mr. Vishnu V, Mr. Arun David H.C., Mrs. Prabhi P, Mr. Jijo George**, **Mr. Surjith C.P**., and **Mr. Prajith** technical staff of KCAET, Tavanur, **Mrs. Nafla K**, Technical assistant, FMTC, KCAET, Tavanur for their selfless help and support throughout my research work.

I would like to express my gratefulness to **Mr. Assainar Haji and family** for giving permission to utilize their black pepper field throughout my research work.

Let me also thank all the teachers, technical staffs, office staffs for their support and cooperation.

I would also like to thank all my friends, juniors and seniors who have helped me in one way or the other for the completion of my research work.

Words are not enough to explain my family's support and prayers throughout my master's period. Thanks to my father, mother and all my relatives for their love and compassion throughout the work.

Finally I acknowledge All India Co-ordinated Research Project (AICRP) and Kerala Agricultural University for financially supporting me in completing my research work in the University.

My thanks remain with all those who have helped me in one way or the other, directly or indirectly for the completion of the research work.

AMSUJA V AJAYAN

Dedicated to my Profession

CONTENTS

LIST OF TABLES

LIST OF FIGURES

LIST OF PLATES

LIST OF APPENDICES

SYMBOLS AND ABBREVIATIONS

%	:	Percentage
+	:	Add
×	:	Multiply
3D	:	3 dimensional
A	:	Ampere
AC	:	Alternating current
Ah	:	Ampere hour
AUTO	:	Automatic
ANN	:	Artificial Neural Network
ANSYS	:	Analysis of Systems.
API	:	Application Programming Interface
BED	:	battery-electric drive
BEV	:	Battery Electric Vehicles
CCD	:	Charge Couple Device
Cm	:	Centimeter
CNN	:	Convolutional Neural Network
CPLD	:	complex programmable logic device
CPU	:	Central Processing Unit
CSI	:	Camera Serial Interface
CTCP	:	Color-Thermal Combined Probability
CUDA	:	Compute Unified Device Architecture
CUDNN	:	CUDA Deep Neural Network
DC	:	Direct Current
DCNN	:	Deep convolutional neural network
DNN	:	Deep Neural Networks
DOF	:	Degree of freedom
DVI	:	Digital Visual Interface
EtherCAT	:	Ethernet for Control Automation Technology
FCN	:	Fully Convolutional Network
FN	:	False negative

FP	:	False positive
Fps	:	Frames per second
G	:	Acceleration due to gravity
GB	:	GigaByte
Gf	:	Gram force
GHz	:	Gigahertz
GND	:	Ground
GPIO	:	General-Purpose Input/Output.
GPS	:	Global Positioning System
GPU	:	Graphics Processing Unit
GRAPES	:	General Rshiny Based Analysis Platform Empowered by Statistics
H	:	Hour
HD	:	High-Definition
HDMI	:	High-Definition Multimedia Interface
HDPE	:	High Density Polyethylene
HSV	:	Hue Saturation Value
I	:	Moment of inertia
I/O	:	Input/Output.
IDE	:	Integrated Development Environment
IEEE	:	Institute of Electrical and Electronics Engineers.
IFS	:	Intuitionistic Fuzzy Set
IoT	:	Internet of Things
IR	:	Infrared
IR LED	:	infrared light-emitting diode
J	:	Joules
K	:	1000
K	:	Radius of gyration or effective radius
KAU	:	Kerala Agricultural University
KCAET	:	Kelappaji College of Agricultural Engineering and Technology
Kg	:	Kilogram

Kgf	:	Kilogram force
kg/cm	:	Kilogram per centimetre
kg-cm	:	Kilogram centimetre
KW	:	Kilowatt
kWh	:	Kilowatt hour
LAN	:	Local area network
LBP	:	Local Binary Pattern
LCD	:	Luminance and Color Difference of Red
LED	:	Light Emitting Diode
m/h	:	Meter per hour
mAh	:	Milliampere/hour
mAP	:	Mean Average Precision
MATLAB	:	Matrix Laboratory
MHz	:	Megahertz
MIPI CSI	:	Mobile Industry Processor Interface - Camera Serial Interface
Mm	:	Millimeter
MPa	:	Mega Pascal
Ms	:	Milliseconds
N	:	Newton
NCRAI	:	Nodal Center for Robotics and Artificial Intelligence
NIR	:	Near-infrared
Nm	:	Newton meter
OpenCV	:	Open Computer Vision
OS	:	Operating system
PASCALVOC	:	PASCAL Visual Object Classes
PHP	:	PHP: Hypertext Preprocessor
PVC	:	Polyvinyl chloride
PWM	:	Pulse Width Modulation
R	:	Distance from the center of force to the joint

R^2	:	R-squared (Coefficient of determination)
RAM	:	Random-access memory
RCNN	:	Region- Based Convolutional Neural Network
RGB	:	Red Green Blue
RGB-D	:	Red Green Blue – Depth
RPi.GPIO	:	Raspberry pi-General-Purpose Input/Output.
Rpm	:	Revolutions per minute
S	:	Seconds
SD	:	Secure Digital
SSD	:	Solid state drives
SVM	:	Support vector machine
TN	:	True negative
TOF	:	Time of flight
TP	:	True positive
UHD	:	Ultra High Definition
USB	:	Universal Serial Bus
V	:	Volt
VGG16	:	Visual Geometry Group 16
W	:	Watts
WHR	:	Width to Height Ratio
XML	:	Extensible Mark-up Language
YOLO	:	You Only Look Once
A	:	Angular acceleration
Ω	:	Angular velocity
Π	:	Pi

Introduction

CHAPTER I

INTRODUCTION

Black pepper (*Pipper nigrum*), known as the “king of spice”, is one of the most widely consumed spices in the world (Wang, *et al*. 2021). India is the third largest producer of black pepper producing 53,000 tons and largely exported from India. The production of the pepper in Kerala is 20,000 tons in 2019 (Anon, 2019).

Black pepper is perennial vine growing on supporting stakes. It can grow up to a height of 10 m, but plant is restricted to a height of 3m. The fruit also called as peppercorns or pepper spikes are having drupes of 5 mm diameter. Generally pepper plucking is done manually by climbing on the tree using bamboo poles, ladders or rope rings. This process of plucking the pepper involves high risk due to falling from the ladder or the bamboo pole. The conventional method results high risk of back pain and musculoskeletal problems to labourers due to repetitive hand motions and ascending and descending on ladders with heavy loads. In future, the labour issue is expected to become more critical in terms of both increasing cost and uncertain availability of skilled labourers. Another conventional method for harvesting is using poles attached with knife for plucking.

Identifying correct stage of maturity is essential to produce high quality pepper spikes. Existing harvesting methods cannot offer harvesting at correct maturity stage. Black pepper is rich in anti-oxidants and anti-inflammatory compounds which helps to balance the blood sugar and cholesterol level. Also it has cancer resisting properties and improves degenerative and damaged brain cells (Meixner, 2019). To ensure the quality of pepper, it should be harvested at its proper maturity stage. The accuracy or precision of harvesting maturity depends on the experience of the person doing the work.

Robotic harvesting is a promising option to harvest black pepper at correct maturity stage and to meet the increasing labour demand. The four functions of robotic harvesting system are i) identifying the matured pepper spike ii) plucking iii) depositing it to a specified location and iv) controlling all the functions. Robotic

arm attached with an end effector and a machine vision system can be used as an effective tool for identifying and harvesting matured black pepper spikes.

KAU developed a machine vision system for identifying matured pepper spikes. This system mainly consists of a sensor, processor and a display unit. Two computer programs were developed using OpenCV – Haar Cascade platform and TensorFlow – faster RCNN platform. These computer programs were coded in python language. TensorFlow – faster RCNN platform had a sensitivity of 77 per cent, specificity of 72 per cent and accuracy of 75 per cent while OpenCV – Haar Cascade platform had a sensitivity of 41 per cent, specificity of 4 per cent and accuracy of 13 per cent. By considering the sensitivity, specificity and accuracy it was concluded that TensorFlow – faster RCNN is better than OpenCV- Haar Cascade platform for identifying matured black pepper spikes.

Hence, it is envisaged to develop a robotic black pepper harvesting system utilizing the developed machine vision system.

Considering the above, a study on the development of robotic black pepper harvesting system is undertaken with the following objectives:

1. Modification of the existing computer program for a machine vision system to identify matured pepper spike.
2. To develop a robotic black pepper harvesting system.
3. Performance evaluation of the developed robotic black pepper harvesting system

Review of Literature

CHAPTER II

REVIEW OF LITERATURE

A brief review of the past research work relevant to different aspects of this research, viz, study of physical properties of black pepper, development of robotic black pepper harvesting system and performance evaluation of robotic black pepper harvesting system are explained in this chapter.

2.1 PHYSICAL PROPERTIES

Agricultural robots were designed based on the features of the target crop (Roshanianfard and Noguchi, 2018). The machine vision system, manipulator, and end effector were designed based on the characteristics of the target fruit. Here reviewed the studies on the properties of target crops to design and develop machine vision systems, manipulators, and end effectors.

Kondo *et al.* (2009) developed a machine vision system for identifying tomatoes for a robotic harvester. Physical properties such as fruit diameter, stem diameter, stem angle, peduncle diameter, and peduncle length are considered for the detection of tomatoes and also for designing the robotic harvester. The developed system had 65 % accuracy.

Vale *et al.* (2010) conducted a study to find the shear strength and shear energy per unit area of saffron stem at different bevel angles and shear velocities. The shear strength and shear energy per unit area, and the force and energy required for picking flowers, are essential parameters in the design and development of harvesting mechanisms. A "Universal testing machine" measured the shear force and energy. The bevel angle of the cutting blade and shear velocity significantly affected shear strength and shear energy per unit stem area. It was concluded that the age of the plants had no significant effect on picking force and energy.

Heidari and Chegini (2011) did a study to determine the shear strength and shearing energy of the rose flower stem. Instron Universal Test Machine was used for the testing. The average shear strength value was 1.63 MPa, and the shearing energy per unit area was 5.16 $mJ.mm^{-2}$. The average shear strength and energy per unit area value decreased with increasing shear velocity.

Ohali (2011) developed a computer vision system for grading date fruits. Three grades of dates were considered, and studied their physical properties such as flabbiness, size, shape, intensity, and defects. For flabbiness measurement, colour intensity distribution at grey level images were used. The size of the fruit was the area covered by the fruit; the shape was the outer profile, the intensity was the number of wrinkles, and the defects were determined from colour intensity. The maximum accuracy of the system was 80%.

Jun *et al*. (2012) developed a machine vision system for automatic grading by extracting the outer features of sweet pepper. They selected a variety of sweet pepper for the study, and three categories were considered for grading. The physical parameters studied include mass, colour, shape, and defect. Several sweet pepper grades were formed and considered for automatic grading based on each property. The overall accuracy was 95%.

Mohammadi *et al*. (2015) developed a system for identifying persimmon fruit using an image processing technique. To identify persimmon fruit, its physical, mechanical, and nutritional properties were studied. The physical properties inspected include colour, diameter, equivalent diameter and arithmetic diameter of the fruit, sphericity, surface area, and aspect ratio. The system on evaluation had an overall accuracy of 90.24%.

Kahandage *et al*. (2017) designed and developed a piece of harvesting equipment for pepper. They considered several factors such as height adjusting, weight-bearing, artificial lighting, easy cutter operation, durability, and safety for designing the equipment. Because the height of vines varies, spikes are at different vine heights, visibility problems due to higher density of leaves and uneven topography of cultivated areas. The maximum height of the pepper vine was 4m, as recommended by the Department of Agriculture. They used the average length of pepper spikes found in the preliminary study to determine the size of the cutter holder and conveying tube.

Roshanianfard and Noguchi (2018) studied the critical parameters to design an end effector for a pumpkin harvester. They used three pumpkin varieties, such

as Hokutokou, JEJEJ, and TC2A, for a physical evaluation. Three experiments were conducted, including physical properties of pumpkin, compression strength test, and bending shear test. The result showed that the designed end-effector could harvest pumpkins with a weight of 6 kg, a volume of 5 ×106 mm^3, and a radius of 110 mm. And the end effector should provide a minimum cutting stress of 4 N mm^{-2} to cut the stem.

Fashi *et al*. (2019) developed a pomegranate grading system based on image processing. Fifteen parameters of 31 monochrome channels were extracted and were given as input to the Artificial Neural Network (ANN) model. Physical properties studied include length, width, circumference, centroid, texture, area, aspect ratio, the diameter of the persistent calyx of the fruit, length of the persistent calyx, and the ratio of the diameter to length of the calyx. The system has 98% accuracy.

Yang *et al*. (2020) developed a robot pumpkin harvester based on the physical dimensions of pumpkin fruit. The weight of a pumpkin fruit usually is around 3 kg or more. It requires a high payload robotic arm to provide enough power to pick up the pumpkin fruits. The hemispherical end effector radius is fixed as 15 cm based on the pumpkin diameter and height. The diameter and height of the pumpkin fruit are less than 25 cm. The torque required to handle the fruit is normally less than 10 Nm, but it becomes 20 Nm when the pumpkin is 5 kg. So, the selected the actuator provides more than 20 Nm torque.

Masood and Jaryani (2021) made a study on the viability of robotic harvesting in chilli pepper. They measured different parameters such as the length of chilli, the diameter of chilli, the diameter of the stem, and the available length of the stem for cutting purposes. The chilli has an average diameter of 29.4 mm, an average length of 113.4 mm, an average stem diameter of 5.6 mm, and an average stem length of 22.1 mm available for cutting. For the design of the cutting mechanism, stem diameter was significant. Also, the distribution of the chilli pepper fruit on the plant is crucial to the robot's accessible and handy space.

Based on these reviews, a preliminary study on the physical properties of matured black pepper spikes was done. The physical properties include the length of the spike, the diameter of the spike, length of the peduncle and diameter of the peduncle, colour of the berries, the diameter of the berries, shear strength of the peduncle, and leaf coverage of the pepper vine.

2.2 DEVELOPMENT OF ROBOTIC BLACK PEPPER HARVESTING SYSTEM

A robotic harvesting system usually consists of a machine vision system performing object detection, a manipulator, an end effector attached to the end of the manipulator for detaching the fruit from the plant and dropping it into the collecting device, and a control unit that include all the electrical components to control the entire harvesting system (Gharakhani *et al*., 2022). Previous research on black pepper harvesting, machine vision systems, manipulators, end effectors, and control units are briefly explained here.

2.2.1 Black pepper harvesting

The conventional way of pepper harvesting includes using bamboo poles or ladders for climbing and harvesting by skilled labour. Another method is using poles attached with knife for plucking. Harvesting black pepper by climbing on ladders is a tedious task. Hence, much research has carried out in developing black pepper harvesting equipment.

Rahul *et al*. (2012) conducted a study to design and develop a pepper plucking equipment. In order to overcome the usability, safety, and ergonomic issue-related problems, five different concepts were established and selected a final model. The final concept was selected based on customer preference. A wire is connected from the hand operating part to the cutting portion in the selected model. The braking mechanism of bicycles has progressed for the cutting of peppercorns. When the hand lever is pressed, the spring gets compressed, resulting in the cutting of peppercorns. The cutting portion was curve-shaped because the stalk's holding is easier with a curve-shaped cutter.

Aneeshya *et al*. (2013) developed and evaluated three models of pepper harvesters based on the efficiency of cutting action and easiness in operation. All

three models consisted of a mild steel cutting unit, aluminium conveying pipe, and a collecting basket. The main concepts adopted were impact, shear, pulling action for proper insertion, cutting, and collecting the spikes. The most efficient and user-friendly model was the one with lightweight, easiness in operation, and minimum loss. A 2 mm thick mild steel sheet was used in the selected model to construct the cutting blades. The two blades were adequately aligned to get the correct cutting action. A hollow rectangular aluminium pipe with an appropriate length was used as the frame, and the cutting tool was fixed on that frame. The cutting action is regulated through the handle break at the bottom of the pipe. A basket was attached just below the cutting tool at an angle to collect and convey the harvested pepper spikes.

Kahandage *et al*. (2017) designed and developed harvesting equipment for black pepper. It consists of a scissor-type cutter, conveying tube, electric bulb, rechargeable battery, height-adjustable telescopic pole, and a weight bearing stand. The spring-loaded scissor-type cutter can be operated manually through the lever fixed to the telescopic pole. An LED torch was fitted at the top of the cutter holder to improve the visibility. A transparent polythene tube was connected with the cutter holder to collect the harvested spikes to the collecting bag. The adjustable range of the telescopic pole was 3-5 m, so the maximum reach of the equipment was 5 m. A locknut was provided to hold the pole at the desired height. Weight bearing tripod with a ball joint was given to support the pole; hence, the equipment can be operated in a vast range of areas without moving the equipment. For harvesting, the operator has to transfer the cutter holder to the spike so that the stalk of the spike is in between two blades and operate the cutter operating lever to harvest the spike. Simultaneously, the holder caught the spike and delivered it through the conveying tube.

Nishanth *et al*. (2020) developed a pepper harvester consisting of a motor, mainframe, harvesting and conveying unit, and collecting bag. The harvesting unit consisted of two stainless steel blades fixed on one of the two front pulleys. The dc motor drove these pulleys; hence these blades cut the pepper stalk by shearing

action. The conveying system made by a rubber belt conveys the cut stalks into the collecting bag. 12 V battery placed in a bag power the harvester for harvesting and conveying the pepper stalk. The average number of panicles harvested using this harvester was 784 per hour, whereas the average number harvested manually was 744 per hour.

2.2.2 Machine vision system

Machine vision systems identify the desired object using machine learning techniques. Robotic harvesters use a machine vision system to identify and locate target fruit on the tree.

Bhartiya and Ashish (2015) developed a machine vision system to identify red rose flowers automatically. An image processing algorithm running on OpenCV (Open Computer Vision) was used for the detection. The XML file needed to detect and identify the rose was created using a cascade trainer in MATLAB. A local binary pattern (LBP) featured cascade classifier was used to detect rose flowers. The single-board computer Raspberry Pi controlled this process by capturing live video through a standard USB webcam and identifying the roses. The machine vision system recognizes the rose flower and makes a circle around the identified rose; it indicates that the rose has been detected.

Bulanon *et al*. (2015) developed a machine vision system to recognize apples from other tree parts like a branch and the leaf and to locate the center of the fruit and its abscission layer. Photos of Fuji apple trees were collected with a color CCD camera having 640×480 pixels. The photos were digitized into a 240×320×24-bit bitmap image using the IEEE 1394 based video capture board and processed on a window-based system. Chromaticity and LCD models were used for apple recognition. And for the segmentation process, they used decision functions derived from these models. Visual Basic programming language was used to write the algorithm. Both chromaticity and LCD models have a success rate of 80%, and the noise rate was below 10%.

Sa *et al*. (2016) developed a unique method for fruit detection using deep convolutional neural networks. They implemented Faster Region-based CNN

(Faster R-CNN) as a classifier and used pictures acquired from two modalities such as colour (RGB) and Near-infrared (NIR). They combined multi-model information (RGB and NIR) with early and late fusion methods and developed a multi-modal Faster R-CNN. It involves bounding box annotation instead of pixel-level annotation, so this methodology is much faster to deploy for new fruits. The model is trained to perform the detection of seven fruits. The entire process takes four hours to annotate and train the new model per fruit.

Lili *et al*. (2017) developed a tomato harvesting robot consisting of a four-wheeled vehicle, a 5-DOF harvesting system, a navigation mechanism, and a binocular stereo vision system. To recognize ripe tomatoes, elliptic template method and Ostu algorithm were used. Images of ripe tomatoes were captured using the point greyGS3 U3-15S5C camera at a 40-100 cm distance from the target with a resolution of 1384×1032. The greyscale images obtained by the normalized color difference method were segmented into foreground and background by Ostu algorithm. Otsu algorithm extracts the target of interest from the picture and the elliptic template method segment the overlapping tomatoes into individual ones. The success rate in detecting ripe tomatoes was 99.3% for the binocular vision system.

Ge *et al*. (2019) introduced a method for identification, instant segmentation, and localization of strawberries on the basis of deep convolutional neural network (DCNN). The developed DCNN model defined four classes, including three ripeness levels of strawberries and deformed strawberries. The ripe strawberries are the easiest to be recognized among the four categories. The localization accuracy was improved by detecting the obstructed fruits and recovering the real size of the fruit with the bounding box method. The width to height ratio (WHR) of final masks was used to detect the occlusions. Moreover, to find the hidden side of the fruit, an enhancement method based on the hardness of the mask profile was suggested.

Hu *et al*. (2019) introduced a method to identify ripe tomatoes by combining an Intuitionistic fuzzy set (IFS) with the Faster R-CNN image detection method. Ripe tomatoes in different configurations such as separate, adjacent, overlapping,

and shaded were labeled in many images to train the Faster R-CNN classifier. The trained Faster R-CNN classifier perfectly and rapidly localize matured tomato, and the RGB color space for the identified tomato region transformed to the HSV color space. Samples were manually segmented to establish the Gaussian density function to remove the background from tomatoes detected by the Faster-RCNN model. Also carried out the morphological processing on the tomato binary map to remove the unnecessary subpixels and separate joined tomatoes. Finally, the IFS edge recognition technology is used to obtain the edge and applies a contour detection method to join edge breakpoints and eliminate the preventable edge points. These processes connect the tomato contour and help get exact values for a tomato's height, width, and center. The proposed method localizes the tomato center more precisely than the Faster R-CNN alone.

Lin *et al*. (2019) developed an algorithm to detect and locate citrus in natural and orchard environments based on red-green-blue-depth images. To capture the RGB-D images, a Kinect V2 sensor with RGB and infrared camera was used. The infrared camera used time of flight (TOF) technology to obtain depth information with a precision below 2mm. The Kinect V2 sensor generates an RGB image of 1920×1080 pixels and a depth image of 512×424 pixels simultaneously at a frame rate of 30 fps. A depth filter segmented RGB-D images to exclude insignificant points. The purpose of segmentation is to remove irrelevant points while focusing on the crucial points that are similar to the target fruits in colour. Bayes classifier was used as the classifier and trained for the RGB feature. Then to group the filtered RGB-D image into a set of clusters, density clustering was used. The density clustering algorithm discloses the cluster center by finding points with relatively larger density and distance. Then SVM (Support vector machine) evaluated the clusters and determined the 3D position and diameter of the citrus fruits.

Peebles *et al*. (2019) made a study to compare Faster-RCNN and Single Shot Multibox Detector (SSD) for identifying asparagus. A dataset of 597 images were used. Out of which 447 images were selected for training, 76 images for testing and 74 images validation purposes. Images were labelled in PASCAL VOC format

using LabelImg. Tensorflow's object detection API was employed to train the networks. The Faster RCNN model was faster-rcnn-inception-v2-coco and the SSD model was ssd-inception-v2-coco. Both models utilized Inceptuion-v2 architecture for their convolutional layers and were pre-trained on Microsoft's COCO dataset. Through the performance evaluation, true positivity (TP), false positivity (FP), false negativity (FN), precision and recall were measured for both models and found that Faster-RCNN network architecture was more suitable for the detection of asparagus.

Song *et al*. (2019) developed a machine vision system for a kiwifruit harvesting robot that can work a full day. Firstly, images of kiwifruit were taken from an orchard at different timing, such as morning, afternoon, and night, with and without flash. They used an ordinary single-lens reflex camera on AUTO mode with a resolution of 2352×1568 to capture the images of kiwifruit. The image dataset comprised 2400 images having 2352×1568 pixel resolution. The labeled image dataset was divided into testing (960) and training (1440) groups. Many photographs were required to train the Faster R-CNN model, so the data augmentation method was applied to enlarge the number of training images. After that, a Faster R-CNN model executed by VGG16 was created and trained. The VGG16 model has an average precision of 87.61%, and correctly detected the kiwifruit images collected under different timing and lighting conditions.

Williams *et al*. (2019) developed a novel multi-arm kiwifruit harvesting robot with a machine vision system algorithm. They used Fully-Convolutional Network (FCN) to perform semantic segmentation of the captured image for identifying kiwifruit. It was trained with 200×200 pixel hand labelled images that were collected from various orchards. Each image was hand-labeled in three classes: calyx (kiwifruit), cane, and wire. Caffe framework (Nvidi caffe) and the Nvidia Digits training system were used for training the model. The results found that 76% of the kiwifruit were detected in the actual situation.

Gao *et al*. (2020) proposed a multi-class apple detection method in dense-foliage fruiting-wall trees based on Faster Region-Convolutional Neural Network.

800 RGB images of apples with 1920 × 1080 pixels were collected under different conditions such as non-occluded, leaf occluded, branch/wire-occluded, and fruit-occluded fruit. Images were annotated by hand with rectangular annotations, and the generated ‘xml’ files were saved. The annotated images were augmented by geometric transformation and image enhancement using the software MATLAB 2018b with the Image processing Toolbox. All the photos were given as the inputs for training and testing the Faster R-CNN based VGG16 model. The training platform included a computer with an Intel Xeon E5-1650 (3.60 GHz) six-core CPU, and a GPU of NVidia TITAN XP 6 GB GPU (3840 CUDA cores) and 16 GB of memory, running on a Windows 7 64-bit system. The software tools included CUDA 8.1, CUDNN 7.5, Python 2.7, and Microsoft Visual Studio 12.0. Overall, the average precision of the model was 0.879, and an average of 0.241 s was needed to process an image.

Santos *et al*. (2020) made an evaluation of two deep learning detection architectures for grape detection: Mask R-CNN, a convolutional framework, for instance, segmentation that is simple to train, and CUDNN 7.5, a single-stage network that can detect objects without a previous region-proposal stage. In this work, a new methodology for image annotation was employed. That is, interactive image segmentation was used to generate object masks, identifying background and occluding foreground pixels. The graph matching-based process uses letterings for the segmentation and transmitting the labels from the model to the input image. To achieve a good annotation, the user repeats the process of scribble marking and graph matching steps. As a final point, the pixels of grape are kept as masks for managed instance segmentation learning. Results showed that the Mask R-CNN network offered better results than YOLO networks.

Zhou *et al*. (2020) designed a sugarcane cutting machine with a machine vision. It consists of an electrical, mechanical, and visual processing unit. The system uses machine vision to detect the sections of sugarcane stalks. FindContours function in OpenCV was used to find the contours of the sugarcane and the outline of the holes. The camera was installed at a height of 310 mm, and the focal length

was 8 mm. For the system's design, the average diameter of the sugarcane was considered, and it was 30 mm. The system's performance was evaluated and found that it has a recognition rate of 93%, and the average time taken for detection was 0.539 seconds.

Meera and Bhaskar (2020) developed a machine vision system for identifying matured black pepper spikes. They developed program in two different platform, one with OpenCV library and Haar cascade classifier and second with TensorFlow library and Faster-RCNN ANN model. TensorFlow – faster RCNN platform had a sensitivity of 0.77, specificity of 0.72 and accuracy of 0.75 while OpenCV – Haar Cascade platform had 0.41 of sensitivity, 0.04 of specificity and 0.13 accuracy. They concluded that TensorFlow-Faster-RCNN platform was better than OpenCV-Haar cascade platform by considering its specificity, sensitivity and accuracy. This machine vision system consist of a webcam as sensor, raspberry pi 4 model B as processor and Raspberry Pi LCD Display Module with a 320x240 resolution as display.

2.2.3 Manipulator

A manipulator is a device used to handle materials without direct human interference. Also, it is a programmable mechanical arm with similar functions to a human arm. The manipulators consist of links connected by joints allowing either rotary motion or linear motion. A manipulator is one of the significant components of a robotic harvester. When the system identifies and locates the target fruit, it moves the end effector to the target fruit.

Henten *et al*. (2002) developed an autonomous robot for harvesting cucumbers in greenhouses. It consists of an autonomous vehicle, a manipulator with seven degrees of freedom, an end-effector with a thermal cutting device, a computer vision system, and a control unit. It has two computer vision systems, one for detecting cucumbers and another for 3D imaging the fruit and the environment. The machine vision system and the control unit enable collision-free motions of the manipulator during harvesting. The field test confirmed the ability of the robot to

pick the cucumber with a success rate of 80%, and the robot needed 45 seconds to pick a single cucumber.

Font *et al*. (2014) developed a robotic fruit harvester by uniting a low-cost stereovision camera and a manipulator with a gripper tool at its end. They made the robotic arm or manipulator by joining five links and a manually interchangeable gripper. The manipulator joints were actuated with six low-cost DC gear motors and are controlled by a Cortex-M4F ARM STM32F407VGT6 microcontroller. This microcontroller controls the motor's speed and velocity and has different connectivity options. To place the gripper in a good position while harvesting, the motor at the base of the manipulator spins 360 º on its x-axis. Then, the motors at joints 2 and 3 can turn 260° on their z-axis to approximate the robotic gripper to the fruit. And the last joint has two degrees of freedom which spin 260° on its z-axis and 360° on its x-axis to enable two specified motions to the robotic gripper.

Roshanianfard and Noguchi (2016) proposed a newly designed robotic arm with 5 DOF for harvesting heavy crops like pumpkin and cabbage. Solidworks 2014 software with JIS standards was used to design, assemble and analyze each harvester component. Using machine design standards, the workspace, required joint torque, and mass center position was calculated. Components were designed with different materials and mass centers to reduce the torque requirement and were compared together. Three models of the robotic arm were made with different servo motor positions and linkage materials. The first model used iron, and the remaining two models used aluminium (AL5202). The results showed that the change in material and servo motor position significantly reduces the torque values.

Zhao *et al*. (2016) proposed the concept of a robotic tomato harvester with dual arms. It consists of a robotic manipulator with dual-arm, interchangeable modular type end-effector, machine vision system with stereoscope camera, communication and control system based on EtherCAT, and graphic user interface. The joints of each manipulator were actuated by direct current servo motors and controlled by the EtherCAT bus.

Lili *et al*. (2017) developed a tomato harvesting robot with five degrees of freedom manipulator. The manipulator is composed of a mechanical arm with four degrees of freedom and an end effector with one degree of freedom, arranged in tandem. The base, shoulder joint, elbow joint, and wrist joint are the major components of the mechanical arm. The results showed that the robotic arm has a load-bearing capacity of 1.5 kg.

Rana and Roy (2017) developed an autonomous robotic arm with 4 DOF similar to a human arm. The entire system consists of a functional arm and a controlling unit. The controlling unit is the signal processing part. It processes the programming language uploaded to the microcontroller and transforms the binary information into voltage variations that will actuate the arm's joints. Arduino Uno R3 was used as the microcontroller, and servo motors actuated each joint of the arm. There are three input wires in a servo motor to control it; two of them are for powering the motor by connecting to the voltage and ground terminal of the power source. And the third wire for data transfer determines the rotation of the motor. The elbow and wrist of the arm were actuated by servo motors with stall torques 15 kg-cm and 14 kg-cm, respectively.

Roshanianfard and Noguchi (2017) proposed a new design of a robotic arm having 5 DOF for harvesting heavy crops like cabbage and pumpkin. This robotic arm is composed of links and joints. The links are pinned together with revolute joints from the base to the end-effector. After the analysis of speed-torque characteristics, motor and driver were selected. In agricultural robots, the speed is secondary; the primary concern is torque. The servo motor’s speed is set to 15 rpm in joint one and 60rpm in joint five. Above these speed values, dynamic torque and inertia increase dramatically. The biggest dynamic torque requires a better power supply to control the servomotors.

Agbaraji *et al*. (2018) designed a robotic arm by estimating the joint torques and examining the motion characteristics. The actuators of the robotic arm joints were selected based on the calculated joint torques. The robot arm comprises links connected by joints, and every joint contains a motor and gears. The joint actuator

determines every possible movement of the robotic manipulator, and the performance of the joint is influenced by the motor torque and the total torque generated at that joint due to load. In the actuator selection steps, it is first necessary to determine the extreme torque needed for each joint. The torque can be calculated by multiplying the weight of the load the motor shaft has to hold with the distance between the load's center of gravity and the joint. The weight includes the weight of motors on the arm and the link arm. These servomotors are lightweight and small, so it helps to reduce the torque requirement of the joint farther back in the arm. The torque applied from the actuators determines the robot arm's operational characteristics, such as distance and velocity. Acceleration is needed to move the arm from the rest position. To find the torque due to angular acceleration, multiply the moment of inertia with angular acceleration at that joint. This work reveals the importance of actuator selection and provides the method of calculating and selecting the actuators properly for different joints in the robot arm.

Bugday and Karali (2019) found that the joint's torque requirement in manipulators increases with prolonging reach length and payload. They made this study by analyzing five robotic arms belonging to different brand. Almost 70 % of the motor's energy is used for lifting redundant weight while operating the robotic arm. So torque requirement can be reduced by reducing the arm's weight at the proper position. This study aims to determine appropriate locations to reduce material from the robot arm by ANSYS shape optimization analysis. To optimize the design, alternative designs were made by changing the material and geometry. Above these, to reduce the weight and identify the best geometric shape, holes were dug at different locations. Results from the precision analysis method showed that the hole drilled on the upper side of the manipulator greatly influences the output parameters like deformation, stress, and robot arm mass. Usually, the deformation due to load decreases with a decrease in the arm's weight. But the situation may reverse based on the geometry and location of the channel. The result showed that after optimization, the robot's weight was reduced by 10 %, stress value by 23 %, and deformation value by 65 %.

Jadeja and Pandya (2019) designed and developed a robotic manipulator having 5-DOF with servo motors positioned at each joint. The joints were found in the base, shoulder, elbow, wrist, and slider. Cortex ARM M3 LPC1768 was chosen as the microcontroller. And the programming language C was used to write the programming code to control the servomotor. The primary function of the microcontroller is to control the rotation of servomotors by generating the pulse width modulation. A servomotor requires 2 ms of pulse duration for rotating the servo at full speed in the clockwise direction.

Williams *et al*. (2019) developed a robotic kiwifruit harvester with multiple arms. It was designed to operate in pergola-style orchards. It consists of a machine vision for object recognition and four robotic arms with end-effectors specially designed for kiwifruit harvesting. The technique used to remove kiwifruit is the same as that done by the people. The end-effector will clasp and rotate the fruit to detach it from the canopy. Through the flexible tube connected to each end-effector, the fruit will reach the conveyor housed inside the harvesting cabinet. Results showed that this harvester could harvest 51% of all kiwifruit within the canopy.

Xiong *et al*. (2019) developed a strawberry harvesting robot to harvest strawberries grown on tabletops in polytunnels. The robot consists of a gripper attached to an industrial arm, a mobile base, and an RGB-D camera. The robotic arm was mounted on the mobile base along with the RGB-D camera. The result showed that the harvester takes an average cycle time of 7.5 seconds for continuously picking single strawberry at a time. 7.5 seconds for the picking operation only; it takes 10.6 seconds when all the procedures are included. The experiments revealed that the robot could pick isolated strawberries with a success rate of 96.8%. But the success rate reduces when it is occluded by leaves or immature fruits themselves. In such situations, the average picking success rate for a single attempt is 53.6% without causing damage to the fruit and 59% when including success with damage.

Daniyan *et al*. (2020) developed a lawn mowing robot. This machine is comprised of an infrared LED/receiver sensor, ultrasonic sensor, power supply unit,

Arduino microcontroller (ATmega328), Raspberry pi, memory card, camera, geared DC motors, and Global Positioning System (GPS). The microcontroller Arduino controls the geared motors alternatively to specify the directions of the lawnmower. The images captured were analyzed through colour algorithm to identify the grasses to be cut. This will helps the robot to make the decision on whether to cut, turn or move forward. A 9 V battery powered the microcontroller. The motors were powered from two 6 V batteries connected in series to get 12 V. The sensors were used for obstacle avoidance and path planning of the geared DC motors, which are powered by the microcontroller itself. The machine's chassis is constructed with aluminium to make the system lightweight.

Kumar and Ashok (2020) designed and fabricated an intelligent seed sowing robot for sowing the seeds at the desired location. The robotic arm takes the seed from the container and plants it in the desired position. It was controlled through the mobile application; once all the positions were set, the robot would automatically sow the seed when the switching button was ON. The robot was navigated through the mobile application by controlling the robot's wheels. This robot consists of stepper motors, dc motors, an ultrasonic sensor, and a linear actuator. The linear actuator opens and closes the valve for distributing the seeds. The Stepper motor driver controls the movement of the motors by receiving the signals from the controller. The ultrasonic sensor detects the obstacles in front of the robot and finds the distance toward them. The ultrasonic sensor sends the signal to the controller, and as a result, the controller stops the robot's movement for further seed sowing.

Siemasz *et al*. (2020) developed a robotic arm with six degrees of freedom that can be used with an external artificial intelligence system. The arm has six rotational joints actuated by stepper motors. They used an Atmega2560 microcontroller to manage each component of the robotic arm. All the actuators of this system were connected to the output of the microcontroller board. And the sensors were connected to the inputs of the microcontroller. Seven bipolar stepper

motors were used to describe the motion of the robotic arm, and the working tool gripper was actuated through a servomotor.

Yang *et al*. (2020) developed a robot pumpkin harvester to solve the lack of the labour force for harvesting pumpkins. This robotic harvester comprises a machine vision system to detect and locate the fruit, a robotic hand-arm, and a moving vehicle. The robotic arm with an end effector was utilized to pluck the fruit and move it to the desired position or container. The robot hand-arm and machine vision system were mounted on the moving vehicle. In the machine vision system, a USB camera was employed to capture the images in the field, and a deep neural network (DNN) based detection algorithm was used to identify the pumpkin position. Generally, pumpkin fruit weighs 3 kg or more; hence a high payload robotic arm is required to pick the pumpkin fruit.

Yurni *et al*. (2020) designed a robotic harvester to identify and pluck green and red tomatoes. This robotic harvester consists of a manipulator, end effector, Arduino, raspberry pi, camera, personal computer, and a proximity sensor. The end effector includes a scissor-type cutter, webcam, and proximity sensor. The pictures of tomatoes were captured through the webcam, and the distance toward the identified tomato was measured using the proximity sensor. Moreover, the scissors on the end effector cut the peduncle of the tomato. The entire system was controlled by Arduino Mega 2560, and Raspberry pi 3 Model B processors and servomotors were used as the actuators at the joints. This robot has 4 DOF, and the servomotors were fixed at the base, joint 1, joint 2, and the end effector. The webcam is considered the robot's eye and makes it occlusion free while approaching and harvesting the tomatoes. The webcam captures the images with a resolution of 320×180 pixels and sends them to the personal computer. After processing the images, the personal computer sends it to the Raspberry pi connected with the robot to locate the tomatoes. As the robot detects the tomatoes, the robotic arm moves to approach the tomato and cuts 3 cm above the tomato. The robot takes an average time of 4.932 seconds to harvest red tomatoes and 5.276 seconds for green tomatoes. Furthermore, the time required for the robot to return to the original

position after detaching the red tomato was 9.676 seconds, and that for the green tomato was 10.586 seconds. Variation in this time was due to varying distance between the robot and the tomato, not the colour of tomato.

Agarwal *et al*. (2021) designed a robotic arm with 5 degrees of freedom. Servomotors stimulated each joint of the robotic arm, and the microcontroller Arduino Uno based on ATmega328P was utilized for controlling the robot. The base and last joint of the robotic arm were fixed, respectively, with servomotors having stall torque of 17 kg-cm and 4.5 kg-cm. And the other three joints were actuated with servomotors having a stall torque of 6.8 kg-cm. Each link of the robotic arm is constructed with aluminium.

Masood and Jaryani (2021) developed a robotic harvester for chilli and conducted a laboratory study. This robot consists of a robotic arm with 5-DOF, Arduino Due board, cutting mechanism, depth camera, and MATLAB TM running machine. DC servo motors actuated each joint of the robotic arm. The robotic arm joints are named base, shoulder, elbow, wrist pitch, and wrist roll, respectively, from base to end-effector. The payload capacity of the arm was 150 g for an operating length of 329 mm and 400 g for minimum working distance. And the robot has a maximum reach of 400 mm. The chillies were detached from the plant by cutting the stem through sharp edge blades actuated with a servomotor have a stall torque of 2 N m. The cutter has two blades; a stationary blade mounted permanently on the ground of the end-effector, and the second moving blade moves about a hinge that lies inside the blade's body. The success rate of cutting improved by enhancing the torque through a set of pinion and gear as the transmission method.

Sanjay *et al*. (2021) proposed a cotton harvester. They utilized image processing, digital analytics, and robotics for identification, harvesting, and storage. In the image processing unit, a high-resolution camera was attached to capture the images of the crop. And the photos were sent to the microprocessor Raspberry pi. The raspberry pi 4 model is stronger, faster, and sleeker than the previous versions of the raspberry pi. The microprocessor processes the image and identifies whether

the cotton balls were opened or not. If the system identifies an opened cotton ball, the arm will move towards the cotton ball to harvest. Otherwise, the machine will move to the subsequent cotton ball for identification. The L293D motor driver with 16 pins runs two DC motors simultaneously and in the desired direction. Moisture sensor lines with LM393 receiver were used to measure the moisture content of the harvested cotton. This robot is comprised of a baler mechanism within the storage unit. It makes cotton bales and helps the farmers easily transport the cotton without wasting power and time. This machine eradicated the harvesting loss and increased the yield by 20–25%, thereby increasing the farmer's profit up to 20%.

Sarkar and Raheman (2021) developed a manually operating planter. It has a robotic arm with two degrees of freedom. The major parts of this planter are the robotic arm, hopper, conveying system, furrow opener and closer, seed tube, and electronic circuit. The robotic arm has a revolute joint and a twisting joint. And the arm is composed of a base plate, supporting frame, bearing holder, and rotating platform. Two Tower Pro MG995 servomotors actuated two joints of the arm. The picking efficiency and holding capacity of the robotic arm were measured as the important performance parameters. Average picking efficiency was 96.84% at a belt speed of 0.12m s^{-1}, and the holding capacity was 25.94 g.

Based on the above review, a manipulator having two degrees of freedom was developed for robotic black pepper harvesting system. It has two joints, which are actuated by servo motors. And it has two links which are made of aluminium hollow rectangular pipe. The use of lightweight aluminium material reduce the load to be taken by the joints.

2.2.4 End-effector

End-effector is the device or tool connected to the manipulator's end to interact with the environment. The structure of the end effector depends on the task the robot will be performing. The robotic harvester has an end effector to the manipulator's end to harvest the target fruit. Most of the end effector consists of sensors, gripping, and cutting mechanisms.

Henten *et al*. (2002) introduced a robotic cucumber harvester, especially in greenhouse cultivation. This robot has an arm attached to an end effector. The end-effector comprises a gripper, suction cup, and a thermal cutting device. The thermal cutting technique employed for harvesting consists of two electrodes carrying a high-frequency electrical potential. When the stalk interacts with the electrodes, it cuts the stem by the high-frequency current between the electrodes. While harvesting, the two fingers of the motorized gripper will grip the stalk of the cucumber, the suction cup will grasp the fruit, and the thermal cutting device will cut the stem of the fruit. After cutting, the suction cup immobilizes the fruit while transporting it to the container.

Feng *et al*. (2008) introduced a robot for harvesting strawberries growing on the hilltop. It has a precise fruit detaching mechanism to avoid any injuries to the fruit while harvesting. The end effector is composed of a pneumatic scissor and pneumatic gripper. During harvesting, firstly, the pneumatic scissor cuts the stem, and then the pneumatic fingers pick the stem and transport it into the conveyor.

Bulanon and Kataoka (2010) developed an end effector that can be mounted to an industrial manipulator for the robotic harvesting of apples. They designed the end effector as the human picks the fruit from the tree. This end-effector is composed of a peduncle holder equipped with two fingers and a wrist. The DC motor will actuate the fingers of the peduncle holder, and it has a gripping force of 11 N and an opening width of 15 mm. This gripping force is enough to hold the fruit because the average weight of the apple is assessed to be less than 400 g. The stepper motor with a torque of 1.5 N m acts as the wrist and rotates the peduncle holder once it squeezes the peduncle. The performance test result showed that it has a success rate of 90 %.

Font *et al*. (2014) developed a gripper tool for fruit harvesting. The gripper tool with a robotic arm and a machine vision system is employed for harvesting purposes. This gripper consists of four fingers; two upper moving fingers and two lower fixed fingers. The moving fingers grab the fruit, and the fixed fingers hold the fruit properly. Lower fixed fingers reduce the pressure needed to catch the fruit

with the moving fingers. A single DC motor was used to open and close the moving fingers. When the torque applied by the motor exceeds a specific value, the system will stop the grabbing procedure to avoid the occurrence of damage to the fruit. Moreover, they gave the gripping fingers a soft foam rubber coating to reduce the pressure applied to the fruit.

Hayashi *et al*. (2014) developed a movable strawberry-harvesting robot comprising a cylindrical manipulator with three degrees of freedom (3-DOF), an end-effector, a machine vision unit, and a tray storage unit. The end-effector consists of a gripper and a photoelectric sensor. The gripper has two fingers, one attached with an interchangeable blade and the other with a stopper. Reflection type photoelectric sensor was used to check the presence of the harvested fruit. The gripper with fingers will detach the fruit, and the photoelectric sensor will confirm its existence. To avoid the injury of fruit while harvesting, a cushioning material was pasted to the finger of the gripper.

Erlingsson *et al.* (2016) designed a compact, precise, and lightweight claw for grasping fruits. The major components of the claw are the mounting platform, servo motor, frame, link, slider, and gripper. The frame was made from an HDPE block, and the mounting platform on the frame was mounted to the robotic arm coupling. The servo motor was fixed on a threaded hole at the center of the frame, and the cut-outs were created in free spaces to reduce the mass. They used a servomotor with stall torque of 17 kg-cm at 6 V and weighing 63 g. Two linkages made of aluminium were connected to each end of the servo hub and each slider assembly. It is used to transform the servo's rotary motion into the slider's linear motion. The gripper made of HDPE was mounted on the slider through a single bolt. And the grippers were lined with a 2 mm thick rubber having a coefficient of friction on a glass surface of 2.

Wang *et al*. (2016) designed a new picking end-effector to improve the automatic harvesting of fresh eating tomatoes. It consists of a fruit stem holder, fruit clamping mechanism, a separating mechanism, and a control unit. Other significant components are the pressure sensor, infrared sensor, sleeve, and gasbag. The

pressure sensor is attached to the gasbag to check the pressure while clamping the fruit. And the infrared sensor at the sleeve to confirm the presence of fruit. The infrared sensor detects the fruit and simulates the air compressor to swell the gasbag when the fruit enters the sleeve. Then the dc motor advised the clamping pliers to clamp the fruit's stem correctly. Moreover, the pressure sensor will measure the pressure between fruit and gasbag to guarantee no injuries to the fruit. Then drive the double-acting cylinder to take the sleeve to shrink to cut off and pick the fruit.

Zhao *et al*. (2016) introduced a tomato harvesting robot with two robotic arms, each having three degrees of freedom. Both the manipulators were attached with end effectors to harvest the tomatoes. The manipulator's function is to position the end effector to the target fruit. The saw-type cutting device was chosen as the end effector, and a motor actuated it through belt and pulley arrangement. A microcontroller controlled the direction and speed of the motor. The posture of the cutter can be adjusted in two directions, X and Y. In the X direction, the blade moves from -45 degrees to 45 degrees with respect to the Y direction, and a four-bar linkage mechanism actuated it. And the Y-direction movement was controlled by a motor with a microcontroller. While harvesting, a vacuum suction cup holds the fruit to resist the shaking of the fruit. This vacuum cup has a diameter of 100 mm, and the vacuum power is set to handle 100 gf to 1 kgf weight.

Lili *et al*. (2017) developed a robotic tomato harvester. It consists of an end effector having one degree of freedom. The robot detaches the tomato from the plant using a shear-type gripper. The gripper was designed by giving equal importance to the steadiness of the gripper and the complexity of the structural control. Grasping, cutting, and separating tomatoes are involved in the harvesting action.

Birrell *et al*. (2019) developed a platform called vegebot. It involves a machine vision system, end effector, and software for the robotic harvesting of iceberg lettuce. They created an end effector which allows damage-free harvesting. A straight cut with high impact must attain enough cutting force to cut the stem. They tested different mechanisms such as a soft gripper with a knife-hand, belt

drive, pneumatic action, and rotary chopping to select the tool which provides the best quality cut and sufficient force. A high power-to-weight ratio was obtained from the pneumatic cutting mechanism, making it suitable for cutting the stem of iceberg lettuce. The end effector used two actuators for grasping and cutting the fruit. And they used a timing belt to transfer the linear motion from a single actuator to both sides of the blade.

Xiong *et al*. (2019) developed a robotic strawberry harvester for strawberries cultivated in polytunnels. The gripper of this harvester has four unique parts for picking, sensing, transporting, and storing. And it consists of a cutter, three active fingers, and three passive cover fingers. These six fingers open simultaneously to swallow the targeted strawberry from below. Then close the fingers to move the stem to the cutting area. The two curved blades of the cutter rotate to cut the stem. The cutter is mounted interior of the fingers to prevent the damage caused to the targeted and surrounding fruits. The blades of the cutter were mounted on a pair of gears; active driving gear and passive driving gear. Active gear is driven by a cable to close the cutter, and passive gear is connected to a return tension spring to open the cutter. Moreover, the gripper has three internal infrared (IR) sensors to identify the target location and move the gripper to the actual cutting position. In addition, the gripper has a container to collect the strawberries continuously. This container has a trapdoor to give out all the strawberries to the storage unit when it is filled. This robot has a success rate of 96.8 % for picking strawberries in a single attempt.

Roshanianfard and Noguchi (2020) developed an end-effector for a pumpkin harvester. A five-fingered hand with an electric drive was chosen as the end effector, and it was designed based on the properties of the pumpkin. This gripper can support varying pumpkin sizes ranging from 76.2 mm to 265 mm in radius. Each finger is comprised of seven elements, and the inner surfaces of each component were equipped with rollers and stabilizers made up of rubber. These rollers and stabilizers are given to prevent crop damage during harvesting and provide distance between the pumpkin surface and blades. Initially, the end-effector is positioned on the top of the pumpkin with opened fingers to approach the target.

Then the end-effector rotates 72° clockwise or anticlockwise to make contact between the blades and the stem. After that, the fingers were moved by the electric actuator to hold the pumpkin and cut off its stem.

Yang *et al*. (2020) developed a robotic pumpkin harvester after conducting a study on the physical properties of pumpkin fruits. The designed robotic hand comprised a base, crank, connecting rod, and a hemispherical end effector with a connecting frame and finger component. The crank is the active link, and connecting rod is the connecting link. The base is attached to the robotic arm, while the crank, connecting rod, and hemispherical end effector are joined by rotating pair. The hemispherical end effector involves three parts of the same shape and is held together by a connecting bracket. The finger component is fixed to the hemispherical end effector by a rotating pair with a torsion spring. Under this spring action, the finger part moves outside. A limiting slot was provided on the upper part of the end effector as an indicator to stop the finger. While harvesting, the finger rotates to a pre-set position and stops when it touches the limiting slot. It acts as a buffer, which prevents the finger from contacting the ground and the pumpkin surface.

Based on the above review, a shear cut mechanism was chosen for harvesting black pepper spikes from its stem. The cutting mechanism consist of a moving blade made up of stainless steel and a stationary cutting edge. The moving blade was driven by a servo motor having a stall torque of 11 kg-cm. There is a collecting pan below the cutting unit to collect the harvested crop directly.

2.2.5 Control unit

Every robot has a control unit to control the entire robot. Generally, the control unit involves microprocessors, sensors, actuators, batteries, and voltage regulators. The control unit continuously reads the sensors and regulates the actuators to achieve the desired function (Ganguly, 2019). This section explains the components of control units used in various works related to robotics.

Logan *et al*. (2012) conducted a study to analyze whether a generator or battery is more suited for a robot based on power density and energy density. The

results showed that batteries could power robots that require a small amount of energy. The batteries are easily rechargeable, clean, and quiet. But the long-duration operations needing large amounts of energy can be powered by a generator weighing much less than the equivalent energy stored in batteries.

Pa and Wu (2012) developed a hexapod robot to collect information from the surroundings. This robot collects environmental information by walking and transmits it to the computer via Bluetooth. Servomotors were used to execute the robot's walking movement through 12 servomotors and connecting rods. CPLD (complex programmable logic device) was used to control the servomotors by generating desired pulse width for PWM. Through the pulse width modulation (PWM) technique, servos can be rotated or held at any angle. This robot uses servomotors with a torsion of 7.2 kg per cm at 4.8 V and 8 kg per cm at 6 V. At 4.8 V, the rotation speed of the motor reaches 0.33 s per 60deg, and at 6 V, it reaches 0.27 s per 60deg

Senthilkumar *et al*. (2014) proposed an image capturing technique in an embedded system based on the Raspberry pi board. The system is comprised of a camera, Raspberry pi, and a monitor. The camera will capture the image, and the raspberry pi board will process the image recognition programs. The monitor previewed the captured image and indicated it to the user. Raspberry Pi is the microprocessor, and its main parts are a processing chip, power supply, memory, USB ports, and Ethernet port. A CSI connector on the microprocessor can deliver 1080p HD video recording at 30fp or 5 MP resolution images. So the raspberry pi IR camera plugs directly into this CSI port. The result showed that this system quickly runs the image capturing process and recognition algorithm. And the data flow smoothly between raspberry pi and the camera.

Deepan *et al*. (2015) developed an intelligent robotic hand that mimics human hand movements. To extract the human hand gesture, they used vision-based interaction techniques. The system has a camera to capture the motion of the human hand, and a Raspberry pi processor controls the entire setup. Face deduction and

skin color recognition are used to distinguish the hand in the video. This hand has five fingers, each having four degrees of freedom actuated by DC motors.

Pannu *et al*. (2015) developed a prototype of an autonomous car with raspberry pi as the processing unit. An HD camera and an ultrasonic sensor were used to collect information from the real world and transfer it to the processor. Four servomotors actuated the wheels of the car, and the motor driver IC L293D was used. 8 AA batteries were used to provide power to the motors. The motor pins were connected to the GPIO pins of raspberry pi via jumper wires for controlling the servos. The frames to mount the raspberry pi, camera, and ultrasonic sensor to the car were made up of aluminium material. They write the programming code in the python language because python language allows the user to convey the concepts in fewer lines of code. The RPi.GPIO Python library permits reading and writing the General-purpose input-output pins on the raspberry pi within a Python script.

Teja and Manohari (2015) developed a vehicle with stereo vision and raspberry pi as a processor. They used Raspberry pi model B, a 3.5 W computer with multiple input-output interfaces and a 700 MHz ARM1176JZF-S processor. Two webcams used in this assembly are connected to the USB port and the motors to the GPIO pins of the raspberry pi. The Raspberry Pi mainly uses Linux kernel-based operating systems. The programming code written in python language controls the motors connected to the General purpose Input-Output (GPIO) pins. The GPIO pins can be organized as either general-purpose input or general-purpose output.

Christian and Shukla (2016) proposed a method to monitor and control multiple servo motors through a web browser using an embedded system. Raspberry pi 2 was used as the microcontroller, and the software included Raspbian operating system, PHP, and Python language. Raspberry pi has 40 GPIO pins for input and outputs to control multiple servo motors. Servos are controlled by sending them a variable-width pulse via a control wire. When the microprocessor instructs the servo to move, the servo will rotate to that position and hold at that position.

When an external force acts on the servo motor while the servo is in the holding position, the servo resists moving out of that position. The torque rating is the maximum amount of force a servo can handle.

Sustek *et al*. (2017) provided essential awareness about controlling DC motors and servo motors with raspberry pi 2B by developing a prototype. Raspberry pi 2B has one GB of RAM, 4-core 900 MHz processor, HDMI video output, four USB 2.0 ports, and 40 - pin GPIO header. GPIO pins are standard pins in the integrated circuit of Raspberry. The purpose or behavior of these GPIO pins is not defined, which can be programmed according to the need. Python module or library RPi.GPIO imported into the main control program can be used for the proper functioning of GPIO pins. The brain of the system Raspberry Pi 2B is sufficient to run and control the DC motors and servo-motors.

Asafa *et al*. (2018) developed a robotic vacuum cleaner for home and office use. The robot is powered by three lithium-ion Polymer batteries (28.8 V DC) rechargeable via an embedded AC-DC adapter. These batteries are lightweight and have high electrochemical potential and energy density. The total current consumption of the system is 1102 mAh. The capacity of the selected battery is 2200 mAh, so when fully charged, it can continuously work for two hours. They used an LM7805 voltage regulator to step down the voltage from 28.8 V to the required 5 V.

Lagnelov *et al*. (2021) conducted a cost analysis based on a simulated vehicle system with 50 KW self-driving battery-electric drive (BED) tractors. The study shows that BED systems have high timeliness cost than diesel systems. But the annual cost was smaller in BED tractors due to saving in operational costs. Battery aging had a vital effect on the cost associated with it. But the use of batteries superior to 50 KWh or multiple batteries significantly extends the lifetime of the batteries.

Based on the above reviews, electrical components such as raspberry pi, servo motors and batteries were selected for the development of robotic black pepper harvesting system. Python module RPi.GPIO was imported to raspberry pi and used

for providing signals to the servo motors. Two 12 V valve regulated lead acid batteries connected in parallel are used for powering the system. Buck converter as used to step down voltage from 12 V to voltages required by each components.

2.3 PERFORMANCE EVALUATION OF ROBOTIC BLACK PEPPER HARVESTING SYSTEM

The performance of the robotic harvester should be evaluated in actual field conditions. The performance of the machine vision system has to be tested separately to find the accuracy and precision of detection. Performance parameters used by various researchers to evaluate the machine vision system and robotic harvester are explained here.

Hayashi *et al*. (2014) developed a movable robotic strawberry harvester comprised of a machine vision system, manipulator, an end-effector, and a storage unit. The operational distance traveled per hour was considered as the work efficiency. So its working efficiency was 102.5 m h^{-1}, and the successful harvesting rate was 54.4%.

Kahandage *et al*. (2017) designed and developed a harvesting equipment for pepper. The performance of the developed equipment was compared with the manual harvesting by considering actual capacity, theoretical capacity, efficiency and damages to the spikes and leaves in both methods. Capacity was the amount of black pepper harvested in unit time. While calculating the theoretical capacity, time taken for resting, moving and other losses were not considered. But in the case of actual capacity, every time losses for resting, moving, and adjusting the equipment and the ladder were taken into account. The ratio between the actual capacity and theoretical capacity gives the efficiency. The theoretical capacity, actual capacity and efficiency of mechanical harvesting equipment were 7.03 kg h^{-1}, 5.2 kg h^{-1} and 74% respectively while corresponding figures of manual method were 8.7 kg h^{-1}, 5.3 kg h^{-1} and 61% respectively. Damages to the vine and spikes were negligible in both methods. Efficiency and capacity of manual harvesting and mechanical method was compared by t test and found that equipment has a significant difference in harvesting efficiency and no significant difference in actual capacity.

The average actual field capacity of skilled male laborers was 5.2 kg h^{-1} while it was 5.06 kg h^{-1} for unskilled female laborers. This result shows that, any labour without considering skill or gender can operate the harvesting equipment with the same capacity.

Lili *et al*. (2017) developed a robotic tomato harvester consisting of an end effector attached to a robotic arm with five degrees of freedom, a four-wheeled steering system, a binocular stereo vision system, and a navigation system. The robotic arm has a maximum load-bearing capacity of 1.5 kg. And the success rate of the vision system in detecting ripe tomatoes is 99.3%. The positioning error becomes less than 10 mm when the distance is smaller than 600 mm. The time taken by the harvester to recognize and pluck a single tomato is almost 15 seconds. And the success rate is 86 %.

Gan *et al*. (2018) conducted a study that combines color and thermal images for immature green citrus fruit detection. They created a new Color-Thermal Combined Probability (CTCP) algorithm to effectively fuse the information from the thermal and color pictures. Faster R-CNN was used for fruit detection in color images, and Multi-level Hough circle detection was applied for fruit detection in the thermal image. The result showed that the model with Faster R-CNN on colour images has a recall rate of 78.4 %, and it increased to 90.4 % when using fused information from colour and thermal images. But while using combined data from colour and thermal images, the precision decreased from 96.7 % to 95.5 %.

Birrell *et al*. (2019) developed a platform called vegebot to automate iceberg lettuce harvesting. The vision system detected 69 matured lettuces during the field test, but the harvester attempted to pick only 60 lettuces. Because the remaining lettuces were out of range of the robotic arm, among these sixty attempts, thirty-one attempts were successful, and twenty-nine were failures. The system takes an average cycle time of 31.7 seconds, but the grasping and cutting require only 2 seconds. The cycle time can be reduced by making the strongest arm and lightweight end effector. The lettuce localization and detachment success rates were 91 % and 97 %; therefore, the harvest success rate was 88%. The damage rate of

the harvester was 38%, which is ratio of the number of damaged lettuce harvested to the total number of lettuce harvested.

Lin *et al*. (2019) introduced an RGB-D image-based algorithm to detect and locate citrus in actual field conditions. It was developed for robotic harvesting. The performance of the system were evaluated using the parameters precision, recall, and F1 score. Precision is the ratio between the number of true positives and the number of detection in the images. And recall is the ratio between the number of true positives and the total number of fruits in the pictures. The F1 score can be calculated using the equation 2× (Precision × Recall) / (Precision + Recall). A higher F1 score indicates better performance of the detection system. The developed algorithm's precision, recall, and F1 scores were 0.9839, 0.8634, and 0.9197, respectively. The result showed that the developed system is strong enough to detect citrus in natural field conditions.

Williams *et al*. (2019) developed a robotic kiwi fruit harvester with multiple robotic arms. The developed harvester was evaluated by measuring its grip failure, obstacle, knocked-off, drop and cycle time. The harvester fails to cut off the fruit from the plant when attempts to pick is considered a grip failure. Leaves and branches are the hindrances to harvesting, so the number of times the end effector comes in contact with these hindrances that limit its ability to move is taken as the obstacle. The number of non-targeted fruits lost when the harvester collides with the canopy is measured as Knocked-off. The number of fruits lost while harvester detaching and dropping is termed as the drop. This developed robotic harvester can harvest 51% of the total number of fruits within a natural orchard environment. The average cycle time of this harvester is 5.5 seconds per fruit, and it has a capacity of 655 fruits per hour.

Zhang *et al*. (2020) developed a multi-class object detection algorithm using a faster R-CNN model. It is used for detecting apples, trunks, and branches in actual field conditions. They evaluated the system by measuring the parameters such as precision, recall, F1 score, and mean Average precision (mAP). The result showed that the computational time for the detection was 0.45 seconds per image. Also, the

system's mean Average Precision and accuracy were 82.4 % and 72.7 %, respectively.

Masood and Jaryani (2021) studied the viability of a robotic chile pepper. They evaluated the harvester's performance by measuring its localization success rate, detachment success rate, harvesting success rate, cycle time, and damage success rate. The fruit localization success rate was the number of fruits correctly localized out of the total number of ripe fruit taken for the test. The detachment success rate is the number of harvested ripe fruit per total number of localized fruit. Number of successfully harvested ripe fruits per total number of ripe fruits taken for testing is the harvesting success rate. The cycle time includes the time taken for human identification, localization, and fruit detachment. And the damage rate was the number of damaged fruits per total number of localized fruit. The result showed that the localization success rate, detachment success rate, harvest success rate, damage rate and cycle time were 37.7 %, 65.5 %, 24.7%, 6.9 %, and 7 seconds respectively.

Sarkar and Raheman (2021) developed a manually drawn planter with a manipulator having two degrees of freedom. The designed robotic arm has a higher picking efficiency of 96.84 % at a conveyor belt speed of 0.12 m s^{-1}. The holding capacity of the arm was evaluated at different sizes of onion and found that it has a maximum capacity of 25.94 g. One cycle time of operation includes time for picking, lifting, carrying, and dropping the onion in the seed tube and returning to the initial position. The cycle time of the process ranges from 3 to 8 seconds. To determine the power consumption of robotic arm, the current consumed by all the servomotors while picking, carrying, and releasing the onion was measured using an ammeter and multiplied by the voltage (6V). The result showed that the weight to be carried is directly proportional to the power consumed. 25. 76 W was the power consumption when the weight of the onion was 25.96 g.

From the reviews mentioned above the performance parameters selected for this research were; sensitivity of the system, specificity of the system, time taken for identification, capacity of the system, effectiveness index of the system, time

taken for cutting, time taken for the entire operation, harvesting loss and drying loss. The machine parameters such as overall dimension of the system, overall weight of the system and power requirement of the system should also be measured.

Materials and Methods

CHAPTER III

MATERIALS AND METHODS

This chapter explains the methodology used for the development and performance evaluation of robotic black pepper harvesting system. The whole process is explained as study of physical properties of black pepper, development of robotic black pepper harvesting system and performance evaluation of developed robotic black pepper harvesting system.

3.1 PHYSICAL PROPERTIES

The study of physical properties of black pepper was carried out to measure and analyse properties and its values that can directly or indirectly affect the design and development of robotic black pepper harvesting system. The physical properties include length of the spikes, diameter of the spikes, weight of the spike, colour of berries, diameter of berries, length of the peduncle, diameter of the peduncle, shear strength of pepper peduncle and leaf coverage of black pepper vine were studied. Two different varieties of black pepper, *Karimunda* and *Panniyur 1* were considered for the study. The samples were collected from Kattappana in Idukki district, Tavanur in Malappuram district, and Thannithode in Pathanamthitta district. These measurements were taken from 100 samples.

3.1.1 Length of spikes

Length of black pepper spikes were taken for the estimation of the size of a black pepper spike. It was measured as the total length from the top end of black pepper spike to its bottom tip excluding the peduncle length.

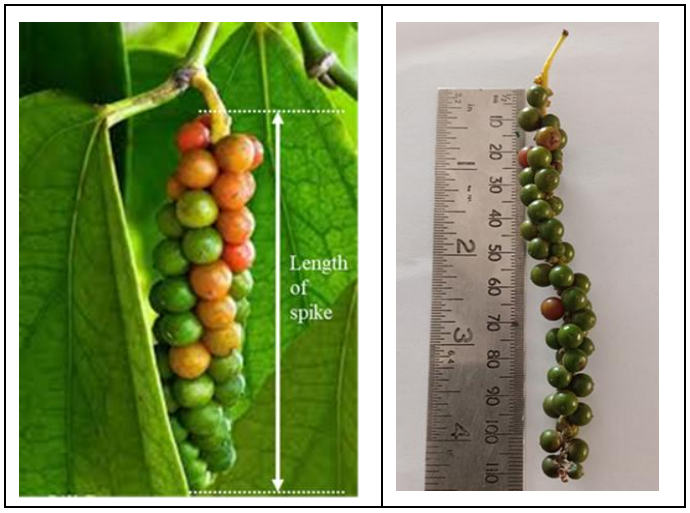

Plate 3.1 Length of spikes

3.1.2 Diameter of spikes

Diameter of the pepper spikes at three levels viz. top end, middle and bottom was measured for size estimation. The average of three values were recorded as average diameter of spikes. The diameter of spikes was measured using a vernier calliper.

Plate 3.2 Diameter of spikes

3.1.3 Weight of spikes

Weight of each pepper spikes were measured using weighing balance. It was measured for 100 samples in both *Panniyur 1* and *Karimunda* variety.

3.1.4 Colour of berries

The colour value was measured using the RGB colour model and it was measured using a program code written in python language. It was measured separately for both *Panniyur 1* and *Karimunda* variety.

3.1.5 Diameter of berries

The diameter of the berries were measured using a vernier caliper. It was measured for 100 samples in both *Panniyur 1* and *Karimunda* variety.

3.1.6 Length of the peduncle

It is the stem attaching the fruit to the plant. Its length is measured from the top end of the pepper spike to the node on the stem. It was measured using a steel rule.

Plate 3.3 Length of the peduncle

3.1.7 Diameter of the peduncle

The diameter of the peduncle was measured for the size estimation of the pepper peduncle.

Plate 3.4. Diameter of the peduncle

3.1.8 Shear strength of the peduncle

The shear strength of the peduncle was calculated from the shear force and cross sectional area of the peduncle. Shear force was determined using EZ-SX Texture Analyzer with the operation software TRAPEZIUM X. The cutting probe (blade) with 2.95 mm thick and 30 degree angle was used for this test. The shear strength of the peduncle at two different speed such as 0.1mm s^{-1} and 1mm s^{-1} were determined. Shear strength can be calculated using the equation,

$$\text{Shear strength (N mm}^{-2}) = \frac{\text{Shear force, N}}{\text{Cross sectional area, mm}^2} \quad \ldots\ldots (3.1)$$

3.1.9 Leaf coverage of black pepper vine

Leaf coverage of black pepper over the supporting element was studied. A sample of 50 black pepper vines were observed for conducting this study. Leaf coverage was measured as the horizontal distance measured from the supporting tree to the extreme end of the black pepper covered. The dimension from four sides were measured. The 95^{th} percentile of the observed values was considered for further study.

Plate 3.5 Texture analysis of peduncle of black pepper spike

Plate 3.6 Leaf coverage of black pepper vine

3.2 DEVELOPMENT OF ROBOTIC BLACK PEPPER HARVESTING SYSTEM

Robotic black pepper harvesting system consist of a machine vision system to identify matured black pepper spikes, manipulator, end effecter, and a control unit. Proposed model of robotic black pepper harvesting system was designed using the software SolidWorks version 2020 as shown in figure 3.1 along with name of each component. Each component of the robotic black pepper harvesting system were discussed here.

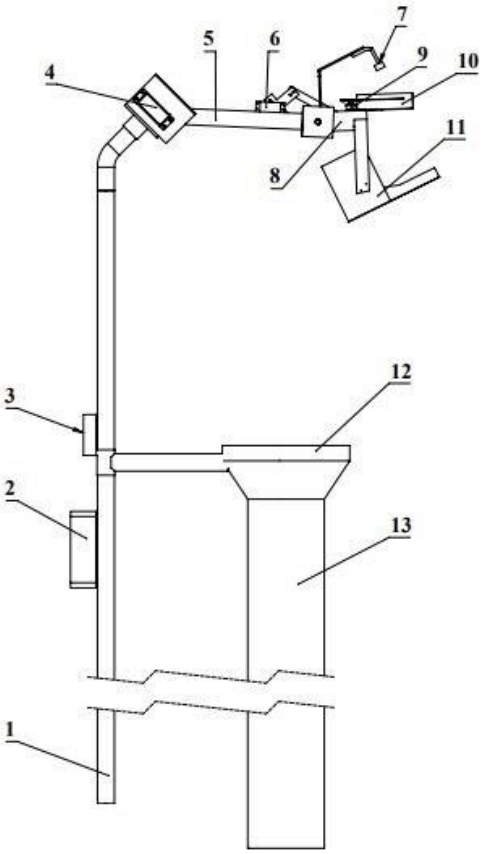

1. Supporting rod
2. Buck converters
3. Processor (Raspberry pi) with display
4. Shoulder joint (Servo motor 1)
5. Shoulder link
6. Elbow joint (Servo motor 2)
7. Sensor (Camera)
8. Elbow link
9. Cutting motor (Servo motor 3)
10. Cutting unit
11. Collecting pan
12. Collecting hopper
13. Conveying unit

Fig. 3.1 Designed robotic black pepper harvesting system.

3.2.1 Machine vision system

The machine vision system developed by Meera (2020) explained in article 2.2 for identifying matured black pepper spikes was used in this project. The machine vision system consist of a sensor (a USB web camera), a processor (raspberry pi) and display unit.

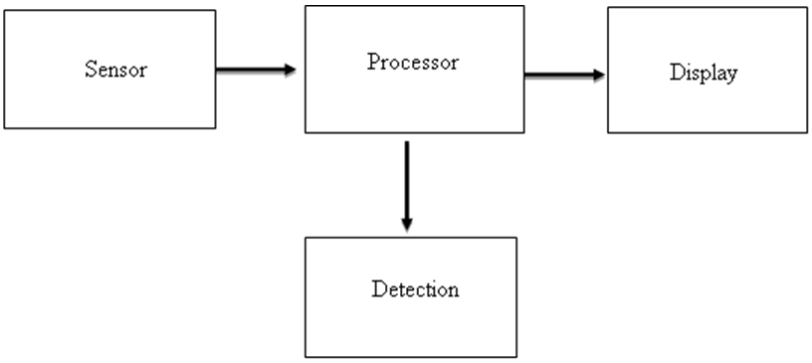

Fig. 3.2 Block diagram of machine vision system

The system used TesnsorFlow as detection library and faster-RCNN as classifier. The computer assisted program was coded in python language. The details of each components were described here,

3.2.1.1 Sensor

In this system USB camera of Logitech was used as the sensor to capture the images of black peppers. It can capture image at a speed of 30 fps. It has a height of 15 cm, width of 7.5 cm and weight of 0.95 g. For the identification process, the maximum distance from the camera was 20 cm and minimum distance was 6 cm.

Plate 3.7 Sensor

3.2.1.2 Processor

In this study Raspberry pi 4 model B was used as the processing unit. This unit have a 64-bit quad-core processor, 4 GB RAM, 2.5 GHz and 5 GHz 802.11b/g/n/ac wireless LAN, Bluetooth 5.0, Gigabit Ethernet port, along with several ports including 2 USB 3.0 ports, two micro HDMI ports enabling 4K UHD video, 2-lane MIPI CSI camera port for connecting a Raspberry Pi camera, 2-lane MIPI DSI display port for connecting a display, 4-pole stereo output and composite video port, micro SD port and a 5V/3A DC power input. The processor speed ranges from 700 MHz to 1.4 GHz. All the operations of the system was controlled by this processor.

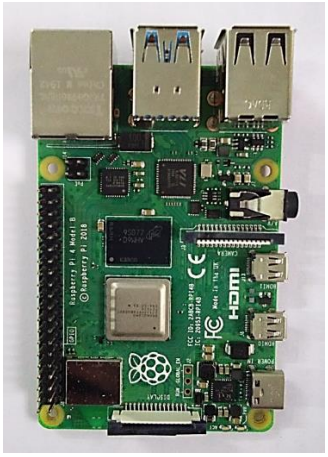

Plate 3.8 Raspberry Pi 4 model B

3.2.1.3 Display unit

The display unit used was a Raspberry Pi LCD Display Module with a 320 × 240 resolution display. It was of the model 3.2 LCD-V4 with 7 × 5 × 1.5 cm side lengths. Its signal input included SPI interface. This monitor had brighter and sharper images with a good resolution display. It was suitable to Raspberry Pi versions of B+, 2B, 3B and 3B+. This display unit was selected due to the compact and wireless nature, being suitable for field works.

Plate 3.9 Display unit

3.2.1.4 Modification of existing computer programme for a machine vision system to identify matured black pepper spikes

In the existing machine vision system for identifying matured black pepper spike, the program was simulated in Jupyter notebook. It was significantly slower the process as each cell have to run separately for the simulation. To make the process faster, the programing code was written and executed in python-based IDE (Integrated Development Environment) "Thonny". Hence the entire program can be simulated by running a single command line thus making the process faster. For the working of machine vision system in the IDE Thonny offline, TensorFlow and IPython were installed separately in the Raspberry Pi.

The prior computer code was altered in order to recognise matured black pepper spikes. Special codes must be provided to upload the files from Google Drive to the working environment of the Jupyter notebook since the codes were performed inside the notebook. However, the current system performed the detection locally, so there is no need to transfer the files from Google Drive. Shortening the programming code is beneficial. Additionally, the cv2 module was used to display the detection result in a new window in full screen mode. In earlier research, the system was tested utilising previously recorded movies and photos. As a result, the programming code was created in a way that allowed testing uploads of videos and photographs from the drive. However, in the current system, the code was changed to enable real-time webcam capture of the films and photographs.

Additionally, programmes were added to interact with the end effector's servomotor when it recognises a mature black pepper spike.

3.2.2 Manipulator

The developed robotic black pepper harvesting system has a manipulator with two degree of freedom. It has two rotational joints which rotates about its horizontal axis. Each joint was actuated by a servo motor. The specifications of the servo motors were selected based on the maximum torque required by the structure and possible loads. Aluminium material was chosen for the construction of manipulator of robotic black pepper harvesting system, because of its light weight, strength and easy availability. Each component of the manipulator are discussed here,

3.2.2.1 Shoulder link

An aluminium hollow square pipe of dimension 31.75 × 31.75 × 1.0 mm was used for the construction of this link. This link has a length of 300 mm and weighs 117 g. A C clamp was riveted on the supporting rod having a height of 1.5 meter and outer diameter of 3.3 cm. The servomotor1 of stall torque 6.0 N m was riveted to this clamp. The servomotor horn was allowed to pass through the provision provided in the shoulder link. So that the link was powered by servo motor. Another C clamp was fixed on the elbow side of this link. This C-clamp was made by folding an aluminium sheet having dimensions 240 × 60 × 1.0 mm and was used to connect shoulder link and elbow link.

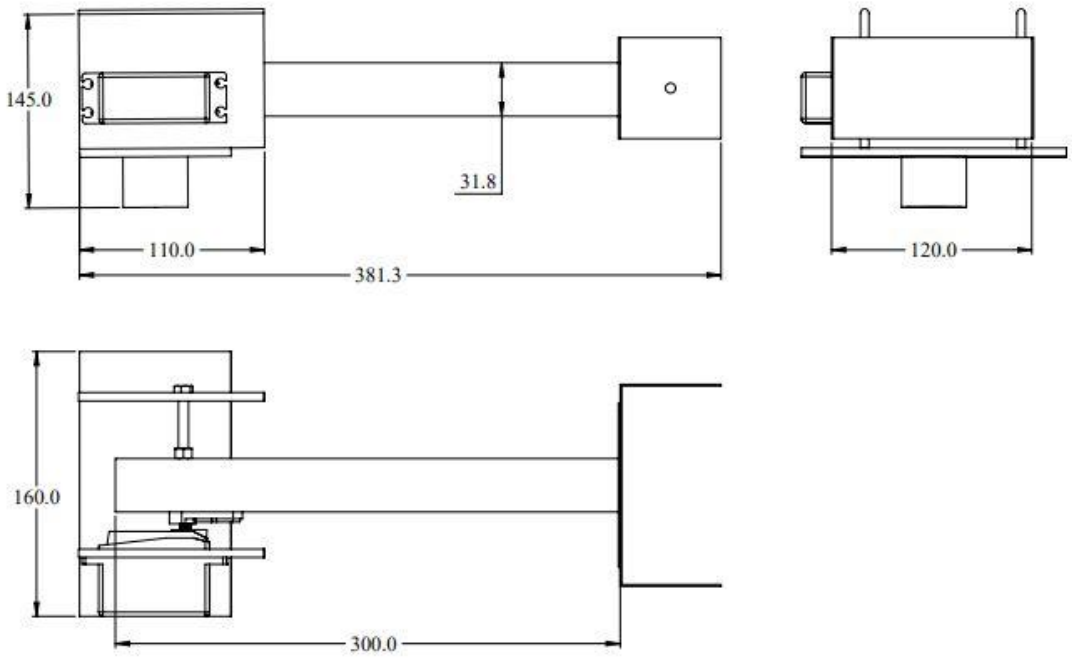

Fig. 3.3 Shoulder link

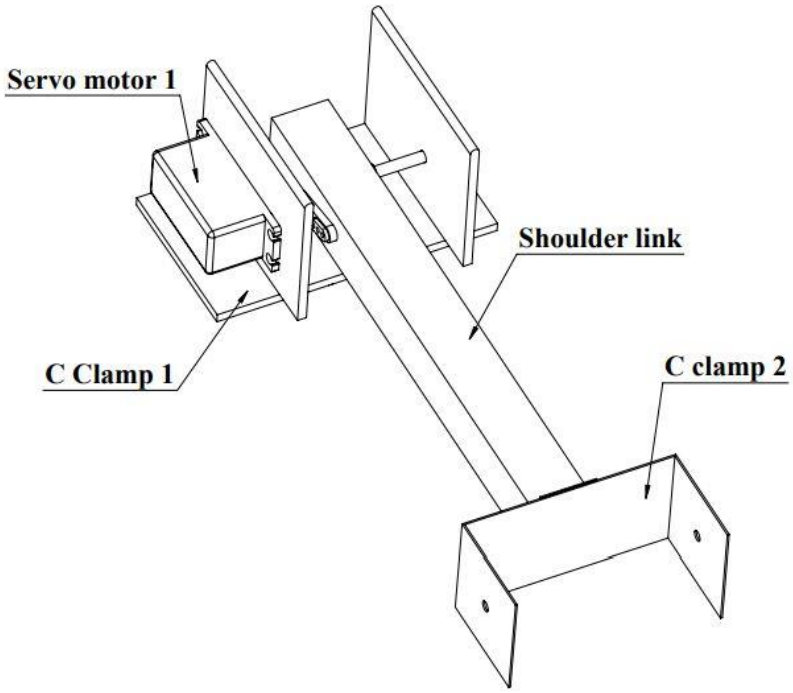

Fig. 3.4 Isometric view of the shoulder link

3.2.2.2 Elbow link

An aluminium hollow pipe having a dimension of 61.5 mm × 38.1 mm × 1 mm was used for the construction of this link. It has a total length of 135 mm to accommodate all the necessary components such as a cutting motor, cutting blade assembly, and camera. And it weighs 60.3 g.

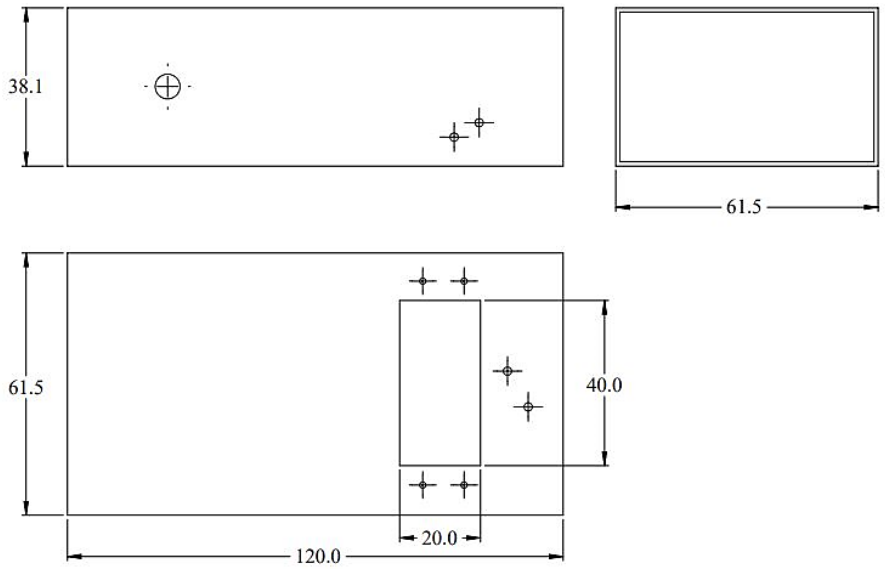

Fig. 3.5 Elbow link

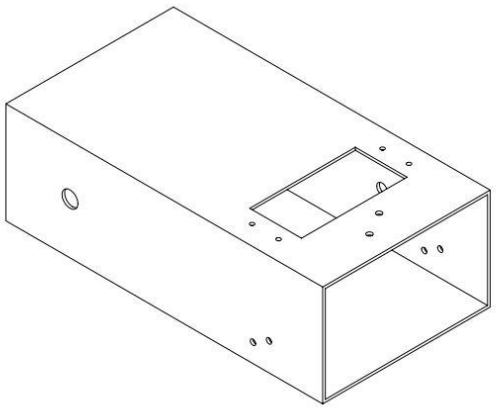

Fig 3.6 Isometric view of elbow link

3.2.2.3 Servo motors

The servo motors were selected based on the torque required at each joint. The torque calculation should start from the last joint and then proceed to the first joint. The calculations are explained here,

Total torque required for a servo motor = … (3.2)

Torque due to force of gravity on links and payload

+Torque due to angular acceleration of links and payload

(Automaticaddison, 2020)

Torque due to force of gravity on links and payload = $m \times g \times r$ …… (3.3)

(Khurmi, 2019)

m = Mass the servo motor has to lift

g = Acceleration due to gravity

r = Distance from the center of force to the joint

Torque due to angular acceleration of links and payload, $\tau = I \times \alpha$ …… (3.4)

(Khurmi, 2019)

I = Moment of inertia

α = Angular acceleration

3.2.2.3.1 Torque required at elbow joint

The values used for the torque calculations are:

Mass of the elbow link, Mb = 0.124 kg

Mass of the cutting blade assembly with servo motor, Me = 0.0831 kg

Mass of the camera with stand, Mc = 0.097 kg

Mass of the collecting pan, Mp = 0.0895 kg

Distance from the center of gravity of elbow link to elbow joint, Lb = 0.0675 m

Distance between cutting blade assembly and elbow joint, Le = 0.075 m

Distance between camera with stand and elbow joint, Lc = 0.055 m

Distance between collecting pan and elbow joint, Lp = 0.0905 m

Torque due to gravitational force $= \big((Mb \times Lb)+(Me \times Le)+(Mc \times Lc)+(Mp \times Lp)\big) \times g$

$= ((0.124 \times 0.0675)+(0.0831 \times 0.075)+$

$(0.097 \times 0.055)+(0.0895 \times 0.0905)) \times 9.8$

$= 0.275$ Nm

$= 2.75$ kg cm

Torque due to angular acceleration = $I \times \alpha$

I= Moment of inertia

α= Angular acceleration

Angular acceleration will be same for both the motor and link, since they are connected to each other. Assume that the motor should move 20 degree ($\frac{\pi}{9}$ radian) in 1 second. Figure 3.7 shows the graph of angular velocity ω (radians/second) vs time t (seconds). Acceleration is the slope of the velocity curve.

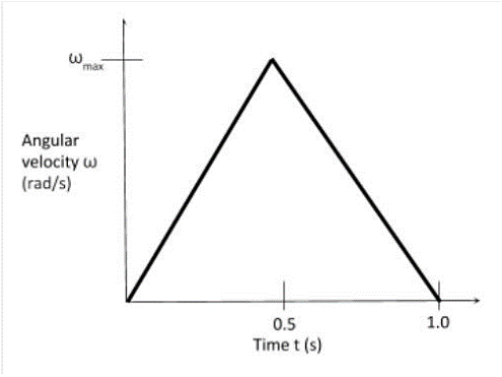

Fig. 3.7 Graph between angular velocity and time

$$\text{Angular acceleration} = \frac{\text{Change in angular velocity}}{\text{Change in time}} \quad \ldots\ldots (3.5)$$

The area of the curve is equal to the distance the servo motor needs to move.

….. (3.6)

Area underneath the curve (Area of triangle) =($^1/_2$)×(base)×(height)

The distance the servo motor needs to move is 20º, which is equal to $^\pi/_9$ radians.

$$^\pi/_9 = (\,^1/_2)\times(1.0)\times(\omega_{max})$$

$$\omega_{max} = \,^\pi/_{4.5} \text{ rad s}^{-1}$$

Since α is the slope of the curve,

$$\alpha = \left(\frac{\text{Change in y}}{\text{Change in x}}\right)$$

$$= (\,^{\frac{\pi}{4.5}}/_{0.5})$$

$$= \,^\pi/_{2.25} \text{ rad s}^{-2}$$

Moment of inertia, $I=m\times k^2$ …… (3.7)

m = Mass

k = Radius of gyration or effective radius

Assume that the rotational inertia of the motor is negligible as compared to the link. Therefore moment of inertia of motor equal to 0 kg m^2

Moment of inertia of cutting blade assembly with motor, $Ie = Me \times Le^2$

$$= 0.0831 \times 0.075^2$$

$$= 0.00047 \text{ kg m}^2$$

Moment of inertia of camera with stand, $Ic = Mc \times Lc^{\,2}$

$$= 0.097\times0.055^2$$

$$= 0.0003 \text{ kg m}^2$$

Moment of inertia of collecting pan, $Ip = Mp \times Lp^2$

$$= 0.0895\times0.0905^2$$

$=0.00073 \text{ kg m}^2$

Moment of inertia of the elbow link about the edge,

$$Ib = \left(\left(\frac{1}{12}\right) \times Mb \times \left(a^2 + b^2\right)\right) + (Mb \times h^2) \qquad \ldots\ldots\ldots (3.8)$$

a = 0.0381 m (breadth of the link)

b = 0.135 m (Length of the link)

h = 0.0435 m (Distance from the central axis to the edge)

$$Ib = \left(\left(\frac{1}{12}\right) \times 0.124 \times \left(0.0381^2 + 0.135^2\right)\right) + \left(0.124 \times 0.0435^2\right)$$

$=0.0019 \text{ kg m}^2$

Torque due to angular acceleration = $I \times \alpha$

$= (Ib + Ie + Ic + Ip) \times \alpha$

$= (0.0019 + 0.00047 + 0.0003 + 0.00073) \times \left(\frac{\pi}{2.25}\right)$

$= 0.00475 \text{ kg m}^2 \text{ s}^{-2}$

$= 0.00475 \text{ N m}$

$= 0.0475 \text{ kg cm}$

Total torque at elbow joint = 2.75 kg cm + 0.0475 kg cm

= 2.8 kg cm

= 0.28 N m

Elbow joint is between shoulder link and elbow link, it rotates about its axis at a fixed limit of 90 to 180 degree.

TowerPro MG996R digital high torque servo motor was selected as elbow joint. It has a stall torque of 0.94 N m at a voltage of 4.8 V and 1.1 N m at a voltage of 6.6 V. At 4.5 V its operating speed is 0.19sec/60 degree (53 rpm) and at 6.6 V

its operating speed is 0.15sec/60 degree (54 rpm). It has metal gear with 25 number of teeth. Its length is 40.7 mm, width is 19.7 mm and height is 42.9 mm. It weighs 55 g.

3.2.2.3.2 Torque required at shoulder joint

Shoulder joint was mounted on the C clamp 1of shoulder link and this C clamp was fixed to the supporting rod.

Thus, the values used for the torque calculations are:

Mass of link 1, Ma = 0.163 kg

Mass of elbow joint, Mj = 0.055 kg

Distance from shoulder joint to the centre of gravity of the link 1, La =0.15 m

Distance between cutting blade assembly and shoulder joint, Le1 = 0.435 m

Distance between the camera and shoulder joint, Lc1 = 0.415 m

Distance between collecting pan and shoulder joint, Lp1 = 0.4505 m

Distance between elbow joint and shoulder joint, Lj = 0.216 m

Torque due to gravitational force = ((Ma × La) + (Mj × Lj)+(Me × Le1)

$$+ (Mc \times Lc1) + (Mp \times Lp1)) \times g$$

$$= \begin{pmatrix} (0.163\times0.15)+(0.055\times0.216)+(0.0831\times0.435)+ \\ (0.097\times0.415)+ (0.0895\times0.4505) \end{pmatrix} \times 9.8$$

$$=1.5 \text{ N m}$$

$$=15 \text{ kg cm}$$

Torque due to angular acceleration = I×α

Moment of inertia of shoulder link about the edge, Ia

$$= ((1/12) \times Ma \times (a1^2+b1^2)) + (Ma\times h1^2)$$

a1= 0.03175 m (Breadth of shoulder link)

b1=0.3 m (Length of shoulder link)

h1=0.12 m (Distance from the central axis to the edge)

$Ia = \left(\left({}^{1}/_{12}\right)\times 0.163\times\left(0.03175^2+0.36^2\right)\right)+(0.163\times 0.12^2)$

$= 0.0036$ kg m^2

Moment of inertia of cutting blade assembly with motor, Ie1 = Me × Le1

$= 0.0831 \times 0.435^2$

$= 0.016$ kg m^2

Moment of inertia of camera with stand, Ic = Mc × $Lc1^2$

$= 0.097 \times 0.415^2$

$= 0.017$ kg m^2

Moment of inertia of collecting pan, Ip = Mp × $Lp1^2$

$= 0.0895 \times 0.4505^2$

$= 0.02$ kg m^2

Moment of inertia of elbow joint, Ij = Mj × Lj

$= 0.055 \times 0.216^2$

$= 0.0026$ kg m^2

The angular acceleration about shoulder joint is same as that of the elbow joint.

Therefore, angular acceleration, $\alpha = {}^{\pi}/_{2.25}$

Torque due to angular acceleration = (Ia+Ie1+Ic+Ip+Ij)×α

$= (0.0036 + 0.016 + 0.017 +$

$0.02 + 0.0026) \times ({}^{\pi}/_{2.25})$

$= 0.083$ N m

$= 0.83$ kg cm

Total torque at shoulder joint = 15 kg cm+0.83 kg cm

= 15.83 kg cm = 1.583 N m

Ultra torque quarter scale 60 kg cm metal gear servo motor was selected as shoulder joint. It has a stall torque of 6 N m at a voltage of 8.4 v and 5.8 N m at a voltage of 6 V. At 8.4 V its operating speed was 0.13 sec/60 degree (77 rpm) and at 6 V its speed was 0.17sec/60 degree (59 rpm). This selected servo motor has a length of 65 mm, width of 30 mm and a height of 48 mm. And it weighs 0.17 kg and operating voltage is 6 V to 8.4 V.

3.2.3 End effector

Robotic black pepper harvesting system used shear type cutting mechanism with a collecting pan as the end effecter. The details of each component of the end-effector is discussed below.

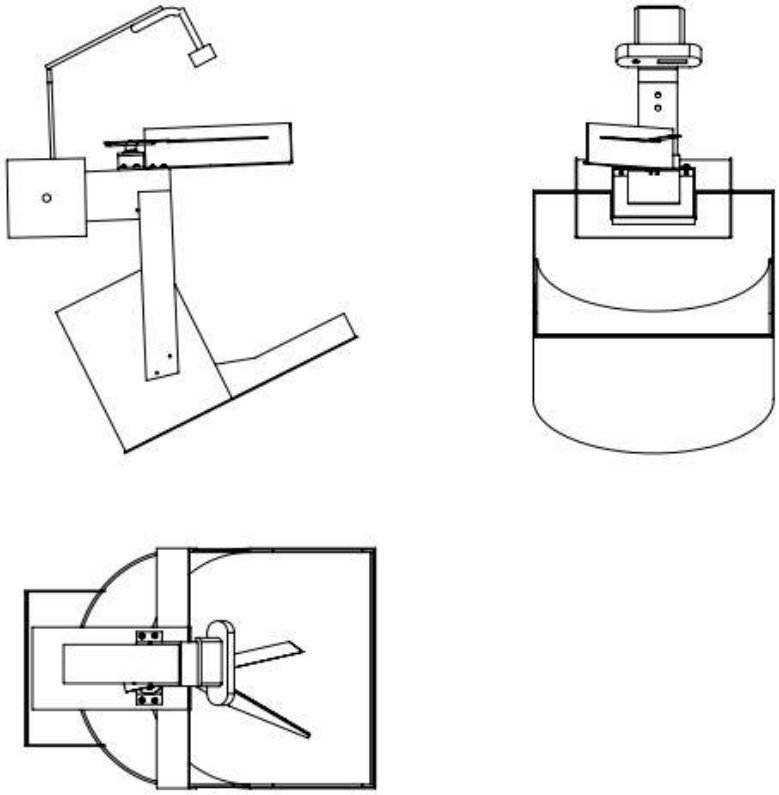

Fig. 3.8 End effector

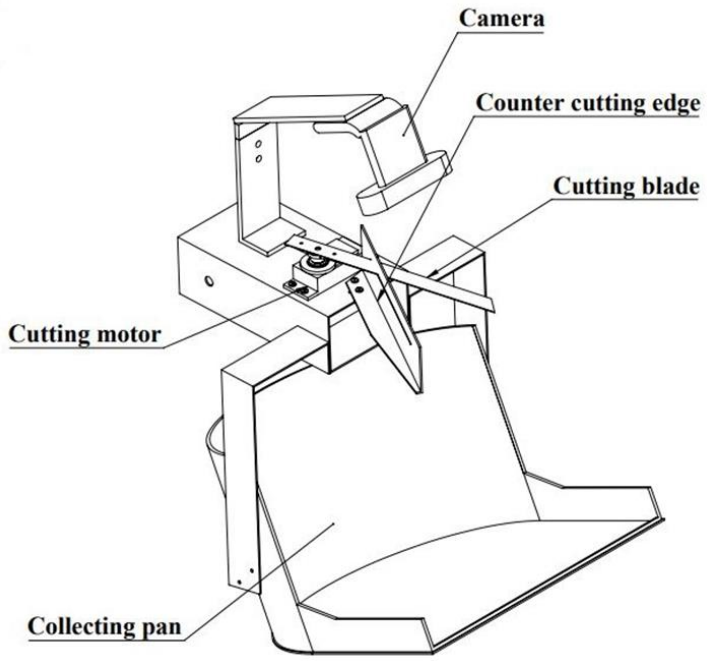

Fig. 3.9 Isometric view of end effector

3.2.3.1 Cutting unit

The shear cut mechanism was selected as the best method for harvesting matured black pepper spikes, following the procedure used for the pepper harvester by Aneeshya *et al*. (2013) as in article 2.2.1.

The cutting unit consists of two components, a movable cutting blade and a stationary counter cutting edge. The cutting blade is controlled by TowerPro MG996R digital high torque servo motor having a stall torque of 1.1 Nm. The maximum torque is applied when the motor is operated at 6 V. A slot was provided in the counter cutting edge and the cutting blade is allowed to pass through that slot. Movable cutting blade and counter cutting edge was made with stainless steel and aluminium sheet respectively. The counter cutting edge and servo motor were fixed to the space provided in elbow link, and the cutting blade was fixed on the servo motor. The cutting blade has a length of 14 cm, width of 1cm and thickness of 0.05 cm on sharp edge and 0.1 cm on other edge. The counter cutting edge has a length of 15 cm, height of 3 cm, and width of 0.1 cm.

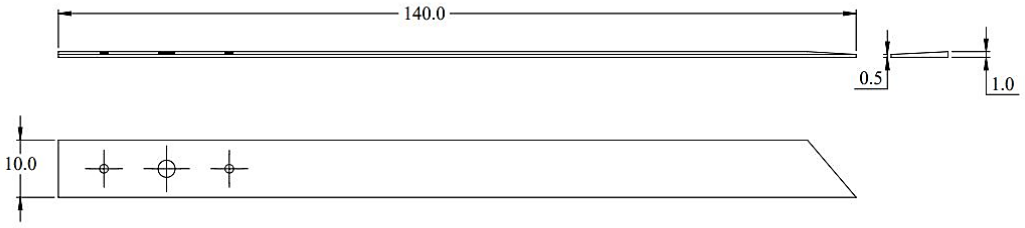

Fig. 3.10 Cutting blade

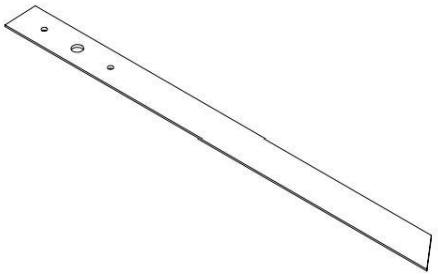

Fig. 3.11 Isometric view of cutting blade

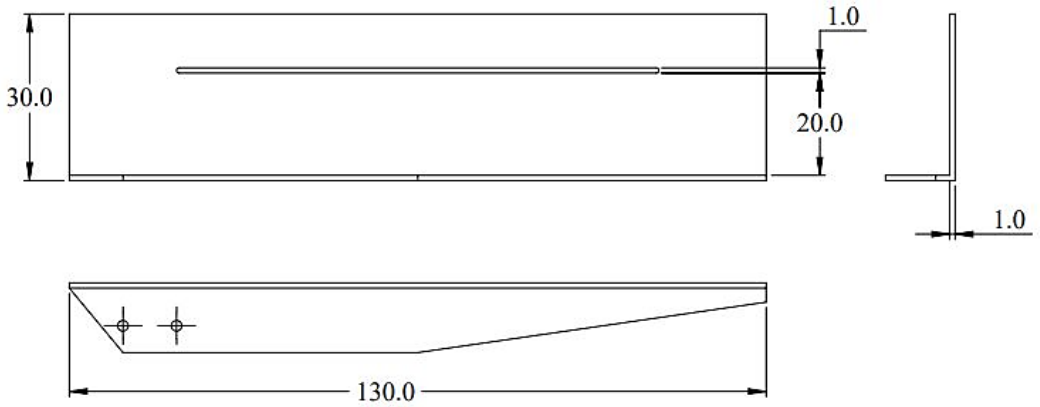

Fig. 3.12 Counter cutting edge

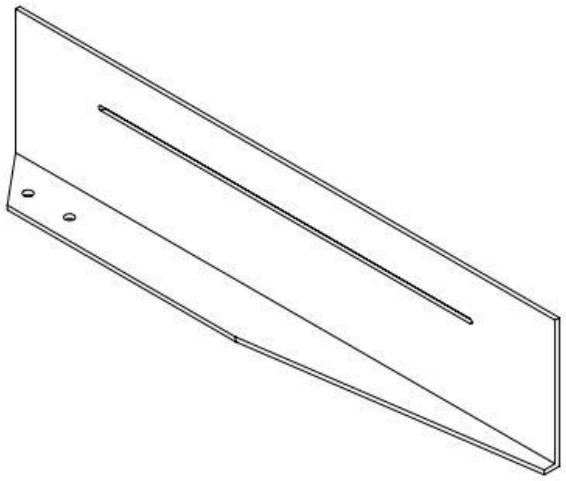

Fig. 3.13 Isometric view of counter cutting edge

3.2.3.2 Collecting pan

It is used to collect the harvested black pepper spikes immediately after the cut. This pan was made up of plastic material and attached to elbow link at an angle of 30 degrees to safely convey the harvested black pepper to the collecting hopper.

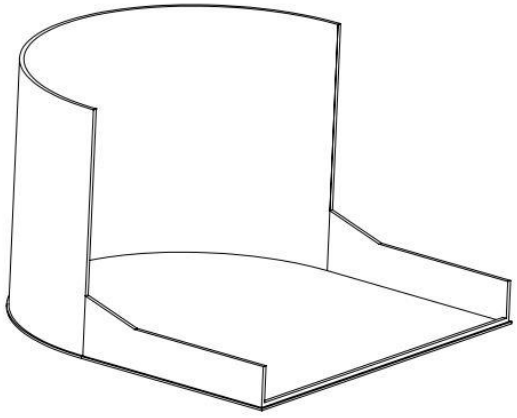

Fig. 3.14 Collecting pan

3.2.4 Control unit

The control unit include all the electrical components such as sensor, processor, servo motors, battery, and buck converters. The specifications of sensor, processor and servo motors were already explained. The details of buck converters and battery were discussed here,

3.2.4.1 Buck converter

It is used for converting main supply voltage such as 12 V, down to lower voltages needed by servo motors and raspberry pi. Shoulder joint requires 8 V, elbow joint requires 6 V, cutting motor requires 6 V, and raspberry pi with display unit requires 5 V input voltages. Two kind of buck converters were used in this work.

24V/12V to 5V 5A Power Module DC-DC XY-3606 power converter was used to step down voltage from 12 V to 5 V, for giving power to raspberry pi with the display unit. Only because of the presence of USB output, it was selected for powering raspberry pi. Its maximum working voltages ranges from 9 to 36 V and the output voltage was 5.2 V.

LM2596S DC-DC buck converter power supply was used for giving power supply to servo motors. It converts voltage from 12 V to 6 V and 8V required by the servo motors. Its input voltage ranges from 3 to 40 V and output voltage range from 1.5V to 35 V with an output current range of 2-3 A.

Plate 3.10 Buck converter

3.2.4.2 Battery

The battery for powering the robotic black pepper harvesting system was selected based on different criteria such as voltage rating, current rating and type of battery. The steps involved in selecting the battery is discussed here.

Current consumption of each and every electrical component were noted and was calculated the total current consumption. Here the electrical components are Raspberry pi 4 model B, 4.3 inch DSI LCD, USB camera, servo motors, and USB extension hub. Current consumption of each component is detailed below,

Raspberry pi with LCD display = 3 A

USB camera = 0.216 A

Servo motor (Shoulder joint) = 1 A

Servo motors (Elbow joint and cutting motor) = 1.2 A

Total current consumption = 5.416 A

Total time the robot have to work = 3 h

Assume that the robotic black pepper harvesting system need to run continuously for 3 h.

$$\text{Total Battery supply (Ah)} = \text{Time (h)} \times \text{Total current consumption (A)} \quad \ldots\ldots (3.9)$$

Total Battery supply $= 3 \times 5.416$

$= 16.248$ Ah

As per the calculations, the total battery supply should be 16.248 Ah. Based on the criteria described above two lead acid battery with voltage 12 V and current 9 Ah was selected. These batteries are connected in parallel to get an output of 18 Ah and 12 V. So the system can work continuously for 3.3 h.

The circuit diagram of robotic black pepper harvesting system is shown in figure 3.15.

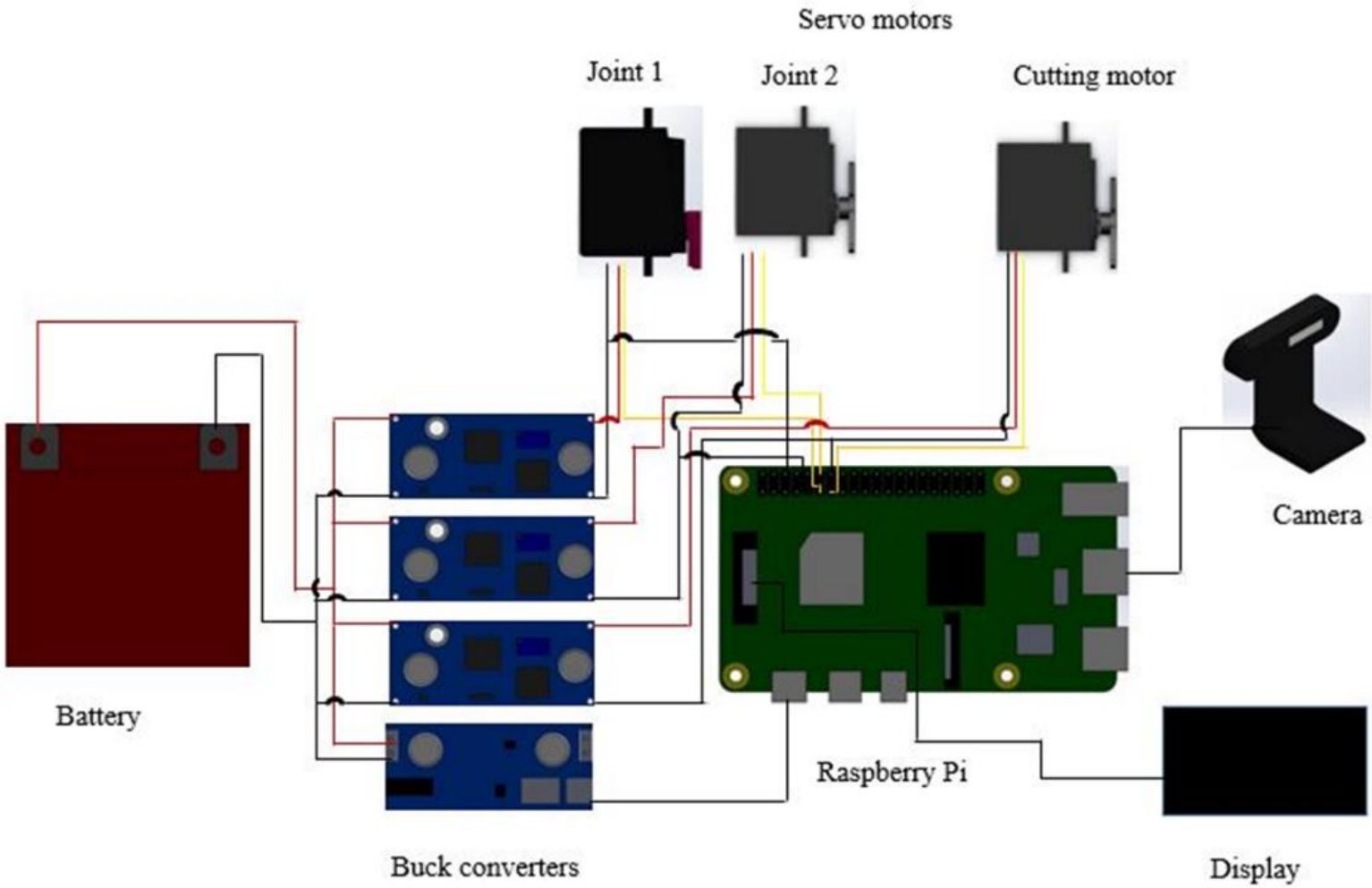

Fig. 3.15 Circuit diagram of robotic black pepper harvesting system

Servo motors have three input and two of them supply power to the motor and the third input controls how much the servo turns. To control the servo motor with Raspberry pi, connect the voltage and ground line of the servo to the external power supply and the remaining data wire to one of the GPIO pin of raspberry pi as shown in figure 3.16. The ground pin of every external power supply should be connected to the GND pin of Raspberry pi. In the selected servo motors, the red wire was the positive terminal, brown wire was the negative (ground) terminal and yellow wire was the data pin.

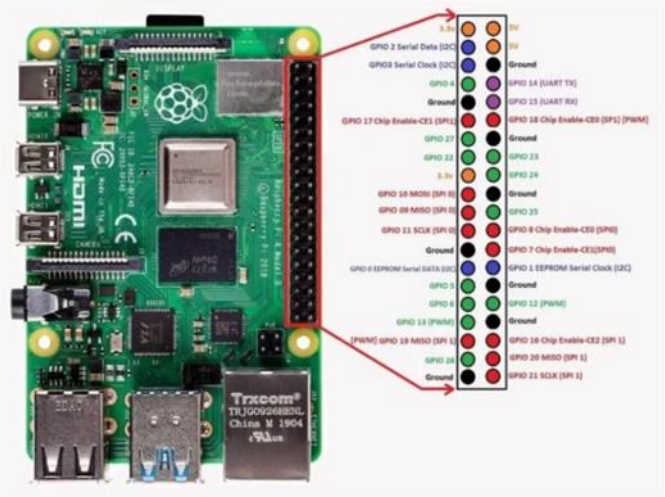

Fig 3.16 The pin configuration of Raspberry Pi 4 model B

There are three servo motors in the developed robotic black pepper harvesting system. Data pin of first servo motor (shoulder joint) was connected to the GPIO pin 11, second motor (Elbow joint) to the GPIO pin 12, and that of third motor (Cutting motor) to the GPIO pin 13. All the servo motors were controlled using the library RPi.GPIO installed on Raspberry pi.

Each servo motors were powered from two batteries connected in parallel having a voltage of 12 v and current of 18 Ah. But the voltage requirement for each servo motor was different. To step down the voltage from 12 v, different buck converters were used. The negative terminal of all the buck converters powering the servo motors were connected to the GND (Ground) pins 6, 9 and 14 of Raspberry Pi.

3.3 PERFORMANCE EVALUATION OF ROBOTIC BLACK PEPPER HARVESTING SYSTEM

The performance evaluation of the developed robotic black pepper harvesting system was carried out using the selected performance parameters. The developed system was evaluated for both the *Panniyur 1* and *Karimunda* variety of black pepper. This section has been subdivided in to two subheadings, performance evaluation of machine vision system and performance evaluation of robotic black pepper harvesting system. The performance of robotic black pepper harvesting system is also compared with existing method of harvesting.

3.3.1 Performance evaluation of machine vision system

The performance of machine vision system was evaluated by measuring sensitivity, specificity, and accuracy of the system and time taken for identification.

3.3.1.1 Sensitivity of the system

It is a statistical measure for the performance of a detection model. It measures the proportion of actual positives that are detected as such. It is also the rate of true positive. The maximum value of sensitivity for a good model is unity. It is calculated using following equation

$$\text{Sensitivity} = \frac{\text{Total true positives}}{\text{Total true positives} + \text{Total false negative}} \quad \ldots (3.10)$$

True Positive is when the object is present in the frame and the model detects it correctly. In this study, true positive is correctly identifying the matured pepper spike.

False negative is when the model incorrectly identifies the negative class in the frame. In this study, false negative is showing no detection when, there are positive objects in the frame.

3.3.1.2 Specificity of the system

It is another statistical measure for evaluating performance of a detection model. It measures the proportion of actual negatives that are correctly detected as such. It is also the true negative rate. The maximum value of specificity for a good model is unity. It is calculated as following equation

$$\text{Specificity} = \frac{\text{Total true negatives}}{\text{Total true negatives} + \text{Total false positives}} \quad \ldots (3.11)$$

True negative is when the model correctly identifies the negative class. In this study, true negative is identifying the negative objects in the frame.

False Positive is when the model incorrectly detects the positive class. In this study, false positive is incorrectly identifying the matured pepper spike in its absence.

3.3.1.3 Accuracy of the system

It is a statistical measure for consistency of the performance of developed model. It is the ratio of total number of true positives and true negatives to the total number of observations. It is calculated as following equation

$$\text{Accuracy} = \frac{\text{True positive} + \text{True negatives}}{\text{True positives} + \text{True negatives} + \text{False positives} + \text{False negatives}} \quad \ldots (3.12)$$

3.3.1.4 Time taken for identification

The time taken by the developed machine vision system for the detection of matured black pepper was calculated. The time taken for detection was measured using the written programming code.

3.3.2 Performance evaluation of robotic black pepper harvesting system

To evaluate the performance of robotic black pepper harvesting system in the field, capacity of the system, effectiveness index, time taken for cutting, time taken for the entire operation, harvesting loss and drying loss were measured.

3.3.2.1 Capacity

The capacity of the system is the amount of black pepper harvested per unit time. It is measured in kilogram per hour and number of spikes per hour. The time taken for one cycle of operation and the amount of black pepper spikes harvested in one cycle were measured. One cycle of operation include moving up of robotic arm, harvesting process and moving down of robotic arm. Time taken for transporting the system from one black pepper spike to the next black pepper spike was also include in one cycle time. Capacity of the developed system can be calculated using the equation,

$$\text{Capacity } (\text{kg h}^{-1}) = \frac{\text{Amount of black pepper spikes harvested during one cycle of operation}}{\text{Time taken for one cycle of operation}} \quad \ldots (3.13)$$

$$\text{Capacity (spikes h}^{-1}) = \frac{\text{Number of black pepper spikes harvested in one cycle of operation}}{\text{Time taken for one cycle of operation}} \quad \ldots (3.14)$$

3.3.2.2 Effectiveness index

It is the measure of percentage of matured pepper spikes harvested correctly. Select 10 black pepper spikes and operate the system for harvesting, then count the number of spikes harvested correctly. The effectiveness index is the ratio of number of matured black pepper spikes harvested correctly to the total number of selected black pepper spikes. It was expressed in percentage. Effectiveness index can be calculated using the equation,

$$\text{Effectiveness index of the system} = \frac{\text{Number of black pepper spikes harvested at correct maturity}}{\text{Total number of selected black pepper spikes}} \times 100 \quad \ldots (3.15)$$

3.3.2.3 Time taken for cutting

Time taken by the system for cutting and separating the identified matured black pepper spike from the plant was measured during the field test. The time taken by the servo motor to move the blade and make the cut was 0.18 seconds, it is fixed in the program. The blade take 36 degrees of rotation for making the cut.

3.3.2.4 Time taken for the entire operation

Time taken for both detection and harvesting of a single black pepper spike was measured during the field test. The test was carried out for 150 black pepper spikes. This time of operation include time for holding the system in proper position, time for detection and time for making the cut.

3.3.2.5 Harvesting loss

Harvesting loss include the amount of immature black pepper berries harvested. The harvesting loss can be calculated using the equation,

$$\text{Harvesting loss} = \frac{\text{Amount of under matured black pepper berries}}{\text{Total amount of black pepper berries harvested}} \times 100 \quad .. (3.16)$$

Harvesting loss was calculated immediately after the harvest of pepper berries.

3.3.2.6 Drying loss

It can be expressed as the weight loss in percentage of moisture escaped from the sample after drying. The moisture content of the samples of black pepper berries were measured immediately after harvesting and after sun drying. The Infrared moisture meter was used to measure the moisture content of the sample. The moisture content of the samples were occasionally measured to reduce it to 10 %, which is the safe moisture content for storage. Drying loss can be calculated using the equations,

$$\text{Drying loss} = \frac{\text{Initial weight - Weight after drying}}{\text{Initial Weight}} \times 100 \quad \ldots (3.17)$$

$$\text{Initial weight} - \text{Weight after drying} = \text{Bone dry matter} \times (\text{Initial moisture content (db) - Final moisture content (db)}) \quad \ldots (3.18)$$

(Sahay and Singh, 2001)

3.3.2.7 Statistical analysis

The t-test (Welch unpaired t-test) was carried out to find out the significant difference between existing method of harvesting and robotic black pepper harvester in terms of the capacity, effectiveness index, harvesting loss and drying loss at 5% level of significance. The statistical analysis was carried out with the help of KAU-GRAPES software.

Results and Discussion

CHAPTER IV

RESULTS AND DISCUSSION

The physical properties of black pepper, development of robotic black pepper harvesting system and performance evaluation of robotic black pepper harvesting system are explained in detail and the results are discussed in the chapter.

4.1 PHYSICAL PROPERTIES

The physical properties of black pepper were studied in two varieties of pepper such as *Karimunda* and *Panniyur 1*. The studied properties include length of spikes, diameter of spikes, weight of spikes, colour of berries, diameter of berries, length of the peduncle, diameter of the peduncle, shear strength of pepper peduncle, and leaf coverage of black pepper vine. The result obtained in the study is shown in the Table 4.1

Table 4.1 Physical properties of black pepper

Sl. no	**Property**	***Karimunda***			***Panniyur 1***		
		Range	Average	Standard deviation	Range	Average	Standard deviation
1	Length of spikes, cm	4.5-13.8	10.4	1.9	7.0-18.0	12.8	2.4
2	Diameter of spikes, cm	0.77-1.3	1.1	0.13	0.86-1.7	1.3	0.17
3	Weight of spikes, g	2.1– 13.6	7.8	2.6	3.8- 17.1	10.1	3.1
4	Colour of berries	(20, 39, 3) - (255, 224, 111)			(35, 54, 10)–(255, 240, 100)		
5	Diameter of berries, cm	0.3– 0.5	0.42	0.07	0.45– 0.7	0.59	0.09

Table 4.1 Continued

Sl. no	**Property**	***Karimunda***			***Panniyur 1***		
		Range	Average	Standard deviation	Range	Average	Standard deviation
6	Length of the peduncle, cm	0.4-2.1	1.2	0.37	0.8 -30	1.3	0.34
7	Diameter of the peduncle, cm	0.1 - 0.20	0.17	0.03	0.1 - 0.15	0.17	0.14
8	Shear strength of pepper peduncle, N mm^{-2}						
	Cutting speed, 0.1 mm s^{-1}	1098-3987	1718.6	647	1090-3313	1671.0	515
	Cutting speed, 1 mm s^{-1}	981-3664	1535.1	589	998-3809	1544.5	606
9	Leaf coverage of black pepper vine, cm						
	Leaf coverage		10.00 - 91.00		45.3	15.3	
	95th percentile of data		76.00				

4.1.1 Length of spikes

From the data as shown in Table 4.1, the *Karimunda* variety was having a length of about 4.5-13.8 cm and *Panniyur 1* was having a length of 7.0-18.0 cm excluding the peduncle. For *Karimunda* variety, an average length (without peduncle) of 10.4 cm was obtained and in *Panniyur 1* variety, an average length (without peduncle) of 12.8 cm was obtained. *Panniyur 1* variety was having more length than *Karimunda*. Appendix VIII shows all the replications of the length of the spikes.

4.1.2 Diameter of spikes

From the Table 4.1, it is observed that, in the *Karimunda* variety, minimum diameter was 0.77 cm and maximum diameter was 1.30 cm. In case of *Panniyur 1* variety the minimum diameter found was 0.86 cm and maximum diameter was 1.70 cm. The average diameter of the *Karimunda* variety was obtained as 1.10 cm and *Panniyur 1* variety had 1.30 cm. From the results, it was found that in case of diameter of spikes *Panniyur 1* variety is larger than *Karimunda*. All the replications are depicted in the appendix IX.

4.1.3 Weight of spikes

In *Karimunda* variety, minimum weight of the pepper spike was 2.1 g and maximum weight was 13.6 g. In case of *Panniyur 1* variety, weight of the spike ranges from 3.8 g to 17.1 g. From the Table 4.1, it is observed that, the average weight of spike in *Karimunda* variety was 7.8 g and *Panniyur 1* variety was 10.1 g. The result showed that, the spike's weight of *Panniyur 1* is higher than that of *Karimunda* variety. All the replications are depicted in the appendix X

4.1.4 Colour of berries

The colour of the matured black pepper was measured using the RGB value. The RGB value of colour image ranges from [0, 0, 0] to [255, 255, 255]. From the observations, it was found that the RGB values for *Karimunda* variety ranged from (20, 39, 3) and (255, 224, 111) and in *Panniyur 1* variety, value ranged from (35, 54, 10) - (255, 240, 100). On evaluating using a python module, it was found that RGB value of matured black pepper spikes is ranging from (20, 39, 3) to (255, 240, 100). All the readings are shown in the appendix XI.

4.1.5 Diameter of berries

For *Karimunda* variety, minimum diameter of berry was 0.30 cm and maximum diameter was 0.50 cm. In case of *Panniyur 1* variety, minimum was 0.45 cm and maximum was 0.70 cm. The average diameter of *Karimunda* was 0.42 cm and *Panniyur 1* was 0.59 cm. The diameter of berries of *Panniyur 1* variety

was larger than *Karimunda*. Appendix XII shows all the replications of the diameter of berries.

4.1.6 Length of the peduncle

For *Karimunda* variety, minimum peduncle length was 0.40 cm and maximum peduncle length was 2.10 cm. In case of *Panniyur 1* variety the minimum peduncle length was 0.80 cm and maximum peduncle length was 3.00 cm. The average peduncle length of *Karimunda* variety was obtained as 1.20 cm and *Panniyur 1* variety was 1.30 cm. From the results, it was found that *Panniyur 1* variety having more peduncle length than *Karimunda* variety. Appendix XIII shows the length of the peduncle data.

4.1.7 Diameter of the peduncle

In the *Karimunda* variety, minimum diameter of peduncle was 0.10 cm and maximum diameter of peduncle was 0.20 cm. In case of *Panniyur* 1 variety the minimum peduncle diameter was 0.10 cm and maximum peduncle diameter was 0.15 cm. The average peduncle diameter of *Karimunda* variety was obtained as 0.17 cm and *Panniyur 1* variety as 0.17 cm. From the results, it was found that both *Karimunda* and *Panniyur1* variety having same peduncle diameter. Appendix XIV provides all the replications of the peduncle diameter.

4.1.8 Shear strength of the peduncle

The shear strength of the peduncle of black pepper spike was obtained from the texture analyzer data. The shear strength of the peduncle at a cutting speed (shear velocity) of 0.1 mm s^{-1} obtained as 1718.58 N mm^{-2} for *Karimunda* variety and 1671 N mm^{-2} for *Panniyur* 1 variety. At a cutting speed (shear velocity) of 1 mm s^{-1}, shear strength obtained as 1535.06 N mm^{-2} for *Karimunda* variety and 1544.50 N mm^{-2} for *Panniyur 1* variety as shown in Table 4.1. And the appendix XV shows all the replications of shear strength calculation.

4.1.10 Leaf coverage of black pepper vine

From the Table 4.1, it is observed that, the maximum leaf coverage of black pepper vine ranges from 10 cm to 91 cm. The 95th percentile of the data was 76cm. All the replications of leaf coverage of black pepper and calculations are depicted in the appendix XVI.

From the result it was observed that, the *Panniyur 1* variety is having higher spike length, spike diameter, spike weight, peduncle length and berry diameter than the *Karimunda* variety. Peduncle diameter is almost same for both the varieties. Shear strength of both the varieties are almost same, resulting in no change in the force requirement for cutting the peduncle of the pepper spike.

4.2 DEVELOPMENT OF ROBOTIC BLACK PEPPER HARVESTING SYSTEM

Based on the data obtained for the properties of black pepper, a robotic black pepper harvesting system was developed. The system comprised of a machine vision system, manipulator, end-effector and a control unit.

4.2.1 Machine vision system

The machine vision system consist of a USB webcam as sensor, Raspberry pi 4 model B as processor and Raspberry pi LCD module as display unit as shown in plate 4.1. The detection was made in TensorFlow-Faster RCNN platform and the program was written in python language. Python IDE “Thonny” was used for writing and executing the program**.**

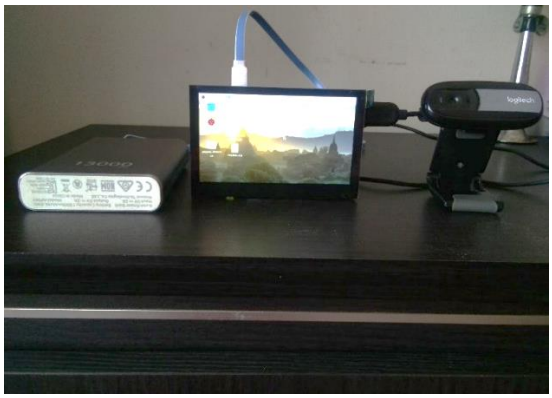

Plate 4.1 Machine vision system

Modification were done in the computer program of machine vision system to identify matured black pepper spikes. The modified programming code is given below,

```
import tensorflow as tf

import os

import cv2

tf.gfile = tf.io.gfile

import time

# Enable Eager Execution for Tensorflow Version < 2

tf.compat.v1.enable_eager_execution()

from object_detection.utils import ops as utils_ops

from object_detection.utils import label_map_util

from object_detction.utils import visualization_utils as
vis_util

import pathlib

import numpy as np

from IPyton.display import clear_output

import time

import pil.Image

from io import BytesIO

import IPython.display

from matpltlib import pyplot as plt

os.environ['PYTHONPATH']='/home/pi/Desktop/pepper_detec
tion/models-master/research'
```

```
MODEL_PATH='/home/pi/Desktop/pepper_detection/mobile_saved_model'
LABEL_PATH='/home/pi/Desktop/pepper_detection/saved_model/label_map.pbtxt'
def load_model(model_name):
    model_dir = model_name
    model_dir = pathlib.Path(model_dir)
    print(model_dir)
    model=tf.compat.v2.saved_model.load(str(model_dir))
    model = model.signatures['serving_default']
    return model
t1 = time.time()
model = load_model(MODEL_PATH)
PATH_TO_LABELS = LABEL_PATH
category_index=label_map_util.create_category_index_from_labelmap(PATH_TO_LABELS, use_display_name=True)
t2 = time.time()
time_taken = t2 - t1
print(f"Time taken to load model : {time_taken} sec")
def run_inference_for_single_image(model, image):
    image = np.asarray(image)
    # The input needs to be a tensor, convert it using `tf.convert_to_tensor`.
    input_tensor = tf.cnvert_to_tensor(image)
    # The model expects a batch of images, so add an axis with `tf.newaxis`.
```

```
input_tensor = input_tensor[tf.newaxis,...]
# Run inference
output_dict = model(input_tensor)


# All outputs are batches tensors.
# Convert to numpy arrays, and take index [0] to
remove the batch dimension.
# We're only interested in the first num_detections.
num_detections=int(output_dict.pop('num_detections'
))
output_dict={key  value[0,  :num_detections].numpy()
for key,value in output_dict.items()}
output_dict['num_detections'] = num_detections
# detection_classes should be ints.
output_dict['detection_classes']=output_dict['detec
tion_classes'].astype(np.int64)
#pdb.set_trace()
# Handle models with masks:
if 'detection_masks' in output_dict:
    # Reframe the the bbox mask to the image size.
    detectionmasks_reframed=utils_ops.reframe_box_m
    asksto_image_masks(out_dict['detection_masks'],
    output_dict['detection_boxes'],image.shape[0],
    image.shape[1])
    detection_masksreframed=tf.cast(detection_masks
    _reframed > 0.6, tf.uint8)
```

```
        output_dict['detection_masks_reframed']=detecti
        on_masks_reframed.numpy()
    return output_dict
#Use 'jpeg' instead of 'png' (~5 times faster)
def array_to_image(a, fmt='jpeg'):
     #Create binary stream object
     f = BytesIO()
     #Convert array to binary stream object
     PIL.Image.fromarray(a).save(f, fmt)
     return IPython.display.Image(data=f.getvalue())
    VIDEO_PATH='/home/pi/Downloads/PEPPER RED_0001.mpg'
cam = cv2.VideoCapture(0)
#d = IPython.display("",display_id=3)
#d2 = IPthon.display.display("",display_id=4)
import matpltlib.pyplot as plt
time_per_frame = []
while True:
    try:
    t1 = time.time()
    ret, frame = cam.read()
    frame=cv2.cvtColor(frame, cv2.COLOR_BGR2RGB)
    output_dict=  run_inference_for_single_image(model,
    frame)
    vis_util.visualize_boxes_and_labels_on_image_array
    output_dict['detection_boxes'],
```

```
            output_dict['detection_classes'],
            output_dict['detection_scores'],
            category_index,
            instance_masks=output_dict.get('detection_masks
            _reframed', None),
            use_normalized_coordinates=True,
            line_thickness=7,
            min_score_thresh=0.55)
        im = array_to_image(frame)
        p1 = plt.imshow(frame)
        cv2.imshow('bklah',cv2.cvtColor(frame,cv2.COLOR_RGB
        2BGR))
        boxes = output_dict['detection_boxes']
        max_boxes_to_draw = boxes.shape[0]
        scores = output_dict['detection_scores']
        min_score_thresh=.55
        classes = output_dict['detection_classes']
        if cv2.waitKey(1) & 0xFF == ord('q'):
            break
        t2 = time.time()
        time_taken = t2-t1
        time_per_frame.append(time_taken)
        s = f"""{int(1/(time_taken))} FPS"""
    except KeyboardInterrupt:
        print()
```

```
cam.release()
IPython.display.clear_output()
print ("Stream stopped")
print(f"Average time taken: {round
(np.mean(time_per_frame), 2)}seconds”)
break
```

The plate 4.2 represents the real time detection of matured black pepper spike by the modified machine vision system.

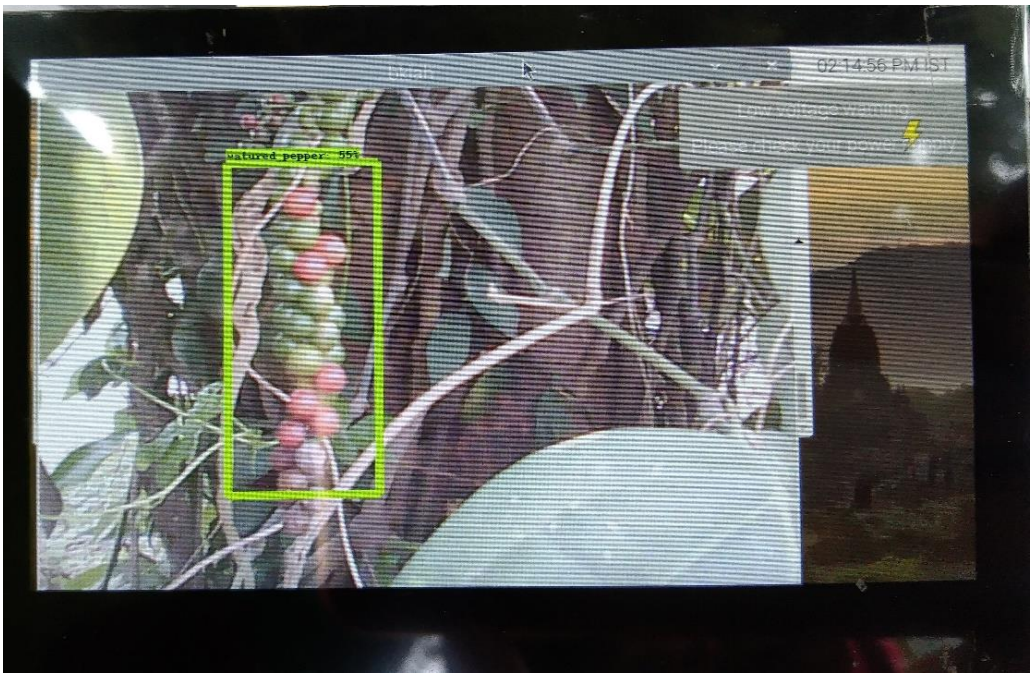

Plate 4.2 Real time detection of matured black pepper spike

4.2.2 Manipulator

The developed manipulator has 2 DOF and the joints are actuated by servo motors. From the Table 4.2, it is observed that, the torque required for the elbow joint is 0.28 N m, so TowerPro MG996R digital high torque servomotor with a stall torque of 1.1 N m is used to actuate elbow joint. And the torque required for shoulder joint is 1.583 N m, so Ultra torque quarter scale servo motor with a stall torque of 6 N m is used to actuate shoulder joint. The servo motors actuate the links

at an angular velocity of 20 degree per second. For moving up the manipulator to action position, shoulder link rotates from 162 degree to 90 degree for lifting the shoulder link 72 degree up and elbow joint hold elbow link in 90 degree. For moving down the manipulator to the home position, the shoulder joint rotates from 90 degree to 162 degree for moving down the shoulder link. For moving down the elbow link, the elbow joint rotates from 90 degree to 18 degree. And for dropping the harvested pepper spike directly to the collecting hopper and conveying system, the elbow rotates again from 18 degree to 144 degree because the collecting pan was attached to elbow link. The Fig. 4.1 represents the direction of motion of shoulder and elbow joints in the manipulator. The shoulder and elbow joint take 69 seconds to move from the home position to the action position. And the joints take 80 seconds to return to the home position after dropping the spike into the collecting unit.

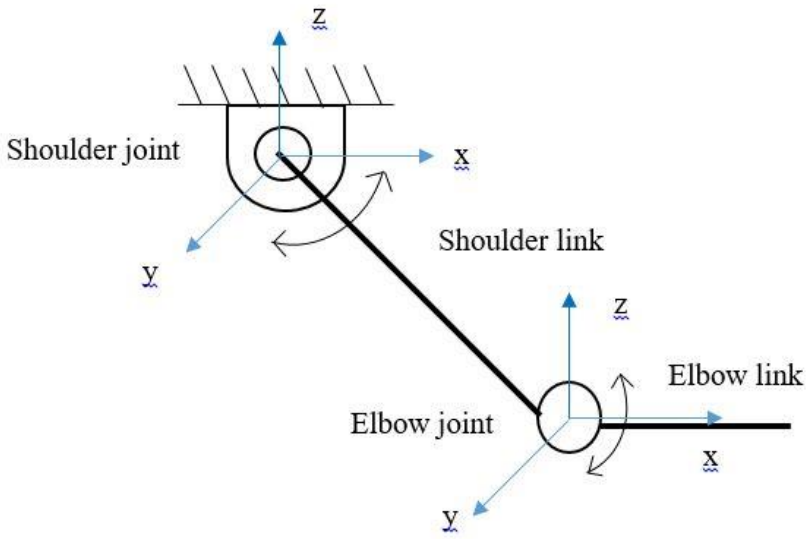

Fig. 4.1 Line diagram representing the movements of joints in the manipulator

Table 4.2 Joints specifications

Sl. No.	Joint	Speed, (rpm)	Static torque, N m	Dynamic torque, N m	Torque, N m
1	Shoulder joint	3.33	1.5	0.083	1.583
2	Elbow joint	3.33	0.275	0.00475	0.28

Table 4.3 Link specifications

Sl. No.	Link	Dimension (cm) Length× Width ×Height	Weight, g	Material
1	Shoulder link	300 × 31.75 × 31.75	117	Aluminium
2	Elbow link	135 × 61.5× 38.1	60.3	Aluminium

4.2.3 End effector

The end-effector consist of cutting unit, and collecting pan. The specification of the components are shown in Table 4.4. Shear cut of the blade is actuated by a TowerPro MG996R servo motor having a stall torque of 1.1 N m. The cutting blade cut the peduncle at a speed of 17.5 mm s^{-1}. The servo motor actuating the cutting blade was capable for providing necessary force to cut the peduncle of black pepper spikes at a speed of 17.5 mm s^{-1}. Fig. 4.2 shows the direction of motion of the cutting blade in the end effector.

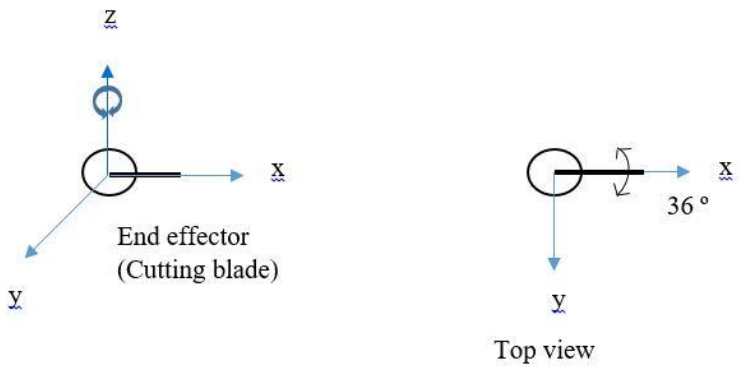

Fig. 4. 2 Line diagram represents the direction of motion of cutting blade in the end effector.

Table 4.4 Specification of cutting unit and collecting pan

Sl. No.	Parameter	Specification
1	Cutting blade	
	Length × Width × Thickness, cm	14 × 1×0.1
2	Counter cutting edge	
	Length× Width × Height, cm	13 ×0.1 × 3
3	Collecting pan	
	Length × Width × Height	20 × 18.5 × 12

Plate 4.3 End-effector

The specification of developed robotic black pepper harvesting system is shown in the Table 4.5

Table 4.5 Specification of robotic black pepper harvesting system

Sl. No.	Particulars	Dimensions
1	Overall dimensions	
	Length × width × height, cm	59 × 18 × 162
	Weight of the system, kg	2.1
	Power requirement of the system, watt	32.4
	Degree of freedom (DOF)	(2-DOF manipulator + 1-DOF end-effector)
	Power supply	12 V, 18 Ah lead acid battery
	Material	Aluminium, PVC, steel, plastic
2	Specification of manipulator	
	Reach, cm	51.5
	Number of links	2
	Degree of freedom (DOF)	2
	Type of joints	Revolute joints
	Material	Aluminium
3	Specification of end-effector	
	Degree of freedom (DOF)	1
	Type of cutting mechanism	Shear cut
	Length × width × height, cm	20 × 18 × 19
4	Specification of collecting hopper and conveying unit	
	Upper diameter of collecting hopper, cm	21
	Bottom diameter of collecting hopper, cm	15
	Height of collecting hopper, cm	10
	Diameter of conveying unit, cm	15
	Length of conveying unit, cm	100
	Material of conveying unit	Fabric
5	Specification of supporting rod	
	Height of the supporting rod, cm	1500
	Inner diameter of supporting rod, cm	2.43
	Outer diameter of supporting rod, cm	3.34
	Material	PVC

(A) (B)

Plate 4.4 Developed robotic black pepper harvesting system: (A) Home position, (B) Action position

4.2.4 Control unit

The program for actuating the servo motors at shoulder joint, elbow joint and end effector were written in python language. The program was written and executed in python IDE "Thonny". The computer program for controlling the manipulator and end effector by actuating the servo motors are discussed here,

4.2.4.1 Computer program for moving up the manipulator

The computer program for moving the manipulator up by controlling the servo motors at shoulder joint and elbow joint is given below.

```
import RPi.GPIO as GPIO
import time
f=0
s=0
fServoPin = 11
sServoPin = 12
GPIO.setmode(GPIO.BOARD)
GPIO.setup(fServoPin,GPIO.OUT)
GPIO.setup(sServoPin,GPIO.OUT)
fpwm = GPIO.PWM(fservoPin,50)
spwm = GPIO.PWM(sservoPin,50)
fpwm.start(11)
spwm.start(7)
for i in range(162,90,-1):
    positionf=1./18.*(i)+1
    fpwm.Changedutycycle(positionf)
    time.sleep(0.1)
fpwm.stop()
```

4.2.4.2 Computer program for moving down the manipulator

The computer program for moving the manipulator down by controlling the shoulder joint and elbow joint is shown below.

```
import RPi.GPIO as GPIO
import time
f=0
s=0
fServoPin = 11
sServoPin = 12
GPIO.setmode(GPIO.BOARD)
GPIO.setup(fservoPin,GPIO.OUT)
GPIO.setup(sservoPin,GPIO.OUT)
fpwm = GPIO.PWM(fServoPin,50)
spwm = GPIO.PWM(sServoPin,50)
fpwm.start(7)
spwm.start(7)
for i in range(90,108,+1):
    positionf=1./18.*(i)+1
    fpwm.Changedutycycle(positionf)
    time.sleep(0.05)
for i in range(90,72,-1):
    positions=1./18.*(i)+1
    spwm.ChangeDutyCycle(positions)
    time.sleep(0.05)
for i in range(108,126,+1):
    positionf=1./18.*(i)+1
    fpwm.Changedutycycle(positionf)
    time.sleep(0.05)
for i in range(72,54,-1):
    positions=1./18.*(i)+1
    spwm.Changedutycycle(positions)
    time.sleep(0.05)
```

```
for i in range(126,144,+1):
    positionf=1./18.*(i)+1
    fpwm.Changedutycycle(positionf)
    time.sleep(0.05)
for i in range(54,36,-1):
    positions=1./18.*(i)+1
    spwm.Changedutycycle(positions)
    time.sleep(0.05)
for i in range(144,162,+1):
    positionf=1./18.*(i)+1
    fpwm.Changedutycycle(positionf)
    time.sleep(0.05)
for i in range(36,18,-1):
    positions=1./18.*(i)+1
    spwm.Changedutycycle(positions)
    time.sleep(0.05)
for i in range(18,144,+1):
    positions=1./18.*(i)+1
    spwm.Changedutycycle(positions)
    time.sleep(0.05)
fpwm.stop()
spwm.stop()
```

4.2.4.3 Computer program for controlling end-effector

Computer program for controlling the servomotor connected to the cutting blade while identifying matured black pepper spikes is shown below.

```
import tensorflow as tf
import os
import cv2
```

```
tf.gfile = tf.io.gfile
import RPi.GPIO as GPIO
import time
# Enable Eager Execution for Tensorflow Version < 2
tf.compat.v1.enable_eager_execution()
from object_detection.utils import ops as utils_ops
from object_detection.utils import label_map_util
from object_detection.utils import visualization_utils
as vis_util
import pathlib
import numpy as np
from IPython.display import clear_output
import time
import PIL.Image
from io import BytesIO
import IPython.display
from matpltlib import pyplt as plt
# Function to control the servomotor attached to the
cutting unit.
def actuate_servo():
    GPIO.setmode(GPIO.BOARD)
    servopin=13
    GPIO.setup(servopin,GPIO.OUT)
    pwm=GPIO.PWM(servopin,50)
    pwm.start(6)
```

```
    for i in range(72,36,-1):
        position=(1./18.)*i + 1
        pwm.Changedutycycle(position)
        time.sleep(0.005)
    for i in range(36,72,+1):
        position=(1./18.)*i + 1
        pwm.Changedutycycle(position)
        time.sleep(0.005)
    pwm.stop()
os.environ['PYTHONPATH']='/home/pi/Desktop/pepper_detection/models-master/research'
MODEL_PATH='/home/pi/Desktop/pepper_detection/mobile_saved_model'
LABEL_PATH='/home/pi/Desktop/pepper_detection/saved_model/label_map.pbtxt'
def load_model(model_name):
    model_dir = model_name
    model_dir = pathlib.Path(model_dir)
    print(model_dir)
    model=tf.compat.v2.saved_model.load(str(model_dir))
    model = model.signatures['serving_default']
    return model
t1 = time.time()
model = load_model(MODEL_PATH)
#warm up
```

```
#input_tensor = tf.convert_to_tensor(np.ones((500, 500, 3), dtype='uint8'))
# model(input_tensor)
PATH_TO_LABELS = LABEL_PATH
category_index=label_map_util.create_category_index_from_labelmap(PATH_TO_LABELS, use_display_name=True)
t2 = time.time()
time_taken = t2 - t1
print(f"Time taken to load model : {time_taken} sec")
def run_inference_for_single_image(model, image):
    image = np.asarray(image)
# The input needs to be a tensor, convert it using `tf.convert_to_tensor`.
    input_tensor = tf.convert_to_tensor(image)
# The model expects a batch of images, so add an axis with `tf.newaxis`.
    input_tensor = input_tensor[tf.newaxis,...]
# Run inference
    output_dict = model(input_tensor)
# All outputs are batches tensors.
# Convert to numpy arrays, and take index [0] to remove the batch dimension.
# We're only interested in the first num_detections.
    num_detections=int(output_dict.pop('num_detections'))
```

```
    output_dict={key:value[0,:num_detections].numpy()fo
    r key,value in output_dict.items()}
    output_dict['num_detections'] = num_detections
# detection_classes should be ints.
    output_dict['detection_classes']=output_dict['detec
    tion_classes'].astype(np.int64)
#pdb.set_trace()
# Handle models with masks:
    if 'detection_masks' in output_dict:
        # Reframe the the bbox mask to the image size.
        detection_masks_reframed=utils_ops.reframe_box_
        masks
        to_image_masks(output_dict['detection_masks'],
        output_dict['detection_boxes'],image.shape[0],
        image.shape[1])
        detection_masks_reframed=tf.cast(detection_mask
        s_reframed > 0.6, tf.uint8)
        output_dict['detection_masks_reframed']=detecti
        on_masks_reframed.numpy()
    return output_dict
#Use 'jpeg' instead of 'png' (~5 times faster)
def array_to_image(a, fmt='jpeg'):
    #Create binary stream object
    f = BytesIO()
    #Convert array to binary stream object
    PIL.Image.fromarray(a).save(f, fmt)
```

```
    return IPython.display.Image(data=f.getvalue())
    VIDEO_PATH='/home/pi/Downloads/PEPPER RED_0001.mpg'
cam = cv2.VideoCapture(0)
#d = IPython.display("",display_id=3)
#d2 = IPthon.display.display("",display_id=4)
import matpltlib.pyplt as plt
time_per_frame = []
while True:
    try:
        t1 = time.time()
        ret, frame = cam.read()
        frame = cv2.cvtColor(frame, cv2.COLOR_BGR2RGB)
        output_dict=run_inference_for_single_image(mod
        el,frame)
        vis_util.visualize_boxes_and_labels_on_image_a
        rray( frame,output_dict['detection_boxes'],
       output_dict['detection_classes'],
       output_dict['detection_scores'],
       category_index,
       instance_masks=output_dict.get('detection_masks
       _reframed', None),
       use_normalized_coordinates=True,
       line_thickness=7,
       min_score_thresh=0.55)
       im = array_to_image(frame)
```

```
            p1=plt.imshow(frame)
            cv2.imshow('bklah',cv2.cvtColor(frame,cv2.COLOR
            _RGB2BGR))
            boxes = output_dict['detection_boxes']
            max_boxes_to_draw = boxes.shape[0]
            scores = output_dict['detection_scores']
            min_score_thresh=.55
            classes = output_dict['detection_classes']
            # classes_size = 1
# Servomotor get actuated when it detect a matured black
pepper spike.
        for i in range(classes.size):
            if(classes[i]==1and
            scotes[i]>min_score_thresh):
                actuate_servo()
            else:
                print('Move to next position')
        if cv2.waitKey(1) & 0xFF == ord('q'):
            break
        t2 = time.time()
        time_taken = t2-t1
        time_per_frame.append(time_taken)
        s = f"""{int(1/(time_taken))} FPS"""
        #d2.update(Ipython.display.HTML(s))
except KeyboardInterrupt:
```

```
        print()
        cam.release()
        IPython.display.clear_output()
        print ("Stream stopped")
        print(f"Average                                    time
    taken:{round(np.mean(time_per_frame), 2)} seconds")
        break
    GPIO.cleanup()
```

4.2.5 Working

The main components of robotic black pepper harvesting system are, machine vision system for the identification of matured black pepper spikes, manipulator with 2 DOF, end-effector to make the harvesting, and a control unit.

Switch on the battery for starting the system. Initially the system take almost 2 minutes for booting the raspberry pi. Then open a terminal and execute the code for running the program. It has three programming code. First code for the detection of matured black pepper spike and also to actuate the servo motor connected to the cutting blade assembly. The cutting action of the end-effector occurs automatically when it detects a matured black pepper spike. The second program was for actuating the shoulder joint and elbow joint together to move the arm upwards. The third program for moving down the arm and dropping the harvested pepper spike to the conveying unit by actuating shoulder joint and elbow joint together.

Code to execute first program (To actuate machine vision system and end-effector)

cd Desktop/pepper_detection/models-master/research

python3 machine_vision.py

Code to execute second program (To moving the arm upward)

cd Desktop/pepper_detection/models-master/research

sudo python servo12up.py

Code to execute third program (To moving down the arm and dropping the harvested pepper spikes to the conveying unit)

cd Desktop/pepper_detection/models-master/research

sudo python servo12down.py

First run the code of machine vision system, then a new window will appear. Through which the cutting blade and pepper spikes can be monitored from the ground itself. It take almost one minute to execute this program. Then run the code for lifting the robotic arm upward. The arm move at a speed of 20º per second. Then hold the entire system in front of each black pepper spikes manually. The system will identify whether the black pepper spike is matured or not. If it identify a matured black pepper spike, the servo motor connected to the cutting blade assembly will actuate and move the blade from its 0º to 36º and return back to 0º. The angle between the cutting blade and counter cutting edge was 36º. If the system identifies a green black pepper, the message "move to the next position" will be displayed on the screen as shown in plate 4.5. After continuously harvesting almost 25 spikes, run the third code to move down the robotic arm to the home position and drop it to the conveying unit. Then the harvested black pepper spikes can be directly collecting in a sack or container held below the conveying unit. This is the one cycle of harvesting. Repeat this same procedure for continuing the harvesting process. But from the second cycle onwards the program can be run simply by pressing the up arrow key and the enter key on the keyboard. After completing the harvesting process, shutdown the Raspberry pi and switch off the power supply.

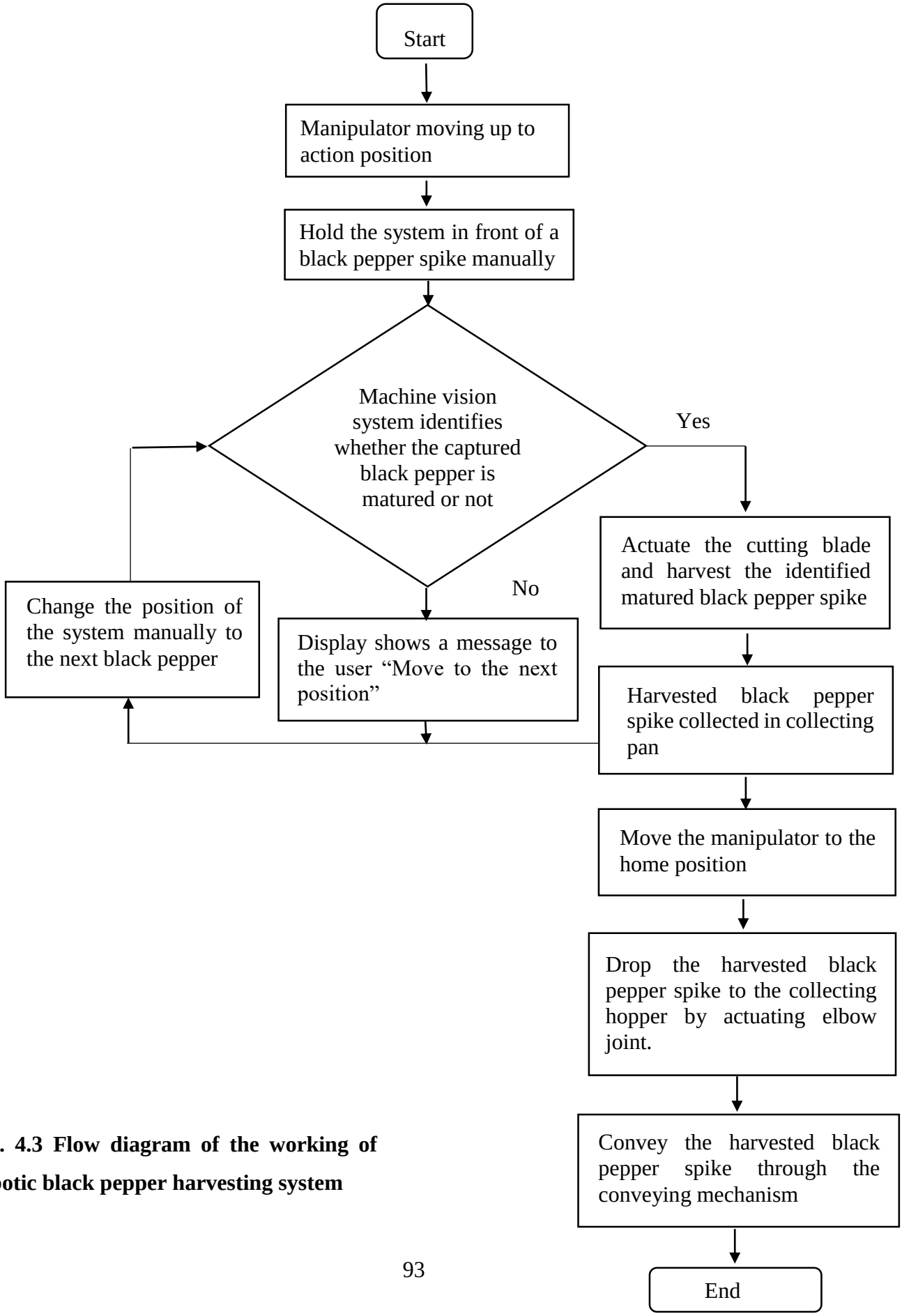

Fig. 4.3 Flow diagram of the working of robotic black pepper harvesting system

Plate 4.5 Display showing the message to change the position

The developed robotic black pepper harvesting system has a machine vision system with TensorFlow-faster RCNN as a detection platform, a camera as a sensor, raspberry pi as processor and a display unit, a manipulator with two degrees of freedom, an end effector with a cutting unit and collecting pan, and a control unit. The processor raspberry pi controlled the whole system through programming codes written in python language, and the system was powered by a 12 V, 18 Ah battery power supply.

4.3 PERFORMANCE EVALUATION OF ROBOTIC BLACK PEPPER HARVESTING SYSTEM

The developed robotic black pepper harvesting system was evaluated for their performance are discussed below and the sample calculations are shown in appendices.

4.3.1 Performance evaluation of machine vision system

The modified machine vision system for the identification of matured black pepper spike was evaluated for their performance in two varieties of black pepper such as *Karimunda* and *Panniyur1*, are discussed here. The performance of machine vision system is shown in Table 4.6 and the sample calculations are shown in appendix XVII.

Table 4.6. Performance evaluation of machine vision system

Sl. No.	Parameter	Varieties	
		Karimunda	***Panniyur 1***
1	True positives (TP)	55	59
2	True negatives (TN)	27	23
3	False positives (FP)	8	7
4	False negatives (FN)	10	11
5	Sensitivity, %	85	84
6	Specificity, %	77	77
7	Accuracy, %	82	82
8	Time taken for identification, seconds	0.43	0.43

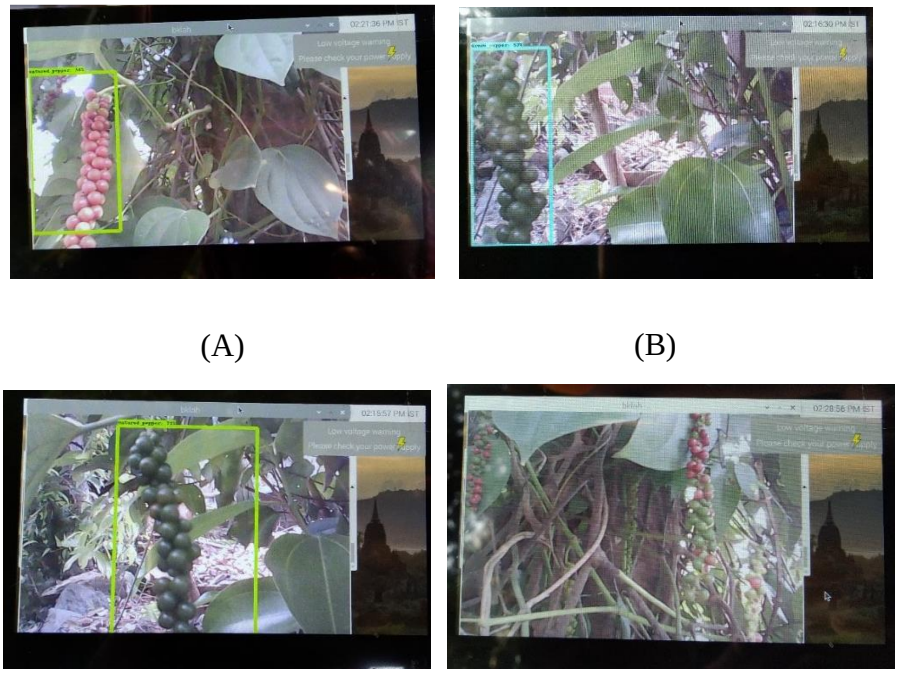

(A) (B)

(C) (D)

Plate 4.6 Performance evaluation of machine vision system to identify matured black pepper spikes: (A) True positive, (B) True negative, (C) False positive, (D) False negative

4.3.1.1 Sensitivity of the system

The performance evaluation of modified machine vision system for identifying matured black pepper spikes in TensorFlow-FasterRCNN platform, with two varieties of black pepper such as *Karimunda* and *Panniyur 1* is shown in Table 4.6. The sensitivity of the system in *Karimunda* variety was 85 % and in *Panniyur 1* variety was 84 %. The result showed that there is no significant difference between the sensitivity of machine vision system in both *Karimunda* and *Panniyur 1* variety. In the study conducted by Meera (2020) explained in article 2.2, the sensitivity of the developed machine vision system for identifying matured black pepper spike obtained as 78 %. The modified machine vision system has higher sensitivity than the system developed by Meera (2020). Also the modified machine vision system has high sensitivity than the work done by Gan *et al*. (2018).

4.3.1.2 Specificity of the system

The system were evaluated with two varieties of black pepper such as *Karimunda* and *Panniyur 1*. Table 4.6 showed that the specificity of the system in both *Karimunda* variety and *Panniyur 1* variety was 77 %. In the similar study conducted by Meera (2020) explained in article 2.2, specificity of the developed machine vision system to identify matured black pepper spikes obtained as 71 %. The modified machine vision system has higher specificity than the previous work done by Meera (2020), so the robotic black pepper harvesting system based on this system will be able to have less harvesting loss.

4.3.1.3 Accuracy of the system

The system was evaluated for two varieties of black pepper such as *Karimunda* and *Panniyur 1*. From the Table 4.7 it was clear that the accuracy of the system in both *Karimunda* and *Panniyur 1* variety was 82 %. In the study done by Meera (2020, the accuracy of the developed machine vision system to identify matured black pepper spikes obtained as 75 %. Modified machine vision shows higher accuracy as compared to the previous system developed by Meera (2020). The modified machine vision system has higher accuracy than the work done by Zhang *et al*., (2020).

4.3.1.4 Time taken for identification

For the performance evaluation of modified machine vision system, the time taken for detection was also measured for both *Karimunda* and *Panniyur 1* variety. For *Karimunda* variety time for detection ranged from 0.41 to 0.46 seconds, and the average time taken was 0.43 seconds. In the case of *Panniyur1* variety, time for detection ranged from 0.41 to 0.46 seconds, and the average time for detection was 0.43 seconds. It indicated that the time for detection does not vary with the variety of black pepper. In the study done by Meera (2020, the time taken for the detection of matured black pepper spikes obtained as 0.42 seconds. The modified machine vision system takes lesser time for detection than the work done by Zhang *et al*., (2020).

The performance evaluation of the machine vision showed that the sensitivity, specificity, accuracy, and time taken for identification are almost the same for the *Karimunda* and *Panniyur 1* variety. Also, the sensitivity, specificity, and accuracy values of the modified machine vision system were higher than that of the previous system.

4.3.2 Performance evaluation of robotic black pepper harvesting system

The developed robotic black pepper harvesting system evaluated for its performance is discussed below and the sample calculations are shown in the appendices. The result obtained in this study is shown in Table 4.7.

Table 4.7 Performance evaluation of robotic black pepper harvesting system

Sl. No.	**Parameter**	**Observed value**	
		Karimunda	***Panniyur1***
1	Capacity of the system, kg h^{-1}	3.5	4.6
	Capacity of the system, Spikes h^{-1}	562	683
2	Effectiveness index of the system, %	81	82
3	Time taken for single cut, seconds	0.18	0.18

Table 4.7 Continued

Sl. No.	Parameter	Observed value	
		Karimunda	***Panniyur1***
4	Time taken for the Entire Operation, seconds	6.6	6.3
5	Harvesting loss, %	4.9	7
6	Drying loss, %	39	66

Plate 4.7 Performance evaluation of robotic black pepper harvesting system

4.3.2.1 Capacity

The capacity of the system in terms of kg h^{-1} ranged from 2.4 to 4.6 kg h^{-1} for *Karimunda* variety and from 3.7 to 5.8 kg h^{-1} in *Panniyur 1* variety. In *Karimunda* variety, the capacity in terms of spikes h^{-1} ranged from 507 to 632 spikes h^{-1}, and in *Panniyur 1*, it ranged from 522 to 667 spikes h^{-1}. The result from Table 4.7 showed that the robotic black pepper harvesting system has an average capacity of 3.5 kg h^{-1} and 562 spikes h^{-1} for *Karimunda* variety and 4.6 kg h^{-1} and 583 spikes h^{-1} for *Panniyur 1* variety. The developed robotic black pepper harvesting system has less capacity than the work done by Williams *et al*. (2019). The decrease in capacity was due to higher operating time,

as major portion of it was allotted for holding the system in proper position and also for transporting the system manually from one position to another. Wind was another factor which affect the harvesting of black pepper spikes, it increases the time taken for harvesting.

4.3.2.2 Effectiveness index

The result showed that, the effectiveness index of the system ranged from 70 % to 100 % in *Karimunda* variety and from 70 % to 90 % in *Panniyur 1* variety. The robotic black pepper harvesting system has an average effectiveness index of 81 % for *Karimunda* and 82 % for *Panniyur* 1 as shown in Table 4.7. The developed robotic black pepper harvesting system has higher effectiveness index than the work done by Hayashi *et al.* (2014) explained in article 2.4 and lesser effectiveness index than the work done by Birrell *et al.* (2019) explained in article 2.4. The effectiveness index of developed robotic black pepper harvesting system is in the acceptable range.

4.3.2.3 Time taken for cutting

The time taken by the servo motor to move the blade and make the cut was 0.18 seconds, it was fixed in the program.

4.3.2.4 Time taken for the entire operation

The minimum time taken for the entire operation was 5.4 seconds in *Panniyur 1* variety and 5.9 seconds in *Karimunda* variety. The maximum time taken was 7.4 seconds in *Panniyur 1* variety and 7.8 seconds in *Karimunda* variety. The result showed that the average time taken for the entire operation was 6.3 seconds in *Panniyur1* variety and 6.6 seconds in *Karimunda* variety. Because Panniyur 1 variety's pepper spikes are more closely spaced than karimunda's. The time for entire operation taken by the developed robotic black pepper harvesting system is higher than the work done by Williams *et al*., (2019) explained in article 2.4 and lesser than the work done by Masood and Jaryani (2021) explained in article 2.4. The time taken by the developed robotic black pepper harvesting system was within the range.

4.3.2.5 Harvesting loss

In *Panniyur 1* variety, the minimum harvesting loss was 6.5 % and maximum harvesting loss was 7.8 %. Whereas in *Karimunda* variety, the minimum harvesting loss was 3.6 % and maximum was 6 %. Result in Table 4.7 showed that the average harvesting loss of robotic black pepper harvesting system was 7.0 % in *Panniyur 1* variety and 4.9 % in *Karimunda* variety. The developed robotic black pepper harvesting system has less harvesting loss than the work done Birrell *et al*. (2019) explained in article 2.4.

4.3.2.6 Drying loss

The drying loss in *Panniyur 1* variety ranged from 61 % to 70 %, and in *Karimunda* variety it ranged from 34 % to 44 %. The result from Table 4.7 showed that the average drying loss was 66 % in *Panniyur 1* and 39 % in *Karimunda*.

The performance evaluation of the robotic black pepper harvesting system in two varieties showed that the system has a higher capacity with *Pannyur 1* than the *Karimunda* variety. Also, the harvesting loss and drying loss were more significant in *Panniyur 1* variety as compared to the *Karimunda* variety. But the effectiveness index, time taken for a single cut, and time taken for the entire operation were almost the same for both the varieties.

4.3.2.7 Comparison between manual harvesting and robotic black pepper harvesting system.

The developed robotic black pepper harvesting system was compared with the manual harvesting method for their performance, are discussed below. Table 4.8 shows the comparative performance of black pepper harvesting by two methods in *Karimunda* and *Panniyur 1* variety.

Table. 4.8 Black pepper harvesting by manual method and developed robotic black pepper harvesting system

Sl. No.	Parameter	*Karimunda*		*Panniyur 1*	
		Manual harvesting	**Robotic harvesting**	**Manual harvesting**	**Robotic harvesting**
1	Capacity, spikes h^{-1}	1052	562	1654	583
	Capacity, kg h^{-1}	6.3	3.5	10.8	4.6
2	Effectiveness index, %	40	81	38	82
3	Harvesting loss, %	15.3	4.9	17.5	7.0
4	Drying loss, %	56	39	81	66

4.3.2.7.1 Capacity

The result from Table 4.8 showed that, in *Karimunda* variety the average capacity of developed robotic black pepper harvesting system was 562 spikes h^{-1} and 3.5 kg $h^{-1}$and that of manual harvesting was 1052 spikes h^{-1} and 6.3 kg h^{-1}. From the results, it is found that the capacity of robotic black pepper harvesting system was lesser than the manual harvesting in both the varieties.

Statistical analysis using t-test (Welch unpaired t-test) showed that there is a significant difference between the capacities of developed robotic black pepper harvesting system as compared to the manual method in both varieties. Table 4.9 and 4.10 shows the result of statistical analysis and the details are depicted in the appendix XXVIII.

Table 4.9 Statistical analysis of capacity (spikes h^{-1}) using t test

Parameter	*Panniyur 1*		*Karimunda*	
	Manual harvesting	**Robotic harvesting**	**Manual harvesting**	**Robotic harvesting**
Mean	1654	583	1052	562
Standard deviation	403.5	40.3	408.13	35.6
Observations	15	15	15	15
Level of significance	5 %		5 %	
Degree of freedom	14.28		14.21	
P value (two tailed)	0		0.000369	
t value	10.238		4.639	
Significance	Significant		Significant	

Table 4.10 Statistical analysis of capacity (kg h^{-1}) using t test

Parameter	*Panniyur 1*		*Karimunda*	
	Manual harvesting	**Robotic harvesting**	**Manual harvesting**	**Robotic harvesting**
Mean	10.84	4.6	6.3	3.5
Standard deviation	1.635	0.612	2.6	0.716
Observations	15	15	15	15
Level of significance	5 %		5 %	
Degree of freedom	17.85		16.1	

Table 4.10 Continued

Parameter	***Panniyur 1***		***Karimunda***	
	Manual harvesting	**Robotic harvesting**	**Manual harvesting**	**Robotic harvesting**
P value (two tailed)	0		0.000874	
t value	13.785		4.074	
Significance	Significant		Significant	

The capacity of the developed robotic black pepper harvesting system is less as compared to manual harvesting in both *Panniyur 1* and *Kariunda* variety.

4.3.2.7.2 *Effectiveness index*

The result from Table 4.8 showed that the average value of effectiveness index of developed robotic black pepper harvesting system was 81 % in *Karimunda* variety and 82 % in *Panniyur 1* variety. Whereas the effectiveness index of manual harvesting in *Karimunda* was 40 % and *Panniyur 1* was 38 %. It is found that effectiveness index of robotic black pepper harvesting system was higher than the manual harvesting in both varieties.

Statistical analysis using t-test (Welch unpaired t-test) showed that there is a significant difference between the effectiveness indexes of developed robotic black pepper harvesting system and manual harvesting in both the varieties. Table 4.11 shows the result of statistical analysis and the details are depicted in the appendix XXIX.

Table 4.11 Statistical analysis of effectiveness index using t test

Parameter	***Panniyur 1***		***Karimunda***	
	Manual harvesting	**Robotic harvesting**	**Manual harvesting**	**Robotic harvesting**
Mean	38	82	40	81
Standard deviation	14.736	6.761	21.38	9.2
Observations	15	15	15	15
Level of significance	5 %		5 %	
Degree of freedom	19.64		18.97	
P value (two tailed)	0		0.000001	
t value	-10.511		-6.883	
Significance	Significant		Significant	

The effectiveness index of developed robotic black pepper harvesting system is higher as compared to manual harvesting in both *Panniyur 1* and *Karimunda* variety.

4.3.2.7.3 Harvesting loss

The result from Table 4.8 showed that the average harvesting loss of developed robotic black pepper harvesting system was 7.0 % in *Panniyur 1* variety and 4.9 % in *Karimunda* variety. And the harvesting loss in manual harvesting was 17.5 % in *Panniyur 1* and 15.3 % *Karimunda*.

Statistical analysis using t-test (Welch unpaired t-test) showed that there is a significant difference between the harvesting loss in developed robotic black pepper harvesting system and manual harvesting for both varieties. Table 4.12 shows the result of statistical analysis and the details are depicted in the appendix XXX.

Table 4.12 Statistical analysis of harvesting loss using t test

Parameter	***Panniyur 1***		***Karimunda***	
	Manual harvesting	**Robotic harvesting**	**Manual harvesting**	**Robotic harvesting**
Mean	17.5	7.0	15.28	5.0
Standard deviation	6.217	0.518	3.2	1.2
Observations	5	5	5	5
Level of significance	5 %		5 %	
Degree of freedom	4.06		5.02	
P value (two tailed)	0.019107		0.000989	
t value	3.771		6.858	
Significance	Significant		Significant	

The result showed that harvesting loss in manual harvesting was higher than in robotic harvesting for both the *Panniyur 1* and *Karimunda* variety.

4.3.2.7.4 Drying loss

The result from Table 4.8 showed that the average drying loss of developed robotic black pepper harvesting system was 66 % in *Panniyur 1* variety and 39 % in *Karimunda* variety. And the drying loss in manual harvesting was 81 % in *Panniyur 1* and 56 % *Karimunda*. It is found that drying loss for both varieties in robotic black pepper harvesting system was lesser than manual harvesting.

Table 4.13 Statistical analysis of drying loss using t test

Parameter	*Panniyur 1*		*Karimunda*	
	Manual harvesting	**Robotic harvesting**	**Manual harvesting**	**Robotic harvesting**
Mean	81	66	56	39
Standard deviation	5.805	3.362	6.834	4.438
Observations	5	5	5	5
Level of significance	5 %		5 %	
Degree of freedom	6.41		6.86	
P value (two tailed)	0.002172		0.002423	
t value	4.933		4.665	
Significance	Significant		Significant	

Statistical analysis using t-test (Welch unpaired t-test) showed that there is a significant difference between the drying loss in developed robotic black pepper harvesting system and manual harvesting for both varieties. The amount of moisture content is higher in under matured black pepper berries. So drying loss will be high for under matured berries. Hence the result indicates that, the amount of under matured berries harvested was higher in manual harvesting than robotic harvesting. Table 4.13 shows the result of statistical analysis and the details are depicted in the appendix XXXI.

The comparison between manual and robotic harvesting showed that the capacity of manual harvesting is higher than that of the robotic black pepper harvesting system because manual harvesting takes less harvesting time than robotic harvesting. However, the effectiveness index is higher for the robotic harvesting system in *Karimunda* and *Panniyur 1*. Also, the harvesting and drying losses in manual harvesting are higher than that of robotic harvesting for both varieties.

Summary and Conclusion

CHAPTER V

SUMMARY AND CONCLUSION

One of the most popular spices in the world is black pepper, also known as the "King of Spices." India is where it is primarily produced and shipped from. Typically, peppers are picked by hand. Man must ascend the supporting tree using ladders or bamboo poles. Harvesting was occasionally also done with poles that had knives attached to the ends of them. However, the current harvesting techniques are exceedingly dangerous and unable to provide precision harvesting. Only the individual doing the work has any control over how precisely and accurately harvesting is done.

The most promising solution to the problems farmers encounter when harvesting black pepper is robotic harvesting. A robotic harvester's main tasks include identification, plucking, depositing, and controlling. KAU developed a machine vision system using fasterRCNN as the classifier and Tensorflow as a library to identify matured black pepper spikes. The program was coded in python language. The developed machine vision system consists of a display unit, a Raspberry Pi 4 model B as the processor, and a USB web camera as the sensor.

In order to collect black pepper spikes at the proper stage of maturity, an effort was made to build a robotic black pepper harvesting system. The development process and programming portion were completed at NCRAI, Govt. Engg. College, Thrissur, and KCAET, Tavanur. At the Instructional Farm, KCAET, Tavanur, performance evaluation of upgraded machine vision system and developed robotic black pepper harvesting system were also completed.

The physical characteristics of black pepper, such as the length, diameter and weight of the spike, colour and diameter of the berries, as well as the length, diameter, shear strength of the peduncle, and leaf coverage of the pepper vine, were investigated in order to build a robotic black pepper harvesting system.

According to the study, the average pepper spike measured 10.4 cm for the *Karimunda* variety and 12.8 cm for the *Panniyur 1* type. The spike's diameter was

1.1 cm for the *Karimunda* variety and 1.3 cm for the *Panniyur 1* variety. In the *Karimunda* variety, the average spike weighed 7.8 g, whereas the *Panniyur 1* variety's spike weighed 10.1 g. The colour value range for *Karimunda* was (20, 39, 3) - (255, 224, 111) and in *Panniyur 1* value range was (35, 54, 10) - (255, 240, 100). Berries had an average diameter of 0.42 cm in *Karimunda* and 0.59 cm in *Panniyur 1*. For the *Karimunda* variety, the average peduncle length was 1.2 cm, whereas it was 1.3 cm for the *Panniyur 1* variety. Both the *Karimunda* and *Panniyur 1* varieties' peduncle diameters were measured as 0.17 cm. The shear strength of the peduncle in the *Karimunda* variety was 1718.58 N mm^{-2} at 0.1 mm s^{-1} cutting speed and 1535.06 N mm^{-2} at 1 mm s^{-1} cutting speed. Shear strengths of 1671 N mm^{-2} at 0.1 mm s^{-1} and 1544.50 N mm^{-2} at 1 mm s^{-1} were measured in the *Panniyur 1* variety. The pepper vine's leaf coverage was found to be 76 cm at the 95th percentile.

The machine vision system created by KAU was adapted to operate quickly and without internet access. To speed up the process, Python-based IDE (Integrated Development Environment) "Thonny" was used to write and run the programming code. Tensorflow and Python were installed independently on the Raspberry Pi in order to function the machine vision system without internet connection.

Machine vision system, manipulator, end effector, and control unit are the components of the newly developed robotic black pepper harvesting system. The manipulator's joints and the end effector's blade are operated by servomotors. The system is under total control of the Raspberry Pi microcontroller. Python was used to create the computer programs that controlled the servo motors. The pepper spikes were detached from the pepper vine using a shear-type tool. The manipulator was moved from the home position to the action position, and the machine vision system was activated, through the use of programming codes. After that, manually hold the apparatus in front of each pepper spike. The cutting blade's servo motor will actuate and make the cut when the machine vision system detects a matured black pepper spike.” Move to the next position” message will be indicated on the screen if the pepper spike is not matured. To lower the manipulator to its home

position and drop the harvested pepper spike into the conveying unit, another code needs to be executed. The robotic black pepper harvesting system is 162 cm tall, 18 cm wide, and 59 cm long. The system weighed 2.1 kg, and it needed 32.4 W of electricity. The system was powered by a parallel connection of two lead-acid batteries, each with a voltage and current of 12 V and 9 Ah, respectively.

At the KCAET Instructional Farm, the developed robotic black pepper harvesting system's performance was assessed. For the study, both the *Karimunda* and *Panniyur 1* varieties were taken into account. In the *Karimunda* variety, the system's capacity was 3.5 kg h^{-1} and 562 spikes h^{-1}, effectiveness index was 81%, harvesting loss was 4.9%, and drying loss was 39 %. The entire process, including detection and detachment, was completed by the machine in 6.6 seconds. Similarly, in *Panniyur 1* variety, the system's capacity was 4.6 kg h^{-1} and 683 spikes h^{-1}, effectiveness index was 82 %, harvesting loss was 7.0 %, and drying loss was 66 %. The system takes 6.3 seconds for the entire operation, including detection and detachment. The mechanism takes 0.18 seconds for a single cut in both varieties; this was programmed in. The improved machine vision system's performance evaluation results show that the system has a sensitivity of 85 % in the *Karimunda* variety and 84 % in the *Panniyur 1* variety, a specificity of 77% in both varieties, and an accuracy of 82 % in both. In both cases, the detection time is 0.43 seconds.

At a 5% level of significance, the t-test (Welch unpaired t-test) was used to determine whether there was a significant difference between manual and robotic black pepper harvesting in terms of capacity, effectiveness index, harvesting loss, and drying loss. The results revealed a considerable difference in capacity between manual and robotic black pepper harvesting system. Manual harvesting has a capacity of 1052 spikes h^{-1} and 6.3 kg h^{-1} in the *Karimunda* variety and 1654 spikes h^{-1} and 10.8 kg h^{-1} in the *Panniyur 1* variety. The capacity of robotic harvesting is lower than that of manual harvesting. The decrease in capacity was caused by increased operating time, as a large portion of it was allocated for holding the system in the appropriate position and manually transporting the system from

one location to another. Another factor influencing black pepper spike harvesting was the wind, which extended harvesting time. The effectiveness index for manual harvesting was 40% in *Karimunda* and 38% in *Panniyur 1*, which is lower than the effectiveness index for robotic harvesting. It demonstrates that robotic harvesting outperforms manual harvesting. In manual harvesting, the harvesting loss was 15.3 % for *Karimunda* and 17.5 % for *Panniyur 1*. Manual harvesting resulted in a 56% drying loss for *Karimunda* and an 81% drying loss for *Panniyur 1*. According to the findings, hand harvesting has larger harvesting and drying losses than robotic harvesting.

Future Scope

To make the system truly robotic, a travelling platform for moving around the supporting tree and a telescopic supporting rod for height modification can be built and developed. Locate matured pepper spikes with the RGB-D camera and a localization algorithm to autonomously approach the end effector to the target fruit. In addition, the proposed detection algorithm and end effector can be utilized in conjunction with a drone to enable pepper harvesting. Another future possibility for the enhancement of robotic harvesting of black pepper is the creation of a soft gripper for black pepper.

References

REFERENCES

Agarwal, A. L., Sharma, A.T., Shinde, R.D., and Mahajan, R. 2021. Design and manufacturing of robotic arm for spray-painting application with 5 DOF. *Int. J. of Eng. Res. in Mech. and Civil Eng.*. 6(8): 34-38.

Agbaraji, E.C., Inyiama, H.C., and Dimson, I.O. 2018. Joint Torque and Motion Computational Analysis for Robotic Manipulator Arm Design. *J. of Eng. Appl. Sci*. 12: 1-9.

Aneeshya, K.S.K., Krishnanunni, G.K., and Ganesan, V. 2013. Development of a black pepper harvester. *J. Spices Aromat. Crops*. 22 (2): 127–130

[Anonymous]. 2019. Available:https://www.indiaagristat.com/

Asafa, T.B., Afonja, T.M., Olaniyan, E.A., and Alade, H.O. 2018. Development of a vacuum cleaner robot. *Alexandria Eng. J*. 57: 2911-1920

Automaticaddison. 2020. How to determine what torque you need for your servo motors. Available: https://automaticaddison.com/how-to-determine-what-torque-you-need-for-your-servo-motors/ [18 march 2021]

Ankur, C. 2011. What is loss on drying? And determination of loss on drying. *Pharmaceutical guidelines* Available: https://www.pharmaguideline.com/2011/08/what-is-loss-on-drying-and.html/ [20 December 2021].

Bhartiya, C. and Ashish, P. 2015. Image processing based rose harvesting system using raspberry pi. *Int. J. Eng Technol*. 4(4): 1049-1052

Birrell, S., Hughes, J., Cai, J.Y., and Lida, F. 2019. A field-tested robotic harvesting system for iceberg lettuce. *J. Field Robotics*. 37: 225-245

Bugday, M. and Karali, M. 2019. Design optimization of industrial robot arm to minimize redundant weight. *Eng. Sci.Technol. Int. J*. 22: 346-352

Bulanon, D.M. and Kataoka, T. 2010. A Fruit detection system and an end effector for Robotic harvesting of fuji apples. *Agric. Eng. Int.: the CIGR J.* 12(1): 203-210. Available: http://www.cigrjournal.org

Bulanon, D.M., Kataoka, T., Ota, Y., and Hiroma, T. 2015.A Machine vision system for the apple harvesting robot. *Agric. Eng. Int.: the CIGR J. of Sci. Res. Dev.. Manuscript* PM 01 006. Vol. III

Christian, C.I. and Shukla, Y.B. 2016. Web based multi DC servo motor monitoring, controlling and management using embedded system. *Int. J. of Innovative Res. Comput. Commun. Eng*. 4(5): 9788-9797.

Daniyan, I., Balogun, V., Adeodu, A., Oladapo, B., Peter, J.K., Mpofu, K. 2020. Development and performance evaluation of a robot for lawn moving. *Procedia Manufacturing*.49: 42-48.

Deepan, R., Rajavarman, S.V., and Narasimhan, K. 2015. Hand gesture based control of robotic hand using raspberry pi processor. *Asian J. of Sci. Res.* 8 (3): 392-402. ISSN 1992-1454

Erlingsson, B.F., Hreimsson, I., Palsson, P.I., Hjalmarsson, S.J., and Foley, J.T. 2016. Axiomatic Design of a linear motion robotic claw with interchangeable grippers. *Procedia CIRP*. 53: 213-218.

Fashi, M., Naderloo, L., and Javadikia, H. 2019. The relationship between the appearance of pomegranate fruit and colour and size of arils based on image processing. *Postharvest Biol. Technol*. 154: 52-57.

Feng, G. Qixin, C., and Masateru, N. 2008. Fruit detachment and classification method for strawberry harvesting robot. *Int. J. of Adv. Robotic Syst.* 5(1): 41-48. ISSN 1729-8806.

Font, D., Palleja, T., Tresanchez, M., Runcan, D., Moreno, J., Martinez, D., Teixido, M., and Palacin, J. 2014.A proposal for automatic fruit harvesting by combining a low cost stereovision camera and a robotic arm. *Sensors*. 14: 11557-11579.

Gao, F., Fu, L., Zhang, X., Majeed, Y., Li, R., and Karkee, M. 2020. Multi-class fruit-on-plant detection for apple in SNAP system using Faster R-CNN. *Comput. Electr. Agric.* 176: 105634

Gan, H., Lee, W.S., Alchanatis, V., Ehsani, R., and Schueller, J.K. 2018. Immature green citrus fruit detection using color and thermal images. *Comput. Electr. Agric*. 152: 117-125.

Ganguly, R. 2022. Robot control system – how do Robots work. *Tech-addict*. Available: https://www.the-tech-addict.com/control-system-in-robotics/ [11 April, 2022].

Ge, Y., Xiong, Y. and From, P.J. 2019. Instance segmentation and localization of strawberries in farm conditions for automatic fruit harvesting. *IFAC PapersOnLine*. 52(30): 294-299.

Gharakhani, H., Thomasson, J. A., and Lu, Y. 2022. An end-effector for robotic cotton harvesting. *Smart Agric. Technol*. 2: 1-11. Available: https://doi.org/10.1016/j.atech.2022.100043.

Hayashi, S., Yamamoto, S., Saito, S., Ochiai, Y., Kamata, J., Kurita, M., and Yamamoto, K. 2014. Field operation of a movable strawberry-harvesting robot using a travel platform. *Jpn. Agric. Res. Q.* 48(3): 307-316.

Henten, E.J.V., Hemming, J., Van Tuijl, B.A.J., Kornet, J.G., Meuleman, J., Bontsema, J., and Van Os, E.A. 2002. An autonomous robot for harvesting cucumbers in greenhouses. *Autonomous Robots*.13: 241-258.

Heidari, A., and Chegini, G. 2011. Determining the shear strength and picking force of rose flower. *Electr. J. of Polish Agric. Univ*. 14(2): 1-11. ISSN 1505-0297

Hu, C., Liu, X., Pan, Z., and Li, P. 2019. Automatic Detection of Single Ripe Tomato on Plant Combining Faster R-CNN and Intuitionistic Fuzzy Set. *IEEE Access*. 7: 154683-154696.

Jadeja, Y. and Pandya, B. 2019. Design and development of 5-dof robotic arm manipulators. *Int. J. of Sci. Technol. Res.* 8(11): 2158-2167. ISSN 2277-8616.

Jun, Q., Sasao, A., Shibusawa, S., and Kondo, N. 2012. Extracting external features of sweet peppers using machine vision system on mobile fruits grading robot. *Int. J. Food Engg*. 8(3).

Kahandage, P.D., Weerasooriya, G.V.T.V., Hapuarachchi, A.S.K., and Charithangi, M.P., 2017. Designing, development and performance evaluation of harvesting equipment for pepper (piper nigrum).*Conference paper, ResearchGate*.1-8

Khurmi, R. S. and Khurmi, N. 2019. *A Text book of Engineering Mechanics*. S Chand and Company Limited, Ran Nagar, New Delhi, pp. 551-557.

Kondo, N., Yamamoto, K., and Shimzu, H. 2009. A Machine Vision System for Tomato Cluster Harvesting Robot. *Engg. Agric. Environ. Food*. 2(2): 60-65.

Kumar, P. and Ashok, G. 2020. Design and fabrication of smart seed sowing robot. *Mater. Today: Proceedings*. 1-5. https://doi.org/10.1016/j.matpr.2020.07.432

Lagnelov, O., Dhillon, S., Larsson, G., Nilsson, D., Larsolle, A., and Hansson, P.A. 2021. Cost analysis of autonomous battery electric field tractors in agriculture. *Biosystems Eng.* 204: 358-376.

Lili, W., Bo, Z., Jinwei, F., Xiaoan, H., Shu, W., Yashuo, L., Qiangbing, Z., and Chongfeng, W. 2017. Development of a tomato harvesting robot used in greenhouse. *Int. J. of Agric. Biol. Eng*. 10: 140-149.

Lin, G., Tang, Y., Zou, X., Li, J., and Xiong, J. 2019. In-field citrus detection and localisation based on RGB-D image analysis. *Biosystems Eng*. 186: 34-44.

Logan, D.C., Pentzer, J., Sean, N.B., and Reichard, K. 2012. Comparing batteries to generators as power sources for use with mobile robotics. *J. of Power Sources*. 212:130-138.

Masood, M.U., and Jaryani, M.H. 2021. A study on the feasibility of robotic harvesting for chile pepper. *Robotics*. 10(94): 1-22. Available: https://doi.org/10.3390/robotics10030094

Meera, T. and Bhaskar, S. 2020. Development of a machine vision system to identify matured pepper spikes. M.Tech (Agrl. Eng.) thesis, Kerala Agricultural University, Thrissur.133p

Meixner, M. 2019. 11 Science-Backed Health Benefits of Black Pepper. Available: https://www.healthline.com/nutrition/black-pepper-benefits

Mohammadi, V., Kheiralipour, K., and Varnamkhasti, M. G. 2015. Detecting maturity of persimmon fruit based on image processing technique. *Scientia Hortic.* 184: 123-128.

Nishanth, M.S., Jayan, P.R., Pankaj, M., and Ratnakiran, D.W. 2020. Design, development and evaluation of pepper harvester. *J. of AgriSearch*. 7(2): 82-85.

Ohali, Y. A. 2011. Computer vision based date fruit grading system: Design and implementation. *J. King Saud Univ. – Comput. Inf. Sci*. 23: 29-36.

Pa, P.S. and Wu, C.M. 2012. Robotics and computer-integrated manufacturing. *Robotics Comput.-Integrated Manufacturing*. 28: 351-358.

Pannu, G.S., Dawud, M., and Gupta, P. 2015. Design and Implementation of Autonomous Car using Raspberry Pi. *Int. J. of Comput. Appli*. 113 (9): 22-29.

Peebles, M., Lim, S.H., Duke, M., and McGuinness, B. 2019.Investigation of optimal network architecture for asparagus spear detection in robotic harvesting. *IFAC PapersOnline*. 52(30): 283-287.

Rahul, M., Prakash, V.U., and Gopinath, C. 2012. Design and development of a pepper plucking equipment to facilitate pepper harvesting. *SASTECH J*. 11(2): 74-81.

Rana, M.T. and Roy, A. 2017. Design and construction of a robotic arm for industrial automation. *Int. J. of Eng. Res. & Technol. (IJERT)*. 6(5): 919-922. ISSN: 2278-0181. Available: http://www.ijert.org/

Roshanianfard, A. and Noguchi, N. 2016. Development of a 5DOF robotic arm (RAVebots-1) applied to heavy products harvesting. *IFAC-PapersOnLine*. 49(16): 155-160

Roshanianfard, A. and Noguchi, N.2017. Kinematics analysis and simulation of a 5DOF articulated robotic arm applied to heavy products harvesting. *J. of Agric. Sci*. 24: 91-104

Roshanianfard, A. and Noguchi, N. 2018. Characterization of pumpkin for a harvesting robot. *IFAC PapersOnLine*. 51(17): 23-30.

Roshanianfard, A. and Noguchi, N.2020. Pumpkin harvesting robotic end-effector. *Comput. Electr. Agric*. 174: 105503.

Sa, I., Ge, Z., Dayoub, F., Upcroft, B., Perez, T., and Mccool, C. 2016. Deep fruits: A fruit detection system using deep neural networks. *Sensors*. 16: 1222.

Sahay, K. M. and Singh, K. K. 2001. *Unit Operations of Agricultural Processing*. Vikas Publishing House Pvt Ltd, New Delhi. p107

Sanjay, N.A., Venkatramani, N.R., Harinee, V.S., and Dinesh, V. 2021. Cotton harvester through the application of machine learning and image processing techniques. *Mater. Today: Proc*. 2214-7853.

Santos, T.T., Souza, L.L.D., Santos, A.A.D., Avila, S. 2020. Grape detection, segmentation, and tracking using deep neural networks and three-dimensional association. *Comput. Electr. Agric.*170: 105247.

Sarkar, P. and Raheman, H. 2021. Development of a manually drawn single row onion set planter using a 2 DOF robotic arm. *Agric. Eng. Int.: CIGR J*. 23(2): 181-194

Senthilkumar, G., Gopalakrishnan, K., and Sathishkumar, V. 2014. Embedded image capturing system using raspberry pi system. *Int. J. of Emerging Trends Technol. Comput. Sci*. 3(2): 213-215. ISSN 2278-6856.

Siemasz, R., Tomczuk, K., and Malecha, Z. 2020. 3D printed robotic arm with elements of artificial intelligence. *Procedia Comput. Sci.* 176: 3741-3750.

Song, Z., Fu, L., Wu, J., Liu, Z., Li, R., and Cui, Y. 2019. Kiwifruit detection in field images using faster R-CNN with VGG16. *IFAC PapersOnLine*. 52(30): 76-81.

Sustek, M.,Marcanik, M., Tomasek, P., and Urednicek, Z .2017. DC motors and servo-motors controlled by Raspberry Pi 2B. *MATEC Web of Conferences* 125:02025.

Teja, S. and Manohari, R. 2015. Raspberry pi vehicle with stereo vision. *Int. J. Sci., Eng. Technol. Res*. 4(4): 811-815. ISSN: 2278 – 7798.

Vale, G.H.,Hassan, B.B.S.R., Saeidirad, M.H., and Kianmehr, M.H. 2010. Shear strength of stem and picking force for saffron flowers. *J. Agric. Eng. Res*. 11(3): 41-54.

Wang, G., Yu, Y., and Feng, Q. 2016. Design of end-effector for tomato robotic harvesting. *IFAC-PapersOnLine*. 49(16): 190-193.

Wang, Y., Chen, L., Chaisiwamongkhol, K., Couto, R.A.S., and Compton, R.G. 2021. Electrochemical quantification of piperine in black pepper. *Food Chem*. 339: 127892.

Williams, H.A.M., Jones, M.H., Nejati, M., Seabright, M.J., Bell, J., Penhall, N.D., Barnett, J.J., Duke, M.D., Scarfe, A.J., Ahn, H.S., Lim, J., and MacDonald, B.A. 2019. Robotic kiwifruit harvesting using machine vision, convolutional neural networks, and robotic arms. *Biosystem Eng.* 181:140-156.

Xiong, Y., Peng, C., Grimstad, L., From, P.J., and Isler, V. 2019. Development and field evaluation of a strawberry harvesting robot with a cable-driven gripper. *Comput. Electr. Agric*. 157: 392-402.

Yang, L., Tian, R., Wang, Q., Hoshino, Y., Yang, S., and Cao, Y. 2020. Optimal design and simulation of a robot hand for a robot pumpkin harvesting system. *Int. Robotics Automation J*. 6(1): 1-5.

Yurni, O., Dewi, T., Risma, P., and Nawawi, M. 2020.Tomato harvesting arm robot manipulator; a pilot project. *J. of Phys.: Conference Series*.1500:012003.

Zhao, Y., Gong, L., Liu, C., and Huang, Y. 2016. Dual-arm robot design and testing for harvesting tomato in greenhouse. *IFAC-PapersOnLine*. 49(16): 161-165.

Zhang, J., Karkee, M., Zhang, Q., Zhang, X., Yaqoob, M., Fu, L., and Wang, S. 2020. Multi-class object detection using faster R-CNN and estimation of shaking locations for automated shake-and-catch apple harvesting. *Comput. Electr. Agric*. 173:105384.

Zhou, D., Fan, Y., Deng, G., He, F., and Wang, M .2020. A new design of sugarcane seed cutting system based on machine vision. *Comput. Electr. Agric.* 175:105611.

Appendices

Appendix I

Cost Analysis

Software Development

Total working hours	= 50 hours
Cost per hour	= Rs. 500
Total Cost	= 500× 50
	= 25,000

Hardware Development

USB Camera	= Rs. 2000
Raspberry Pi	= Rs. 5500
DSI display	= Rs. 3500
Servo motors	= Rs. 6000
Battery	= Rs. 7000
Buck converters	= Rs. 1000
Materials for the fabrication	= Rs, 1000
Labour charge	= Rs. 5000
Total cost	= 31000

Total cost of development = Rs. 56, 000

Appendix II

Specification of the sensor

Particulars	Specification
Brand	Logitech
Colour	Black and silver
Item height	15 cm
Item width	7.5 cm
Item weight	0.95 gm
Item model number	Logitech C170 Webcam-1

Appendix III

Specifications of processor

Particulars	Specification
Brand	Raspberry Pi
Series	Pi 4, 4 GB
Colour	Green
Pi Dimensions	9.6×7.3×3.2 cm; 80 Grams
RAM size	4 GB
Maximum memory supported	4 GB
Connectivity Type	Wi-Fi, Bluetooth
Operating System	Chrome OS, Windows 10

Appendix IV

Specifications of display unit

Particulars	Specification
Brand	Raspberry Pi LCD Display Module 3
Manufacturer	WaveShare
Touchscreen	TFT
Resolution	320×240
Dimensions	7×5×1.5
Hardware Interface	SPI
Backlight current	TBD
Backlight	LED

Appendix V

Specification of servomotors

1. Servo motor at shoulder joint

Particulars	Specifications
Name	Ultra Torque Quarter scale 60 kgcm metal Gear Servo Motor
Operating Voltage (VDC)	6 to 8.4
Operating angle	180 degree
Operating Temperature Range	-15ºC to 70ºC
Storage Temperature Range	-30ºC to 80 ºC
Operating Speed (at 6 V)	0.17 sec/60 degree
Operating Speed (at 7.4 V)	0.15 sec/60 degree
Operating Speed (at 8.4 V)	0.13 sec/60 degree
Stall torque (at 6 V)	58 kg.cm
Stall torque (at 7.4 V)	65 kg.cm
Stall torque (8.4 V)	70 kg.cm
Servo wire length	32 cm
Gear Type	Metal
Required Pulse	500us-2500us
Length (mm)	65
Width (mm)	30
Height (mm)	48
Weight (gm)	160

2. Servo motor at elbow joint and cutting unit

Particulars	Specification
Name	TowerPro MG996R Digital High Torque Servo Motor
Operating Voltage (VDC)	4.8 to 6.6
Temperature Range	0 to 55 ºC
Stall Torque (at 4.8 V)	9.4 kg cm
Stall Torque (at 6.6 V)	11 kg cm
Operating Speed (at 4.8 V)	0.19 sec/60 º
Operating speed (at 6.6 V)	0.15 sec/60 º
Dead Band width	1 uS
Gear Type	Metal
No. of teeth	25
Length	40.7 mm
Width	19.7 mm
Height	42.9 mm
Weight	55 gm
Wire length	32 cm

Appendix VI

Specification of Battery

Particulars	Specification
Brand	EXIDE
Model Number	Xplore 12XL9-B Motorcycle VRL 12V
Battery type	VRLA (Valve regulated lead acid)
Battery capacity	9 Ah
Voltage output	12 V
Maintenance free	Yes
With Electrolyte	Yes
Factory charged	Yes
Acid level indicator	Yes
Number of terminals	2
Weight	2.5 kg

Appendix VII

Specification of Buck converters

Particulars	Specifications
Name	24V/12V to 5V 5A Power Module DC-DC XY-3606 Power Converter
Maximum working voltage	9-36 V
Output voltage	5.2 V
Length	63 mm
Width	27 mm
Height	10 mm
Weight	22 g

Particulars	Specifications
Name	LM2596S DC-DC Buck Converter Power Supply
Input voltage	3-40 V
Output voltage	1.5-3.5 V (Adjustable)
Output current	2-3 A
Switching frequency	150 KHz
Conversion efficiency	92 % (Highest)
Load regulation	± 0.5%
Voltage regulation	± 0.5 %
Dimension	45×20×14 mm

Appendix VIII

Length of pepper spike

Sl. No.	Length of pepper spike (cm)			
	With peduncle	Without peduncle	With peduncle	Without peduncle
	Karimunda		*Panniyur 1*	
1	9	8.5	18.5	17
2	9.5	8	12.5	11.5
3	9.5	8.5	17.5	16
4	6	4.5	16	15
5	11	10	18	16.5
6	12	10	9	7
7	11	10	19.5	18
8	12	10.5	17	16
9	9.5	8	16.5	15
10	9	8	16	15
11	11	9	9	8
12	12.5	11	9.5	8.5
13	8	6.5	9.5	8.5
14	13.5	12.5	10.5	9
15	12.5	12	14	12
16	11.5	10.5	9.3	8.3
17	14.5	13	12	10.5
18	13.5	12.5	13	12
19	8.5	8	12.5	11.5
20	12.5	11	13	12
21	11.5	10.3	15.4	13.5
22	11.1	9.8	14.5	13.5
23	12	10.6	14.9	13.5

Sl. No	Length of pepper spike (cm)			
	With peduncle	Without peduncle	With peduncle	Without peduncle
	Karimunda		*Panniyur 1*	
24	12.8	11.2	16	14.7
25	13	12	16.4	15
26	13	11.5	15.7	14.7
27	9	8	17	15.7
28	8.8	7.5	17.8	16.6
29	9	8	16.7	15.5
30	11	10	17.8	16.4
31	9.4	8.3	16	15
32	9	7.5	16.5	15.5
33	7	5.5	13.4	12.1
34	12	11	11.4	9.7
35	11	9	9.8	8.9
36	12.5	11	11.3	8.3
37	9.6	8.1	17.3	16.3
38	9.3	8.7	14	12
39	9.7	8.6	13.6	12.4
40	9.2	8.2	12.8	11.8
41	11.5	9.4	11.9	9.9
42	13.4	11.9	12.7	11.2
43	12.8	12.3	16.4	15.1
44	11.9	10.9	9.7	8.7
45	12.6	11.1	10.3	9.1
46	8.4	6.9	13.5	12.4
47	13.6	12.5	16.5	14.2
48	11.9	11.1	17.3	15.9
49	11.5	10.5	18.1	17.2

Sl. No.	Length of pepper spike (cm)			
	With peduncle	Without peduncle	With peduncle	Without peduncle
	Karimunda		*Panniyur 1*	
50	14	12.5	11.9	10.6
51	13.6	12.7	14.6	13.5
52	8.4	7.9	12.3	11.1
53	12.3	10.8	11.7	10.4
54	13.5	12.9	13.7	12.5
55	11	10.6	14.7	13.3
56	14	12.9	12.8	11.3
57	14.9	13.5	13.6	12.4
58	11.7	10.6	18.5	16.6
59	13.9	12.7	17	15.7
60	9	7.6	13.2	12.2
61	12	10.8	12.3	11
62	14	13.1	11.2	9.8
63	15	13.8	13	12
64	13.9	12.4	12.9	11.7
65	12.9	11.7	13.4	12.1
66	13	11.5	14.2	12.5
67	10	9	15.1	13.8
68	12	11.5	14	12.6
69	14.6	13	13.9	12.6
70	13.5	12	12.9	11.4
71	11.9	11	12.8	11.2
72	14.6	12.7	13.6	12.2
73	13.8	12.1	16	14.8
74	9.4	8.2	15.1	14
75	9	8	16	14.1
76	7.5	6.9	12.9	11.5

Sl. No.	Length of pepper spike (cm)			
	With peduncle	Without peduncle	With peduncle	Without peduncle
	Karimunda		*Panniyur 1*	
77	9.8	7.9	13.5	12.4
78	10.4	9.3	14.3	13
79	15	13.6	13.6	12.4
80	11.2	10.3	17	15.6
81	10.7	10	16.3	15.4
82	12.5	11.5	11.7	9.8
83	13	11.5	13.6	11.9
84	12.9	11.7	11.9	10.9
85	14.1	13	11.6	10.6
86	12.9	11	13.2	11.9
87	13	11.7	13.7	12.9
88	11.3	10	16.6	15.1
89	11.7	10.9	17.3	16
90	13.3	12	12.8	11.5
91	13	12	18.1	16.9
92	11	10.1	14.1	12.8
93	12.3	11.2	13.8	12.3
94	13	11.6	17	16
95	10	9	13.5	12.6
96	14	12.8	16.2	14.7
97	11.9	10.6	14.6	13.1
98	12	11	13.7	12.4
99	11.3	10	13.6	12
100	12	10.9	14.7	13.3
Average	11.6	10.4	14.2	12.8
Standard deviation	2.0	1.9	2.4	2.4

Appendix IX

Diameter of pepper spikes

Sl. No.	Diameter of spike (cm)		Sl. No	Diameter of spike (cm)	
	Karimunda	*Panniyur 1*		*Karimunda*	*Panniyur 1*
1	0.77	1.7	27	1.23	1.6
2	1.17	1.7	28	1.2	1.7
3	0.8	1.47	29	1.2	1.5
4	1.17	0.87	30	1.1	0.88
5	1.27	1.37	31	1.05	1.4
6	1.1	1.33	32	0.97	1.3
7	1.23	1.5	33	0.97	1.51
8	0.83	1.27	34	0.87	1.28
9	1.2	1.27	35	1	1.44
10	1.1	1.43	36	1.28	1.34
11	1.2	1.33	37	1.12	1.11
12	1.1	1.1	38	0.86	1.12
13	1.2	1.1	39	1.3	1.21
14	1.03	1.2	40	1.1	1.11
15	1	1.1	41	1.05	1.21
16	1.03	1.2	42	1.1	1.31
17	0.87	1.3	43	1.14	1.28
18	1.27	1.27	44	1.12	1.46
19	1.1	1.45	45	1.05	1.36
20	1.2	1.35	46	1.23	1.6
21	1.17	1.32	47	1.21	1.4
22	1.1	1.49	48	1	1.28
23	1.2	1.26	49	1.07	1.31
24	1.09	1.42	50	1.12	1.18
25	1.24	1.32	51	1.1	1.2
26	1.1	1.09	52	1.14	1.19

Sl. No.	Diameter of spike (cm)		Sl. No.	Diameter of spike (cm)	
	Karimunda	*Panniyur 1*		*Karimunda*	*Panniyur 1*
53	1.2	1.1	77	1.1	1.3
54	1.12	1.19	78	0.97	1.29
55	1.1	1.29	79	0.87	1.22
56	1	1.26	80	1.17	1.3
57	0.9	1.44	81	1.27	1.27
58	0.97	1.42	82	1.24	1.28
59	0.83	1.32	83	1	1.45
60	0.97	1.09	84	0.96	1.44
61	1.15	1.07	85	0.89	1.32
62	1.2	1.19	86	1.09	1.25
63	1.09	1.2	87	1.11	1.44
64	1.04	1.28	88	1.08	1.37
65	1.21	1.43	89	1.2	1.33
66	1.1	1.3	90	1.13	1.43
67	0.83	1.32	91	1.21	1.21
68	0.95	1.49	92	1.1	1.2
69	0.87	1.26	93	1	1.32
70	1.11	1.42	94	0.95	1.27
71	1.25	1.3	95	1.24	1.33
72	1.13	1.33	96	1.08	1.24
73	1.3	1.1	97	1.1	1.28
74	1.22	1.4	98	1.25	1.4
75	1.2	1.2	99	1.13	0.97
76	1.21	1.34	100	1.3	0.87
Average		1.1			1.3
Standard deviation		0.13			0.17

Appendix X

Weight of the spike

Sl. No.	Weight of the spike (g)		Sl. No	Weight of the spike (g)	
	Karimunda	*Panniyur 1*		*Karimunda*	*Panniyur 1*
1	5	9.9	27	7.1	5.7
2	3	17.1	28	4.9	6.4
3	3.7	8.1	29	6.8	11.5
4	5.1	9.2	30	11.1	10.6
5	4.8	8.8	31	12.4	6.8
6	4.3	11.1	32	11.8	12.7
7	2.6	7.3	33	9.1	13.5
8	2.1	7.1	34	13.4	6.9
9	2.8	3.8	35	12.6	8.9
10	2.9	6.9	36	9.4	9.3
11	4.1	3.9	37	8.9	15.3
12	2.5	10.7	38	7.6	11.8
13	2.9	5.3	39	9.1	15.8
14	4.4	5.6	40	5.9	16.1
15	9	7.5	41	7.8	17
16	8.7	8.2	42	9.4	14.3
17	7.6	6.1	43	6.9	9.7
18	9.3	6	44	7.3	11.8
19	10.1	7.5	45	7.2	13.5
20	9.6	7.7	46	6.8	12.1
21	4.9	8.1	47	6.9	9.4
22	5.8	8.4	48	4.7	8.7
23	6.7	15.3	49	8.3	12.1
24	9.1	9.87	50	10.5	9.7
25	10.1	13.2	51	10.7	9.8
26	6.9	8.9	52	11.8	7.89

Sl. No.	Diameter of spike (cm)		Sl. No.	Diameter of spike (cm)	
	Karimunda	*Panniyur 1*		*Karimunda*	*Panniyur 1*
53	10.6	8.43	77	6.9	11.75
54	13.6	7.95	78	9.9	8.95
55	9.5	5.89	79	10.1	6.58
56	7.9	5.98	80	10.8	7.39
57	7.3	6.79	81	11.3	8.99
58	4.9	11.89	82	10.1	7.89
59	6.8	12.04	83	12.1	6.98
60	10.6	8.98	84	9.78	12.09
61	5.8	13.78	85	8.58	6.98
62	9.8	14.76	86	7.68	9.78
63	3.9	5.78	87	6.43	8.95
64	5.9	9.62	88	4.9	8.08
65	9.4	8.99	89	6.85	7.93
66	10.4	7.98	90	7.77	12.09
67	11.7	12.95	91	6.97	11.78
68	8.1	11.78	92	5.98	13.04
69	7.62	15.29	93	9.3	14.01
70	6.17	16.1	94	6.9	11.79
71	8.65	11.73	95	9.1	10.98
72	9.5	12.98	96	5.98	8.09
73	10.11	11.79	97	6.9	6.97
74	7.8	10.97	98	7.4	11.78
75	9.1	16.74	99	7.7	12.94
76	8.7	14.21	100	8.2	7.98
Average		17.8		10.1	
Standard deviation		2.6		3.1	

Appendix XI

Colour of berries

Sl. No.	RGB Value (Range)	
	Karimunda	*Panniyur 1*
1	(24, 46, 19) - (251, 174, 172)	(93, 34, 9) – (218, 180, 111)
2	(26, 33, 2) - (255, 193, 174)	(93, 70, 13) - (255, 240, 100)
3	(46, 68, 19) - (255, 224,196)	(94, 119, 29) - (251, 255, 110)
4	(79, 53, 26) - (255, 199, 169)	(94, 120, 38) - (252, 205, 110)
5	(47, 39, 3) - (255, 230, 202)	(94, 130, 60) - (255, 205, 101)
6	(52, 25, 0) - (255, 184, 192)	(94, 131, 63) - (255, 135, 101)
7	(69, 75, 40) - (255, 195, 186)	(94, 49, 40) - (255, 135, 125)
8	(105, 128, 79) -(255, 183, 175)	(94, 91, 21) - (255, 156, 110)
9	(40, 76, 32) - (255,225,254)	(95, 120, 19) - (255, 220, 110)
10	(28, 30, 0) - (255, 198, 185)	(95, 123, 28) - (255, 223, 130)
11	(37, 19, 6) - (255, 195, 186)	(97, 136, 39) - (253, 210, 130)
12	(66, 89, 5) - (255, 179, 187)	(98, 121, 19) - (254, 203, 130)
13	(65, 70, 16) - (255, 182, 173)	(35, 54, 1) - (255, 200, 150)
14	(82, 124, 59) - (253, 163, 138)	(44, 52, 7) - (255, 196, 150)
15	(26, 8, 2) - (255, 237, 187)	(45, 52, 15) - (255, 230, 150)
16	(20, 39, 3) - (255, 191, 185)	(52, 61, 7) - (255, 224, 130)
17	(44, 28, 6) - (255, 213, 206)	(57, 72, 15) - (255, 210, 130)
18	(27, 15, 15) - (255, 188, 230)	(64, 85, 23) - (255, 209, 150)
19	(75, 4, 1) - (255, 198, 111)	(66, 84, 11) - (255, 219, 160)
20	(35, 54, 1) - (255, 241, 199)	(93, 34, 9) - (218, 180, 111)

Appendix XII

Diameter of berries

Sl. No	Diameter of berries, cm		Sl. No	Diameter of berries, cm	
	Karimunda	*Panniyur 1*		*Karimunda*	*Panniyur 1*
1	0.45	0.5	26	0.45	0.6
2	0.42	0.65	27	0.42	0.45
3	0.45	0.55	28	0.4	0.5
4	0.5	0.45	29	0.35	0.6
5	0.5	0.7	30	0.3	0.5
6	0.5	0.6	31	0.42	0.7
7	0.45	0.7	32	0.45	0.5
8	0.3	0.7	33	0.5	0.45
9	0.45	0.6	34	0.35	0.6
10	0.5	0.65	35	0.5	0.7
11	0.3	0.7	36	0.3	0.45
12	0.4	0.45	37	0.35	0.5
13	0.35	0.6	38	0.5	0.6
14	0.5	0.6	39	0.45	0.7
15	0.35	0.7	40	0.35	0.45
16	0.3	0.5	41	0.4	0.5
17	0.5	0.6	42	0.42	0.6
18	0.45	0.5	43	0.5	0.65
19	0.3	0.6	44	0.5	0.5
20	0.45	0.45	45	0.45	0.6
21	0.3	0.5	46	0.5	0.7
22	0.35	0.6	47	0.4	0.5
23	0.3	0.7	48	0.3	0.55
24	0.35	0.65	49	0.35	0.65
25	0.45	0.6	50	0.4	0.7

Sl. No	Diameter of berries, cm		Sl. No.	Diameter of berries, cm	
	Karimunda	*Panniyur 1*		*Karimunda*	*Panniyur 1*
51	0.5	0.6	76	0.35	0.65
52	0.3	0.65	77	0.3	0.5
53	0.5	0.7	78	0.4	0.55
54	0.4	0.5	79	0.35	0.5
55	0.42	0.6	80	0.45	0.65
56	0.4	0.5	81	0.3	0.7
57	0.5	0.45	82	0.5	0.45
58	0.45	0.55	83	0.5	0.55
59	0.3	0.65	84	0.35	0.6
60	0.5	0.6	85	0.5	0.65
61	0.45	0.7	86	0.5	0.45
62	0.3	0.45	87	0.4	0.7
63	0.35	0.55	88	0.45	0.55
64	0.4	0.55	90	0.45	0.55
65	0.5	0.6	91	0.5	0.7
66	0.43	0.45	92	0.4	0.6
67	0.45	0.5	93	0.35	0.55
68	0.5	0.65	94	0.5	0.65
69	0.5	0.45	95	0.35	0.45
70	0.4	0.55	96	0.5	0.65
71	0.4	0.65	97	0.4	0.65
72	0.45	0.6	98	0.5	0.7
73	0.5	0.65	99	0.4	0.7
74	0.5	0.6	100	0.4	0.65
75	0.3	0.65			
Average			0.42		0.59
Standard deviation			0.07		0.09

Appendix XIII

Length of the peduncle

Sl. No.	Length of peduncle, cm		Sl. No.	Length of peduncle, cm	
	Karimunda	*Panniyur 1*		*Karimunda*	*Panniyur 1*
1	0.5	1.5	25	1.5	1
2	1.5	1	26	1.2	1.9
3	1	1.5	27	1.3	1
4	1.5	1	28	1.4	1.4
5	1	1.5	29	1.6	1.3
6	2	2	30	1	1.4
7	1	1.5	31	1.5	1
8	1.5	1	32	1	1.3
9	1.5	1.5	33	1.3	1.2
10	1	1	34	1	1.2
11	2	1	35	1	1.4
12	1.5	1	36	1.1	1
13	1.5	1	37	1.5	1
14	1	1.5	38	1.5	1.3
15	0.5	2	39	1	1.7
16	1	1	40	2	0.9
17	1.5	1.5	41	1.5	3
18	1	1	42	1.5	1
19	0.5	1	43	0.6	2
20	1.1	1.2	44	1.2	1
21	1	1	45	1.5	1.2
22	2.1	2	46	1.2	1.3
23	1.5	1.5	47	1.5	1.7
24	0.5	1.3	48	1	1.3

Sl. No.	Length of peduncle, cm		Sl. No	Length of peduncle, cm	
	Karimunda	*Panniyur 1*		*Karimunda*	*Panniyur 1*
49	1	1	75	1	1.9
50	1.5	1.2	76	0.6	1.4
51	1.5	1.1	77	1.9	1.1
52	1.1	2.3	78	1.1	1.3
53	0.8	1.4	79	1.4	1.2
54	1	0.9	80	0.9	1.4
55	1.5	1.3	81	0.7	0.9
56	0.9	1.1	82	1	1.9
57	0.5	1.2	83	1.5	1.7
58	1.5	1.3	84	1.2	1
59	0.6	1.2	85	1.1	1
60	0.4	1.4	86	1.9	1.3
61	1.1	1.5	87	1.3	0.8
62	1.4	1.2	88	1.3	1.5
63	1.1	1.9	89	0.8	1.3
64	1.2	1.3	90	1.3	1.3
65	1.4	1	91	1	1.2
66	1.2	1.3	92	0.9	1.3
67	0.9	1.4	93	1.1	1.5
68	0.5	1.4	94	1.4	1
69	1.6	1.3	95	1	0.9
70	1.5	1.5	96	1.2	1.5
71	0.9	1.6	97	1.3	1.5
72	1.9	1.4	98	1	1.3
73	1.7	1.2	99	1.3	1.6
74	1.2	1.1	100	1.1	1.4
Average		1.2		1.3	
Standard deviation		0.37		0.34	

Appendix XIV

Diameter of the peduncle

Sl. No.	Diameter of the peduncle, cm		Sl. No.	Diameter of the peduncle, cm	
	Karimunda	*Panniyur 1*		*Karimunda*	*Panniyur 1*
1	0.15	0.15	25	0.15	0.2
2	0.15	0.15	26	0.16	0.1
3	0.2	0.2	27	0.15	0.1
4	0.2	0.2	28	0.15	0.15
5	0.16	0.1	29	0.14	0.16
6	0.14	0.2	30	0.1	0.15
7	0.2	0.16	31	0.15	0.15
8	0.2	0.15	32	0.16	0.2
9	0.15	0.1	33	0.2	0.16
10	0.15	0.1	34	0.16	0.15
11	0.2	0.15	35	0.15	0.15
12	0.16	0.1	36	0.2	0.16
13	0.15	0.2	37	0.2	0.15
14	0.2	0.2	38	0.19	0.15
15	0.2	0.15	39	0.16	0.2
16	0.15	0.1	40	0.14	0.2
17	0.1	0.15	41	0.15	0.2
18	0.15	0.2	42	0.19	0.15
19	0.19	0.15	43	0.2	0.14
20	0.16	0.15	44	0.15	0.2
21	0.15	0.15	45	0.15	0.15
22	0.14	0.2	46	0.2	0.16
23	0.2	0.14	47	0.2	0.15
24	0.19	0.16	48	0.15	0.15

Diameter of the peduncle, cm			Diameter of the peduncle, cm		
Sl. No.	*Karimunda*	*Panniyur 1*	Sl. No.	*Karimunda*	*Panniyur 1*
49	0.15	0.15	75	0.15	0.14
50	0.14	0.15	76	0.15	0.16
51	0.15	0.16	77	0.15	0.14
52	0.2	0.14	78	0.19	0.15
53	0.2	0.15	79	0.16	0.15
54	0.15	0.16	80	0.15	0.2
55	0.15	0.15	81	0.14	0.15
56	0.14	0.2	82	0.2	0.19
57	0.16	0.2	83	0.2	0.2
58	0.2	0.15	84	0.15	0.2
59	0.14	0.1	85	0.16	0.2
60	0.15	0.15	86	0.2	0.15
61	0.15	0.1	87	0.2	0.15
62	0.2	0.16	88	0.15	0.16
63	0.2	0.1	89	0.15	0.2
64	0.15	0.16	90	0.16	0.2
65	0.16	0.14	91	0.19	0.15
66	0.19	0.19	92	0.2	0.15
67	0.16	0.2	93	0.15	0.16
68	0.2	0.2	94	0.15	0.16
69	0.16	0.16	95	0.14	0.19
70	0.15	0.19	96	0.15	0.2
71	0.14	0.2	97	0.16	0.15
72	0.2	0.2	98	0.15	1.5
73	0.2	0.15	99	0.2	0.1
74	0.16	0.16	100	0.15	0.1
Average		0.17			0.17
Standard deviation		0.03			0.14

Appendix XV

Shear strength of the peduncle

Cutting speed = 0.1 mm s^{-1}

	Karimunda				*Panniyur 1*			
Sl. No.	**Shear force, N**	**Diameter of the peduncle, mm**	**Cross sectional area of the peduncle, mm^2**	**Shear strength of the peduncle, N mm^{-2}**	**Shear force, N**	**Diameter of the peduncle, mm**	**Cross sectional area of the peduncle, mm^2**	**Shear strength of the peduncle, N mm^{-2}**
1	34.60	0.15	0.02	1958.95	36.00	0.2	0.03	1146
2	35.00	0.15	0.02	1981.60	26.01	0.1	0.01	3313
3	36.01	0.20	0.03	1146.70	36.01	0.2	0.03	1147
4	36.84	0.20	0.03	1173.20	36.84	0.2	0.03	1173
5	33.10	0.16	0.02	1647.09	33.50	0.15	0.02	1896
6	32.40	0.14	0.02	2105.81	36.10	0.2	0.03	1150
7	35.50	0.20	0.03	1130.57	35.76	0.16	0.02	1780
8	36.34	0.20	0.03	1157.32	36.05	0.15	0.02	2041
9	34.43	0.15	0.02	1949.44	35.43	0.16	0.02	1763
10	34.65	0.15	0.02	1961.90	33.65	0.15	0.02	1905
11	33.43	0.16	0.02	1663.27	33.43	0.15	0.02	1892

	Karimunda				*Panniyur 1*			
Sl. No.	**Shear force, N**	**Diameter of the peduncle, mm**	**Cross sectional area of the peduncle, mm^2**	**Shear strength of the peduncle, N mm^{-2}**	**Shear force, N**	**Diameter of the peduncle, mm**	**Cross sectional area of the peduncle, mm^2**	**Shear strength of the peduncle, N mm^{-2}**
12	34.22	0.16	0.02	1702.58	34.22	0.2	0.03	1090
13	33.41	0.15	0.02	1891.58	36.10	0.2	0.03	1150
14	34.49	0.20	0.03	1098.31	34.49	0.18	0.03	1356
15	35.00	0.20	0.03	1114.65	35.00	0.15	0.02	1982
16	34.20	0.15	0.02	1936.31	34.20	0.15	0.02	1936
17	31.30	0.10	0.01	3987.26	36.42	0.2	0.03	1160
18	31.60	0.15	0.02	1789.10	31.60	0.15	0.02	1789
19	33.48	0.19	0.03	1181.26	32.48	0.15	0.02	1839
20	31.70	0.15	0.02	1794.76	33.70	0.15	0.02	1908
Average				1718.58 N mm^{-2}				1671 N mm^{-2}
Standard deviation				647				515

Cutting speed = 1 mm s^{-1}

	Karimunda				*Panniyur 1*			
Sl. No.	**Shear force, N**	**Diameter of the peduncle, mm**	**Cross sectional area of the peduncle, mm^2**	**Shear strength of the peduncle, N mm^{-2}**	**Shear force, N**	**Diameter of the peduncle, mm**	**Cross sectional area of the peduncle, mm^2**	**Shear strength of the peduncle, N mm^{-2}**
1	30.3	0.16	0.02	1507.76	32.00	0.2	0.03	1019.11
2	31.9	0.2	0.03	1015.92	29.90	0.1	0.01	3808.92
3	32.14	0.2	0.03	1023.57	32.14	0.2	0.03	1023.57
4	29.34	0.14	0.02	1906.93	31.34	0.2	0.03	998.09
5	28.76	0.1	0.01	3663.69	30.90	0.15	0.02	1749.47
6	29.38	0.15	0.02	1663.41	33.11	0.2	0.03	1054.46
7	29.54	0.16	0.02	1469.94	31.40	0.16	0.02	1562.50
8	31.1	0.15	0.02	1760.79	32.26	0.15	0.02	1826.30
9	30.56	0.16	0.02	1520.70	31.56	0.16	0.02	1570.46
10	29.75	0.15	0.02	1684.36	29.65	0.15	0.02	1678.70
11	30.76	0.15	0.02	1741.54	29.76	0.15	0.02	1684.93

	Karimunda				*Panniyur 1*			
Sl. No.	**Shear force, N**	**Diameter of the peduncle, mm**	**Cross sectional area of the peduncle, mm^2**	**Shear strength of the peduncle, N mm^{-2}**	**Shear force, N**	**Diameter of the peduncle, mm**	**Cross sectional area of the peduncle, mm^2**	**Shear strength of the peduncle, N mm^{-2}**
12	32.3	0.2	0.03	1028.66	31.35	0.2	0.03	998.41
13	31.76	0.19	0.03	1120.74	30.76	0.16	0.02	1530.65
14	31.12	0.16	0.02	1548.57	31.12	0.15	0.02	1761.92
15	29.55	0.15	0.02	1673.04	28.35	0.15	0.02	1605.10
16	30.1	0.15	0.02	1704.18	30.10	0.15	0.02	1704.18
17	31.97	0.16	0.02	1590.86	31.97	0.2	0.03	1018.15
18	32.4	0.2	0.03	1031.85	28.40	0.15	0.02	1607.93
19	30.8	0.2	0.03	980.89	29.80	0.15	0.02	1687.19
20	33.4	0.2	0.03	1063.69	31.40	0.2	0.03	1000.00
Average				1535.06 N mm^{-2}				1544.5 N mm^{-2}
Standard deviation				589				606

Appendix XVI

Leaf coverage of black pepper vine

Plant Number	Maximum coverage of plant on each side, cm			
	I	II	III	IV
1	85	43	28	10
2	39	48	50	30
3	58	50	59	43
4	61	38	65	72
5	83	43	48	70
6	43	29	39	47
7	67	40	65	74
8	56	47	45	59
9	70	57	48	60
10	60	87	91	40
11	88	80	30	35
12	61	52	33	43
13	63	24	50	47
14	40	44	46	44
15	38	38	43	32
16	68	36	45	40
17	66	44	59	65
18	42	53	48	41
19	55	46	29	37
20	49	42	56	40
21	32	45	36	31
22	50	44	46	56
23	48	43	31	45
24	36	53	33	14
25	51	29	34	38
26	47	57	54	60
Average		45.3		
Standard deviation		15.3		

Plant Number	Maximum coverage of plant on each side, cm			
	I	II	III	IV
27	76	43	37	68
28	41	42	65	57
29	33	23	34	24
30	57	34	39	41
31	42	32	40	91
32	53	55	57	48
33	37	42	23	28
34	37	36	39	29
35	56	31	65	44
36	69	59	45	53
37	32	31	22	32
38	42	44	30	17
39	38	27	33	48
40	39	52	51	52
41	24	27	30	22
42	59	54	37	31
43	39	45	42	30
44	62	27	29	35
45	81	45	39	37
46	53	48	45	35
47	35	28	21	16
48	30	24	29	38
49	37	29	64	28
50	59	55	67	52

Cumulative frequency distribution table

Sl. No.	Class interval	Frequency	Cumulative Frequency
1	10-20	4	4
2	20-30	23	27
3	30-40	52	79
4	40-50	53	132
5	50-60	38	170
6	60-70	17	187
7	70-80	5	192
8	80-90	6	198
9	90-100	2	200

95^{th} Percentile $= l + \frac{\frac{95N}{100} - m}{f} \times C$

l= Lower limit of 95^{th} class

m= Cumulative frequency just before the 95^{th} class

f= Frequency of 95^{th} class

C= Class interval

N= Total number of observations

95^{th} class is the class contain $\frac{95N}{100}$ th observation. That is 190^{th} observation. So the 95^{th} class was 70-80.

l= 70; m= 187; f= 5; C= 10

95^{th} Percentile $= l + \frac{\frac{95N}{100} - m}{f} \times C = 70 + \frac{\frac{95 \times 200}{100} - 187}{5} \times 10$ = 76 cm

Appendix XVII

Performance evaluation of machine vision system

Parameter	*Karimunda*	*Panniyur 1*
True positives (TP)	55	59
True negatives(TN)	27	23
False positives (FP)	8	7
False negatives (FN)	10	11
Sensitivity, %	85	84
Specificity, %	77	77
Accuracy, %	82	82

Sample calculation

1. Sensitivity

Total true positives = 55

Total false negatives = 10

$$\text{Sensitivity} = \frac{\text{Toatl true positives}}{\text{Total true positives} + \text{Total false negative}} \times 100$$

$$= (55 / (55+10)) \times 100 = 85\ \%$$

2. Specificity

Total true negatives = 27

Total false positives = 8

$$\text{Specificity} = \frac{\text{Total true negatives}}{\text{Total true negatives} + \text{Total false positives}} \times 100$$

$$= (27 / (27+8)) \times 100 = 77\ \%$$

3. Accuracy

Total true positives = 55

Total true negatives = 27

Total TP, TN, FP, FN = 100

$$\text{Accuracy} = \frac{\text{True positives + True negatives}}{(\text{True positives + True negatives+ False positives+False negatives})} \times 100$$

$$\text{Accuracy} = ((55+27)/100) \times 100$$

$$= 82\ \%$$

Appendix XVIII

Time taken for identification

Sl. No.	Time taken for identification, sec		Sl. No.	Time taken for identification, sec	
	Karimunda	*Panniyur 1*		*Karimunda*	*Panniyur 1*
1	0.43	0.43	23	0.42	0.43
2	0.42	0.42	24	0.43	0.42
3	0.46	0.41	25	0.44	0.42
4	0.43	0.43	26	0.43	0.43
5	0.44	0.46	27	0.44	0.43
6	0.43	0.44	28	0.46	0.44
7	0.42	0.42	29	0.42	0.42
8	0.42	0.42	30	0.42	0.41
9	0.42	0.43	31	0.43	0.46
10	0.43	0.43	32	0.44	0.43
11	0.43	0.46	33	0.46	0.43
12	0.44	0.42	34	0.43	0.42
13	0.43	0.43	35	0.42	0.44
14	0.42	0.41	36	0.42	0.43
15	0.46	0.44	37	0.43	0.45
16	0.43	0.46	38	0.46	0.46
17	0.44	0.42	39	0.42	0.42
18	0.43	0.42	40	0.42	0.43
19	0.45	0.43	41	0.43	0.44
20	0.46	0.43	42	0.44	0.43
21	0.43	0.42	43	0.43	0.42
22	0.43	0.44	44	0.46	0.44

Sl. No.	Time taken for identification, sec		Sl. No.	Time taken for identification, sec	
	Karimunda	*Panniyur 1*		*Karimunda*	*Panniyur 1*
45	0.44	0.42	73	0.43	0.41
46	0.46	0.42	74	0.44	0.46
47	0.43	0.43	75	0.42	0.45
48	0.46	0.43	76	0.46	0.46
49	0.44	0.46	77	0.43	0.44
50	0.46	0.42	78	0.42	0.43
51	0.42	0.43	79	0.41	0.42
52	0.42	0.46	80	0.45	0.44
53	0.42	0.42	81	0.46	0.46
54	0.42	0.41	82	0.43	0.44
55	0.43	0.42	83	0.42	0.42
56	0.43	0.43	84	0.44	0.41
57	0.42	0.41	85	0.42	0.46
58	0.42	0.42	86	0.42	0.44
59	0.43	0.44	87	0.42	0.46
60	0.42	0.42	88	0.43	0.42
61	0.46	0.43	89	0.43	0.43
62	0.43	0.46	90	0.44	0.41
63	0.42	0.42	91	0.42	0.44
64	0.43	0.42	92	0.46	0.46
65	0.42	0.43	93	0.46	0.43
66	0.43	0.44	94	0.43	0.43
67	0.44	0.43	95	0.42	0.42
68	0.43	0.42	96	0.43	0.44
69	0.42	0.43	97	0.44	0.45
70	0.41	0.46	98	0.46	0.46
71	0.43	0.41	99	0.45	0.43
72	0.43	0.42	100	0.46	0.42

Average time taken for identification, *Karimunda* = 0.43 seconds

Average time taken for identification, *Panniyur 1* = 0.43 seconds

Appendix XIX

Capacity of the system

Karimunda

Cycle number	Time taken for cycle of operation (h)	No. of black pepper spikes harvested in cycle of operation	Weight of black pepper spikes harvested in one cycle of operation (kg)	Capacity of the system (kg h^{-1})	Capacity of the system (number of spikes h^{-1})
1	0.0175	10	0.045	2.55	571
2	0.0186	10	0.082	4.41	537
3	0.0169	10	0.047	2.77	590
4	0.0181	10	0.061	3.38	554
5	0.0158	10	0.038	2.40	632
6	0.0161	10	0.043	2.67	621
7	0.0183	10	0.051	2.78	545
8	0.0194	10	0.069	3.55	514
9	0.0175	10	0.072	4.11	571
10	0.0189	10	0.057	3.02	529
11	0.0172	10	0.070	4.06	581
12	0.0197	10	0.074	3.76	507
13	0.0175	10	0.067	3.83	571
14	0.0186	10	0.086	4.63	537
15	0.0178	10	0.072	4.07	563

Panniyur1

Cycle number	Time taken for cycle of operation (h)	No. of black pepper spikes harvested in cycle of operation	Weight of black pepper spikes harvested in one cycle of operation (kg)	Capacity of the system (kg h^{-1})	Capacity of the system (number of spikes h^{-1})
1	0.0175	10	0.077	4.4	571
2	0.0178	10	0.081	4.6	563
3	0.0169	10	0.084	5.0	590
4	0.0181	10	0.078	4.3	554
5	0.0158	10	0.061	3.8	632
6	0.0161	10	0.060	3.7	621
7	0.0181	10	0.083	4.6	554
8	0.0164	10	0.095	5.8	610
9	0.0175	10	0.085	4.9	571
10	0.0172	10	0.078	4.5	581
11	0.0186	10	0.073	3.9	537
12	0.0192	10	0.091	4.7	522
13	0.0183	10	0.088	4.8	545
14	0.0161	10	0.075	4.6	621
15	0.0150	10	0.088	5.8	667

Sample Calculation

Amount of black pepper spikes harvested in one cycle of operation = 0.045 kg

Time taken for one cycle of operation = 0.0175 h

Numer of black pepper spikes harvested in one cycle of operation = 10

Capacity of the system (kg h^{-1})

$$= \frac{\text{Amount of black pepper spikes harvested in one cycle of operation}}{\text{Time taken for one cycle of operation}}$$

$$= \frac{0.045}{0.0175}$$

$$= 2.55 \text{ kg } h^{-1}$$

Capacity of the system (spikes h^{-1})

$$= \frac{\text{Number of black pepper spikes harvested in one cycle of operation}}{\text{Time taken for one cycle of operation}}$$

$$= \frac{10}{0.0175}$$

$$= 571 \text{ spikes } h^{-1}$$

Panniyur 1

Average capacity of the system = 4.6 kg h^{-1}

Average capacity of the system = 583 spikes h^{-1}

Karimunda

Average capacity of the system = 3.5 kg h^{-1}

Average capacity of the system = 562 spikes h^{-1}

Appendix XX

Effectiveness index of the system

Karimunda

Trial No.	Number of spikes selected	No. of matured pepper spikes harvested	No. of matured pepper spikes not harvested	No. of green pepper spikes harvested	No. of green pepper spikes not harvested	Effectiveness index of the system (%)
1	10	7	1	1	1	80
2	10	9	0	1	0	90
3	10	10	0	0	0	100
4	10	7	0	3	0	70
5	10	7	0	2	1	80
6	10	7	0	3	0	70
7	10	8	0	0	0	80
8	10	8	1	0	1	90
9	10	6	0	3	1	70
10	10	7	0	3	0	70
11	10	8	0	2	0	80
12	10	9	0	1	0	90
13	10	8	1	1	0	80
14	10	8	0	2	0	80
15	10	8	0	2	1	90

Panniyur 1

Trial No.	Number of spikes selected	No. of matured pepper spikes harvested	No. of matured pepper spikes not harvested	No. of green pepper spikes harvested	No. of green pepper spikes not harvested	Effectiveness index of the system (%)
1	10	8	1	1	0	80
2	10	9	1	0	0	90
3	10	6	1	1	2	80
4	10	7	1	1	1	80
5	10	4	2	1	3	70
6	10	8	0	1	1	90
7	10	7	1	1	1	80
8	10	5	1	1	3	80
9	10	6	0	1	3	90
10	10	8	0	1	1	90
11	10	7	1	0	2	90
12	10	8	0	1	0	80
13	10	6	1	2	1	70
14	10	8	1	1	0	80
15	10	8	1	1	0	80

Sample Calculation

Number of black pepper spikes detected correctly and harvested at correct maturity=

Number of matured pepper spikes harvested +Number of green pepper spikes not harvested

Total number of black pepper spikes detected correctly and harvested at correct maturity = 7+1 = 8

Total number of selected black pepper spikes = 10

$$\text{Effectiveness index of the system} = \frac{\text{Number of black pepper spikes detected correctly and harvested at correct maturity}}{\text{Total number of selected black pepper spikes}} \times 100$$

$$= \frac{8}{10} \times 100$$

$$= 80\ \%$$

Karimunda

Average effectiveness index of the system = 81 %

Panniyur 1

Average effectiveness index of the system = 81 %

Appendix XXI

Time taken for the entire operation

Karimunda

Sl. No.	Time taken for the entire operation (seconds)	Sl. No.	Time taken for the entire operation (Seconds)	Sl. No.	Time taken for the entire operation (seconds)
1	7.5	11	6.3	21	6
2	6.6	12	6.1	22	6.6
3	7.3	13	6.2	23	6.6
4	7.2	14	6.1	24	6.1
5	7	15	6.7	25	6.3
6	6.3	16	6.1	26	6.6
7	6.1	17	5.9	27	6.3
8	6.3	18	6.3	28	6.7
9	6.2	19	6.3	29	7.2
10	6.2	20	6	30	7.1

Sl. No.	Time taken for the entire operation (seconds)	Sl. No.	Time taken for the entire operation (Seconds)	Sl. No.	Time taken for the entire operation (seconds)
31	6.6	46	7.8	61	6.8
32	6.8	47	7.2	62	6.8
33	6.3	48	7	63	6.7
34	6.2	49	6.6	64	6.3
35	6	50	7.5	65	6.5
36	6.7	51	6.9	66	6.4
37	6.7	52	7.2	67	6.2
38	6.7	53	7.1	68	6.4
39	6.9	54	6.9	69	6.4
40	6.6	55	6.8	70	6.3
41	6.7	56	6.3	71	6.8
42	6.8	57	6.3	72	6.3
43	6.7	58	6.4	73	6.5
44	6.8	59	6.3	74	6.4
45	7.4	60	6.1	75	6.3

Average time taken for the entire operation = 6.6 seconds

Panniyur 1

Sl. No.	Time taken for the entire operation (seconds)	Sl. No.	Time taken for the entire operation (Seconds)	Sl. No.	Time taken for the entire operation (seconds)
1	6.3	26	6.3	51	5.4
2	6.3	27	6	52	5.7
3	6.1	28	6.1	53	5.8
4	6.5	29	6.3	54	6.1
5	5.7	30	6	55	6.2
6	5.8	31	6.9	56	6
7	6.5	32	6.7	57	5.7
8	7	33	6.3	58	5.8
9	6.3	34	6.4	59	5.9
10	6.8	35	6.3	60	5.4
11	6.7	36	6.4	61	7.1
12	7.3	37	6.7	62	6.9
13	6.6	38	6.6	63	6.3
14	6.7	39	6.3	64	6.5
15	6.5	40	6.4	65	6.3
16	6.6	41	5.9	66	6.8
17	6.3	42	5.6	67	6.3
18	6.9	43	5.7	68	6.9
19	6.6	44	5.7	69	6.5
20	6.8	45	5.6	70	6.4
21	6.1	46	5.9	71	6.6
22	5.9	47	5.4	72	7
23	6.3	48	6	73	7.4
24	6.4	49	5.8	74	7.1
25	5.6	50	5.4	75	6.3

Average time taken for the entire operation = 6.3 seconds

Appendix XXII

Harvesting loss of robotic black pepper harvesting system

	Karimunda			*Panniyur 1*		
Sample	Weight of matured berries (kg)	Weight of under matured berries (kg)	Harvesting loss (%)	Weight of matured berries (kg)	Weight of under matured berries (kg)	Harvesting loss (%)
1	0.0676	0.004	5.6	0.1146	0.008	6.5
2	0.0796	0.003	3.6	0.0898	0.0076	7.8
3	0.0822	0.005	5.7	0.0818	0.0058	6.6
4	0.094	0.006	6.0	0.0856	0.0064	7.0
5	0.076	0.003	3.8	0.1088	0.008	6.8

Sample calculation

Weight of under matured berries = 0.004 kg

Weight of matured berries = 0.0676 kg

$$\text{Harvesting loss} = \frac{\text{Weight of under matured berries}}{\text{Weight of matured berries} + \text{Weight of under matured berries}} \times 100$$

$$= \frac{0.004}{(0.0676 + 0.004)} \times 100$$

$$= 5.6\ \%$$

$$\text{Average harvesting loss (} \textit{Karimunda} \text{)} = \frac{(5.6 + 3.6 + 5.7 + 6.0 + 3.8)}{5}$$

$$= 4.9\ \%$$

$$\text{Average harvesting loss (} \textit{Panniyur 1} \text{)} = \frac{(6.5 + 7.8 + 6.6 + 7.0 + 6.8)}{5}$$

$$= 7.0\ \%$$

Appendix XXIII

Drying loss of robotic black pepper harvesting system

Karimunda

Sample	Initial Weight, Kg	Weight after drying, Kg	Initial moisture content (wb), %	Final moisture content (wb), %	Initial moisture content (db), %	Final moisture content (db), %	Bone dry matter, Kg	Water evaporated, Kg	Drying loss, %
1	0.07	0.04	49	10	96	11	0.04	0.03	43
2	0.08	0.05	50	10	100	11	0.04	0.04	44
3	0.09	0.06	43	10	75	11	0.05	0.03	37
4	0.10	0.07	41	10	69	11	0.06	0.03	34
5	0.08	0.05	42	10	72	11	0.05	0.03	36

Panniyur 1

Sample	Initial Weight, Kg	Weight after drying, Kg	Initial moisture content (wb), %	Final moisture content (wb), %	Initial moisture content (db), %	Final moisture content (db), %	Bone dry matter, Kg	Water evaporated, Kg	Drying loss, %
1	0.12	0.05	71	10	245	11	0.04	0.08	68
2	0.10	0.04	69	10	223	11	0.03	0.06	66
3	0.09	0.03	65	10	186	11	0.03	0.05	61
4	0.09	0.05	73	10	270	11	0.02	0.06	70
5	0.12	0.07	70	10	233	11	0.04	0.08	67

Sample calculation

Initial weight = 0.07 Kg

Weight after drying = 0.04 Kg

Initial moisture content (wb) = 49%

Final moisture content (wb) = 10 %

$$\text{Initial moisture content (db)} = \frac{\text{Moisture content (wb)}}{\text{100- Moisture content (wb)}} \times 100$$

$$= \frac{49}{100-49} \times 100 \quad = 96\ \%$$

$$\text{Final moisture content (db)} = \frac{\text{Moisture content (wb)}}{\text{100- Moisture content (wb)}} \times 100$$

$$= \frac{10}{100-10} \times 100 = 11\ \%$$

Bone dry matter = Initial weight – Initial weight × Moisture content in decimal (wb)

= 0.07- (0.07×0.49)

= 0.04 Kg

Initial weight – Weight after drying = Water evaporated during drying

= Bone dry matter × (Initial moisture content in decimal (db) – Final moisture content in decimal (db))

= 0.04 × (0.96 – 0.11)

= 0.03 Kg

$$\text{Drying loss} = \frac{\text{Initial Weight-Weight after drying}}{\text{Initial weight}} \times 100$$

$$= \frac{0.03}{0.07} \times 100 = 43\%$$

Average drying loss in *Karimunda* = $\frac{43+44+37+34+36}{5} = 39\ \%$

Average drying loss in *Panniyur 1* = $\frac{68+66+61+70+67}{5} = 66\ \%$

Appendix XXIV

Capacity of manual harvesting

Karimunda

Sl. No	Time taken (Minute)	No. of black pepper spikes harvested	Total amount of black pepper spikes harvested (kg)	Capacity of manual harvesting (Spikes h^{-1})	Capacity of manual harvesting (kg h^{-1})
1	0.083	110	0.71	1320	8.52
2	0.083	150	0.89	1800	10.68
3	0.083	92	0.83	1104	9.96
4	0.083	29	0.21	348	2.52
5	0.083	82	0.42	984	5
6	0.083	130	0.56	1560	6.7
7	0.083	86	0.42	1032	5
8	0.083	105	0.53	1260	6.4
9	0.083	36	0.16	432	1.9
10	0.083	98	0.5	735	6
11	0.083	74	0.47	888	5.6
12	0.083	101	0.6	1212	7.2
13	0.083	126	0.8	1500	9.6
14	0.083	56	0.3	672	3.6
15	0.083	78	0.5	936	6

Panniyur 1

Sl. No	Time taken (Minute)	No. of black pepper spikes harvested	Total amount of black pepper spikes harvested (kg)	Capacity of manual harvesting (Spikes h^{-1})	Capacity of manual harvesting (kg h^{-1})
1	0.083	159	0.91	1908	10.9
2	0.083	160	1.03	1920	12.4
3	0.083	154	0.89	1848	10.7
4	0.083	149	0.93	1788	11.1
5	0.083	115	0.70	1380	8.4
6	0.083	106	0.64	1272	7.7
7	0.083	96	0.80	1152	9.6
8	0.083	89	0.85	1068	10.1
9	0.083	92	0.78	1104	9.4
10	0.083	173	0.97	2076	11.6
11	0.083	194	1.16	2328	13.9
12	0.083	184	1.07	2208	12.8
13	0.083	134	0.91	1608	10.9
14	0.083	124	0.98	1488	11.8
15	0.083	139	0.94	1668	11.3

Sample Calculation

Time taken = 0.083hr

Number of black pepper spikes harvested = 110 spikes

Total weight of black pepper spikes harvested = 0.71 kg

$$\text{Capacity, Spikes } h^{-1} = \frac{\text{Number of black pepper spikes harvested}}{\text{Time taken}}$$

$$= \frac{110}{0.083}$$

$= 1320 \text{ spikes h}^{-1}$

$$\text{Capacity, kg h}^{-1} = \frac{\text{Total amount of black pepper spikes harvested}}{\text{Time taken}}$$

$$= \frac{0.71}{0.083}$$

$$= 8.52 \text{ kg h}^{-1}$$

Karimunda

Average capacity of manual harvesting, spikes h^{-1} = 1052 spikes h^{-1}

Average capacity of manual harvesting, kg h^{-1} = 6.3 kg h^{-1}

Panniyur 1

Average capacity of manual harvesting, spikes h^{-1} = 1654 spikes h^{-1}

Average capacity of manual harvesting, kg h^{-1} = 10.8 kg h^{-1}

Appendix XXV

Effectiveness index of manual harvesting

Karimunda

Replication	Total number of black pepper spikes	No. of matured pepper spikes harvested	No. of green pepper spikes harvested	Effectiveness index
1	10	2	8	20
2	10	3	7	30
3	10	5	5	50
4	10	4	6	40
5	10	1	9	10
6	10	6	4	60
7	10	2	8	20
8	10	6	4	60
9	10	3	7	30
10	10	5	5	50
11	10	3	7	30
12	10	4	6	40
13	10	1	9	10
14	10	7	3	70
15	10	8	2	80

Panniyur 1

Replication	Total number of black pepper spikes	No. of matured pepper spikes harvested	No. of green pepper spikes harvested	Effectiveness index
1	10	3	7	30
2	10	4	6	40
3	10	3	7	30
4	10	2	8	20
5	10	5	5	50
6	10	3	7	30
7	10	6	4	60
8	10	7	3	70
9	10	5	5	50
10	10	2	8	20
11	10	4	6	40
12	10	4	6	40
13	10	3	7	30
14	10	2	8	20
15	10	4	6	40

Sample Calculation

Total number of black pepper spikes = 10

Number of matured black pepper spikes harvested = 2

Number of green pepper spikes harvested = 8

$$\text{Effectiveness index} = \frac{\text{Number of matured black pepper spikes harvested}}{\text{Total number of black pepper spikes}}$$

$$= \frac{2}{10}$$

$$= 20\ \%$$

Karimunda

Average effectiveness index of manual harvesting = 40%

Panniyur 1

Average effectiveness index of manual harvesting = 38 %

Appendix XXVI

Harvesting loss of manual harvesting

	Karimunda			*Panniyur 1*		
Sample	Weight of matured berries (kg)	Weight of under matured berries (kg)	Harvesting loss (%)	Weight of matured berries (kg)	Weight of under matured berries (kg)	Harvesting loss (%)
1	0.0785	0.015	16.0	0.1235	0.0118	8.7
2	0.0823	0.019	18.8	0.1227	0.021	14.6
3	0.143	0.016	10.1	0.1134	0.0377	25.0
4	0.132	0.025	15.9	0.1128	0.03	21.0
5	0.0976	0.018	15.6	0.1256	0.0275	18.0

Sample Calculation

Weight of under matured berries = 0.015 kg

Weight of matured berries = 0.0785 kg

$$\text{Harvesting loss} = \frac{\text{Weight of under matured berries}}{(\text{Weight of under matured berries} + \text{Weight of matured berries})}$$

$$= \frac{0.015}{(0.015+0.0875)} = 16.0\ \%$$

Karimunda

$$\text{Average harvesting loss} = \frac{(16 + 18.8 + 10.1 + 15.9 + 15.6)}{5}$$

$$= 15.3\ \%$$

Panniyur 1

Average harvesting loss $= \frac{(8.7 + 14.6 + 25 + 21 + 18)}{5}$

$= 17.5\ \%$

Appendix XXVII

Drying loss of manual harvesting

Karimunda

Sample	Initial Weight, Kg	Weight after drying, Kg	Initial moisture content (wb), %	Final moisture content (wb), %	Initial moisture content (db), %	Final moisture content (db), %	Bone dry matter, Kg	Water evaporated, Kg	Drying loss, %
1	0.09	0.05	52	10	108	11	0.04	0.04	47
2	0.10	0.04	65	10	186	11	0.04	0.06	61
3	0.16	0.07	55	10	122	11	0.07	0.08	50
4	0.16	0.06	63	10	170	11	0.06	0.09	59
5	0.12	0.04	66	10	194	11	0.04	0.07	62

Panniyur 1

Sample	Initial Weight, Kg	Weight after drying, Kg	Initial moisture content (wb), %	Final moisture content (wb), %	Initial moisture content (db), %	Final moisture content (db), %	Bone dry matter, Kg	Water evaporated, Kg	Drying loss, %
1	0.14	0.03	79	10	376	11	0.03	0.10	77
2	0.14	0.04	80	10	400	11	0.03	0.11	78
3	0.15	0.02	88	10	733	11	0.02	0.13	87
4	0.14	0.02	89	10	809	11	0.02	0.13	88
5	0.15	0.04	78	10	355	11	0.03	0.12	76

Sample calculation

Initial weight = 0.09 Kg

Weight after drying = 0.05 Kg

Initial moisture content (wb) = 52 %

Final moisture content (wb) = 10 %

$$\text{Initial moisture content (db)} = \frac{\text{Moisture content (wb)}}{\text{100- Moisture content (wb)}} \times 100$$

$$= \frac{52}{100-52} \times 100 \quad = 108\ \%$$

$$\text{Final moisture content (db)} = \frac{\text{Moisture content (wb)}}{\text{100- Moisture content (wb)}} \times 100$$

$$= \frac{10}{100\text{-}10} \times 100 = 11\ \%$$

Bone dry matter = Initial weight – Initial weight × Moisture content in decimal (wb)

$= 0.09 - (0.09 \times 0.52) = 0.04$ Kg

Initial weight – Weight after drying = Water evaporated during drying

= Bone dry matter × (Initial moisture content in decimal (db) – Final moisture content in decimal (db))

$= 0.04 \times (1.08 - 0.11)$

$= 0.04$ Kg

$$\text{Drying loss} = \frac{\text{Initial Weight-Weight after drying}}{\text{Initial weight}} \times 100$$

$$= \frac{0.04}{0.09} \times 100 = 47\ \%$$

$$\text{Average drying loss in } \textit{Karimunda} = \frac{47+61+50+59+62}{5} = 56\ \%$$

$$\text{Average drying loss in } \textit{Panniyur 1} = \frac{77+78+87+88+76}{5} = 81\ \%$$

Appendix XXVIII

Statistical analysis (Welch unpaired t-test) for comparing the capacity of manual harvesting and robotic harvesting

(i) Capacity (Kg h $^{-1}$)

Parameter	***Panniyur 1***		***Karimunda***	
	Manual harvesting	**Robotic harvesting**	**Manual harvesting**	**Robotic harvesting**
Number of observations	15	15	15	15
Minimum	7.7	3.7	1.9	2.4
Maximum	13.9	5.8	10.7	4.6
Range	6.2	2.1	8.8	2.2
Sum	162.6	69.4	94.7	52.1
Median	10.9	4.6	6.0	3.5
Mean	10.84	4.627	6.313	3.473
Standard error mean	0.422	0.158	0.672	0.185
Confidence intervals mean. .95	0.905	0.339	1.442	0.396
Variance	2.673	0.375	6.778	0.512
Standard deviation	1.635	0.612	2.604	0.716
Coefficient of variation	0.151	0.132	0.412	0.206
t_value	13.785		4.074	

Parameter	*Panniyur 1*		*Karimunda*	
	Manual harvesting	**Robotic harvesting**	**Manual harvesting**	**Robotic harvesting**
Degree of freedom	17.85		16.1	
P value	0		0.000874	
Level of significance	5 %		5 %	
Significance	Significant		Significant	

(ii) Capacity (spikes h $^{-1}$)

Parameter	*Panniyur 1*		*Karimunda*	
	Manual harvesting	**Robotic harvesting**	**Manual harvesting**	**Robotic harvesting**
Number of observations	15	15	15	15
Minimum	1068	522	348	507
Maximum	2328	667	1800	632
Range	1260	145	1452	125
Sum	24816	8739	15783	8423
Median	1668	571	1032	563
Mean	1654.4	582.6	1052.2	561.5
Standard error mean	104.2	10.4	105.4	9.2

Parameter	*Panniyur 1*		*Karimunda*	
	Manual harvesting	**Robotic harvesting**	**Manual harvesting**	**Robotic harvesting**
Confidence intervals mean. .95	223.4	22.3	226	19.7
Variance	162779	1626.8	166567.5	1270.5
Standard deviation	403.5	40.3	408.1	35.6
Coefficient of variation	0.244	0.069	0.388	0.063
t_value	10.238		4.639	
Degree of freedom	14.28		14.21	
P value	0		0.000369	
Level of significance	5 %		5 %	
Significance	Significant		Significant	

Since P-value is <0.05, reject the null hypothesis at 5% level of significance.

Here the null hypothesis is: Average capacity of manual harvesting = Average capacity of robotic harvesting system. It shows that there is a significant difference between the capacity of manual harvesting and robotic black pepper harvesting system in both variety.

Appendix XXIX

Statistical analysis (Welch unpaired t-test) for comparing the effectiveness index of robotic black pepper harvesting system and manual harvesting

Parameter	*Panniyur 1*		*Karimunda*	
	Manual harvesting	**Robotic harvesting**	**Manual harvesting**	**Robotic harvesting**
Number of observations	15	15	15	15
Minimum	20	70	10	70
Maximum	70	90	80	100
Range	50	20	70	30
Sum	570	1230	600	1220
Median	40	80	40	80
Mean	38	82	40	81.3
Standard error mean	3.8	1.7	5.5	2.4
Confidence intervals mean. .95	8.2	3.7	11.8	5.07
Variance	217.1	45.7	457.1	83.8
Standard deviation	14.7	6.8	21.4	9.2
Coefficient of variation	0.388	0.082	0.535	0.113
t_value	-10.511		-6.883	

Parameter	*Panniyur 1*		*Karimunda*	
	Manual harvesting	**Robotic harvesting**	**Manual harvesting**	**Robotic harvesting**
Degree of freedom	19.64		18.97	
P value	0		0.000001	
Level of significance	5 %		5 %	
Significance	Significant		Significant	

Since P-value is <0.05, reject the null hypothesis at 5% level of significance. Here the null hypothesis is: Average effectiveness index of manual harvesting = Average effectiveness index of robotic harvesting system. Result showed that, there is significant difference between the effectiveness index of manual harvesting and robotic black pepper harvesting system in both variety.

Appendix XXX

Statistical analysis (Welch unpaired t-test) for comparing the harvesting loss in robotic black pepper harvesting system and manual harvesting

Parameter	*Panniyur 1*		*Karimunda*	
	Manual harvesting	**Robotic harvesting**	**Manual harvesting**	**Robotic harvesting**
Number of observations	5	5	5	5
Minimum	8.7	6.5	10.1	3.6
Maximum	25	7.8	18.8	6
Range	16.3	1.3	8.7	2.4

Parameter	*Panniyur 1*		*Karimunda*	
	Manual harvesting	**Robotic harvesting**	**Manual harvesting**	**Robotic harvesting**
Sum	87.3	34.7	76.4	24.7
Median	18	6.8	15.9	5.6
Mean	17.4	6.9	15.3	4.94
Standard error mean	2.8	0.23	1.4	0.51
Confidence intervals mean. .95	7.7	0.64	3.9	1.42
Variance	38.6	0.26	10.05	1.30
Standard deviation	6.2	0.5	3.17	1.14
Coefficient of variation	0.356	0.075	0.208	0.232
t_value	3.771		6.858	
Degree of freedom	4.06		5.02	
P value	0.019107		0.000989	
Level of significance	5 %		5 %	
Significance	Significant		Significant	

The P-value is <0.05, so reject the null hypothesis at 5% level of significance.

Null hypothesis is: Average harvesting loss of manual harvesting = Average harvesting loss of robotic harvesting system. It shows that there is a significant difference between the harvesting loss of manual harvesting and robotic black pepper harvesting system in both variety.

Appendix XXXI

Statistical analysis (Welch unpaired t-test) for comparing the drying loss in robotic black pepper harvesting system and manual harvesting

Parameter	*Panniyur 1*		*Karimunda*	
	Manual harvesting	**Robotic harvesting**	**Manual harvesting**	**Robotic harvesting**
Number of observations	5	5	5	5
Minimum	76	61	47	34
Maximum	88	70	62	44
Range	12	9	15	10
Sum	406	332	279	194
Median	78	67	59	37
Mean	81	66	56	39
Standard error mean	2.596	1.503	3.056	1.985
Confidence intervals mean. .95	7.208	4.174	8.485	5.511
Variance	33.7	11.3	46.7	19.7
Standard deviation	5.805	3.362	6.834	4.438
Coefficient of variation	0.071	0.051	0.122	0.114

Parameter	*Panniyur 1*		*Karimunda*	
	Manual harvesting	**Robotic harvesting**	**Manual harvesting**	**Robotic harvesting**
t_value	4.933		4.665	
Degree of freedom	6.41		6.86	
P value	0.002172		0.002423	
Level of significance	5 %		5 %	
Significance	Significant		Significant	

The P-value is <0.05, so reject the null hypothesis at 5% level of significance.

Null hypothesis is: Average drying loss of manual harvesting = Average drying loss of robotic harvesting system. It shows that there is a significant difference between the drying loss of manual harvesting and robotic black pepper harvesting system in both *Panniyur 1* and *Karimunda* variety.

DEVELOPMENT OF ROBOTIC BLACK PEPPER HARVESTING SYSTEM

By

AMSUJA V AJAYAN

(2019-18-011)

ABSTRACT OF THESIS

Submitted in partial fulfilment of the requirements for the degree of

MASTER OF TECHNOLOGY

IN

AGRICULTURAL ENGINEERING

(Farm Machinery and Power Engineering)

Faculty of Agricultural Engineering and Technology

Kerala Agricultural University

DEPARTMENT OF FARM MACHINERY AND POWER ENGINEERING

KELAPPAJI COLLEGE OF AGRICULTURAL ENGINEERING AND TECHNOLOGY, TAVANUR - 679 573

KERALA, INDIA

2022

Abstract

Black pepper is a perennial crop and one of India's most economically significant spices. It has a high commercial value in the market all around the world. Its fruit is harvested, dried, and powdered for many cuisines and processed for many value-added products. Black pepper is a flowering vine growing on supporting stakes. The berries turn from green to red on maturity and are harvested when it starts to turn red. For achieving good quality and good-sized pepper, it should be harvested at its correct maturity stage. Generally, black pepper spikes were harvested manually by climbing on supporting trees using bamboo poles. It is a tedious task because there are chances of falling from ladders while harvesting and also causes some musculoskeletal diseases to the labours. For their time saving and heavy work intensity, farmers harvest almost all the fruits in a range of maturity along with the real matured ones. This practice eventually affects the crop yield and quality. Through robotic harvesting, black pepper spikes can be harvested at correct maturity and also helps to overcome the difficulties faced by the labours. The main functions of robotic harvesting are identification, plucking, depositing, and controlling. KAU developed a machine vision system with the camera as sensor, Raspberry pi 4 model B as the processor, and LCD as the display unit to identify matured black pepper spikes. The programing code was written in python language, and the Tensorflow-faster RCNN platform was used for the detection. Hence, a robotic black pepper harvesting system was developed in the present study, and its performance evaluation was carried out.

The physical properties of black pepper relevant to design and develop a robotic black pepper harvesting system were determined. The developed robotic black pepper harvesting system consists of a machine vision system to identify matured black pepper spikes, a manipulator with 2 DOF, an end-effector with 1 DOF, and a control unit. Servo motors actuated the shoulder and elbow joints of the manipulator and the cutting blades. Shear-type cutting was employed for detaching pepper spikes from the pepper vine. The entire system was controlled by the microprocessor Raspberry pi 4 Model B. For controlling the servo motors, the library RPi.GPIO was installed on raspberry pi, and the programming code was

written in python language. Two lead-acid batteries with a voltage of 12 V and a current 9Ah were connected in parallel to power the entire system. The overall dimension of the developed unit was 59 × 18 × 162 cm, and it weighs 2.1 kg.

The performance evaluation parameters of the machine vision system viz., sensitivity, specificity, and accuracy were respectively as 85 %, 77 %, and 82 % in *Karimunda* variety and 84 %, 77 %, and 82 % in *Panniyur 1* variety. Time taken for detection is 0.43 seconds. Also, the capacity of the developed robotic black pepper harvesting system is 3.5 kg h^{-1} and 562 spikes h^{-1} in the *Karimunda* variety, whereas 4.6 kg h^{-1} and 683 spikes h^{-1} in *Panniyur 1* variety. The effectiveness index, time taken for the entire operation, harvesting loss, and drying loss was 81%, 6.6 seconds, 4.9 %, and 39 % in the *Karimunda* variety and 82 %, 6.3 seconds, 7%, and 66 % in *Panniyur 1* variety respectively. The system takes 0.18 seconds for a single cut for both varieties; it was fixed in the program.

A study was also carried out for manual harvesting and found that manual harvesting has a capacity of 1052 spikes h^{-1} and 6.3 kg h^{-1} in the *Karimunda* variety and 1654 spikes h^{-1} and 10.8 kg h^{-1} in the *Panniyur 1* variety, which is higher than robotic harvesting. The effectiveness index of the manual harvesting was 40% in *Karimunda* and 38 % in *Panniyur 1*, which is lower than robotic harvesting. The harvesting loss and drying loss of manual harvesting are 15.3 % and 56 % in *Karimunda* and 17.5 % and 81 % in *Panniyur 1*, which is higher than robotic harvesting. It was statistically verified and found a significant difference between manual and robotic harvesting in terms of capacity, effectiveness index, harvesting loss, and drying loss at a 5 % level of significance.